

AN ABSTRACT OF THE THESIS OF

David King for the degree of Master of Science in Wood Science and Civil Engineering presented on March 18, 2014

Title: Moisture Effects on Properties of Wood-Composite Assemblies.

Abstract approved:

Jeffrey J. Morrell

Arijit Sinha

Engineered wood composites are used in many structural applications and are intended for dry use. However, these materials may encounter significant amounts of wetting while in service, which can lead to structural failures. This study combined aspects of wood science, mechanics, structural engineering, and mycology to assess changes in material properties of I-joists and small-scale, wood-composite shear walls over extended periods of wetting. Exposure time, total rainfall, and rain days were used to develop predictive models of ultimate flexural failure for I-joists subjected to long-term external exposure. I-joists were experimentally evaluated with a full-scale, six-point bending test followed by a web-flange seam tension test. Bending test failure modes progressed from pure shear to web buckling with prolonged exposure time. Variance in flexural strength nearly doubled after 27 days of exposure. Decreases in flexural strength became significant after 65 days of exposure, reducing capacity by 9%. I-joist flexural strength reduced to 18% after 138 days of exposure. The results

illustrate the detrimental effects of exposure to wetting during construction, and support improved efforts to limit wetting.

Properties of small-scale shear walls were evaluated in a similar study monitoring the effects of moisture exposure and fungal inoculating over time. Shear wall capacity was tested using a lateral point load at various exposure intervals. Initial shear wall capacity increased by 37% as the fasteners corroded, producing better withdrawal resistance. Shear wall assemblies with visual decay experienced losses in capacity ranging from 13 to 61%. Comparisons of moisture and density distributions showed that wetting had an effect on panel properties. Visual evidence of decay in the uplift corner of a shear wall suggests considerable reductions in capacity and should require immediate repair.

© Copyright by David King
March 18, 2014
All Rights Reserved

Moisture Effects on Properties of Wood-Composite Assemblies

by
David King

A THESIS

submitted to

Oregon State University

in partial fulfillment of
the requirements for the
degree of

Master of Science

Presented March 18, 2014
Commencement June 2014

Master of Science thesis of David King presented on March 18, 2014.

APPROVED:

Co-Major Professor, representing Wood Science

Co-Major Professor, representing Civil Engineering

Head of the Department of Wood Science and Engineering

Head of the School of Civil and Construction Engineering

Dean of the Graduate School

I understand that my thesis will become part of the permanent collection Oregon State University libraries. My signature below authorizes release of my thesis to any reader upon request.

David King, Author

ACKNOWLEDGEMENTS

I would like to thank the following people and organizations. Their help with advising, laboratory work, and encouragement have made this work possible.

- Dr. Jeffery J. Morrell – Distinguished Professor, Oregon State University
- Dr. Arijit Sinha – Assistant Professor, Oregon State University
- Milo Clauson – Senior Faculty Research Assistant, Oregon State University
- Camille Freitag – Senior Faculty Research Assistant, Oregon State University
- Connie Love – Senior Faculty Research Assistant, Oregon State University
- Byrne Miyamoto – Oregon State University
- Center for Wood Utilization Research
- Fellow graduate students and friends at OSU
- Faculty and staff in the Wood Science and Engineering Department, OSU
- Faculty and staff in the School of Civil and Construction Engineering, OSU

I would especially like to thank my wife, Sarah and my parents, Tom and Sally for their continued support and interest in my education. I would not be where I am today without their influence in my life.

CONTRIBUTION OF AUTHORS

Dr. Jeffery J. Morrell and Dr. Arijit Sinha have provided significant guidance in writing and directing this research project.

TABLE OF CONTENTS

	<u>Page</u>
1. Introduction	1
2. Literature Review	5
2.1 Oriented Strand Board	6
2.2 Laminated Veneer Lumber	10
2.3 I-Joists	11
2.4 Shear Walls	14
2.5 Literature Cited	16
3. Effects of Outdoor Exposure on Properties of I-joists	19
3.1 Abstract	20
3.2 Keywords	21
3.3 Introduction	21
3.4 Materials and Methods	23
Specimens	23
Exposure	24
Test setup	24
Statistics	26
3.5 Results and Discussion	27
Rainfall and moisture content	27
Bending test	28
Regression	30

TABLE OF CONTENTS (Continued)

	<u>Page</u>
Bending test failure modes	31
Tension test failure modes	34
3.6 Conclusions.....	35
3.7 References.....	36
4. Moisture and Fungal Effects on Wood Composite Shear Walls.....	38
4.1 Abstract	39
4.2 Keywords	39
4.3 Introduction.....	40
4.4 Materials and Methods.....	42
Assemblies	42
Uplift corner	44
Treatments	45
Irrigation system.....	47
Inoculum	48
Moisture content mapping.....	49
Shear wall tests.....	49
Digital image correlation.....	51
Density mapping	52
Culturing	53
Statistics	53

TABLE OF CONTENTS (Continued)

	<u>Page</u>
4.5 Results and Discussion	54
Moisture content mapping.....	54
Shear wall tests.....	60
Digital Image Correlation	67
Density Mapping.....	70
Culturing	74
Conclusions	75
4.6 References.....	76
5. Conclusions	78
Recommendations	79
Continued studies on I-joists.....	79
Continued studies on shear walls and <i>Postia placenta</i> interaction:	80
Bibliography.....	82
Appendices	87

LIST OF FIGURES

<u>Figure</u>	<u>Page</u>
3-1. I-joist bending test setup	26
3-2. Daily rainfall amounts over the 138 day period when I-joists were exposed in Western Oregon	28
3-3. Moisture content and maximum loads of I-joists exposed outdoors in an above ground test for 0 to 138 days in Western Oregon.	29
3-4. Box and whisker plots of capacity (load) and deflection of I-joists exposed to wetting over a 138 day period.....	30
3-5. Various failure modes of I-joist a) ZW, b) ZJ, c) WB, and d) IJ	32
3-6. Maximum load in tension of sections cut from I-joists exposed for 0 to 138 days outdoors in an above ground test in Western Oregon.....	35
4-1. Shear wall assembly configurations a) dry control, b) no corner control, c) wetting only or wetting and fungal exposure.....	46
4-2. Shear wall irrigation system	48
4-3. Shear wall testing apparatus	51
4-4. Typical shear wall wetting patterns a) Type B, b) Type F, c) Type T, d) Type L, e) Type I, f) Type X	55
4-5. Box and whisker plots of shear wall percent weight gain with respect to wetting patterns (moisture content map type).....	60
4-6. Photographs show a) nail withdrawal on frame in uplift corner, b) nail withdrawal on paneling in uplift corner, c) nail pull-through and flake debonding on paneling in uplift corner, and d) cross grain tension on the sill plate in uplift corner of small scale shear wall assemblies	62
4-7. Maximum shear wall capacity as shown by treatment groups	64

LIST OF FIGURES (Continued)

<u>Figure</u>	<u>Page</u>
4-7. Wetted and wetted/fungal inoculated shear wall maximum load versus incubation period	64
4-8. Maximum shear wall capacity as shown by treatment groups	65
4-9. Examples of a) wetted assembly with corroded framing nails, b) dry control shear wall with non-corroded framing nails.	66
4-11. Progressive strain contour plots showing strain in shear walls at a) 0.50 kN, b) 0.94 kN, c) 2.13 kN, d) 2.41 kN, or e) 3.23 kN	68
4-12. Typical density maps of a) dry control and b) wetted/inoculated assemblies	71
4-13. Comparisons between moisture content and Pilodyn maps of a) assembly SW17 b) assembly WC26 c) assembly SW32 and d) assembly WC24. Note: Moisture content contour plots were developed using data points covering the entire shear wall face whereas Pilodyn contour plots were developed using data points covering the ¼ panel in the uplift corner resulting in a tighter grid spacing.	72

LIST OF TABLES

<u>Table</u>	<u>Page</u>
3-1. Effect of exterior exposure on moisture content and physical properties of I-joists	28
4-1: Frequencies of the six moisture content distributions in assemblies exposed for different incubation periods	56

LIST OF APPENDICIES

<u>Appendix</u>	<u>Page</u>
Appendix A - I-joist Project Photographs	88
Appendix B - Derivation of Beam Loading Geometry	92
Appendix C - LabView Programming	96
Appendix D - I-Joist Flexural and Tension Charts with Rain Data	99
Appendix E - I-Joist Flexural Tests Load and Deflection Data	102
Appendix F - I-Joist Tension Tests Load and Deflection Data.....	113
Appendix G - Shear Wall Construction and Testing	116
Appendix H - Moisture Content Maps	121
Appendix I – Pilodyn Contour Plots	142
Appendix J - Shear Wall Load and Deflection Curves	155
Appendix K - Digital Image Correlation Strain Maps	160

LIST OF APPENDIX FIGURES

<u>Figure</u>	<u>Page</u>
A-1. End View of I-joist Exposure Rack	89
A-2. Side View of I-joist Exposure Rack.....	89
A-3. Hold down Strips on I-joist Exposure Rack	90
A-4. Flexure Test Set-up	90
A-5. Tension Test Set-up	91
C-1. LabView Graphical User Interface	97
C-2. LabView Programming.....	98
D-2. Moisture content and maximum loads of 356 mm deep I-joists exposed outdoors in an above ground test for 0 to 566 days in Western Oregon.	100
D-2. Cumulative Rainfall during Exposure Period	101
E-1. Load vs. Deflection Curve for C1, C2, C3, and C4	103
E-2. Load vs. Deflection Curve for C5, C6, and C7	103
E-3. Load vs. Deflection Curve for 4449, 4601, 4 613, and 4615	104
E-4. Load vs. Deflection Curve for 4641, 4642, 4691, and 4693	104
E-5. Load vs. Deflection Curve for 4635, 4570, 4697, and 5747	105
E-6. Load vs. Deflection Curve for 4454, 4456, 4483, and 4495	105
E-7. Load vs. Deflection Curve for 4494, 4498, 4552, and 4643	106
E-8. Load vs. Deflection Curve for 4656, 4660, 4692, 4696.....	106
E-9. Load vs. Deflection Curve for 4402, 4411, 4450, and 4459	107
E-10. Load vs. Deflection Curve for 4546, 4614, 4658, 4680, and 5773	107

LIST OF APPENDIX FIGURES (Continued)

<u>Figure</u>	<u>Page</u>
E-11 Load vs. Deflection Curve for 4402, 4411, 4450, and 4459	108
E-12. Load vs. Deflection Curve for 4546, 4614, 4658, 4680, and 5773	108
E-13. Load vs. Deflection Curve for 14C01, 14C02, 14C04, and 14C05	109
E-14. Load vs. Deflection Curve for 14C06, 14C07, 14C08, 14C09, and 14C10.....	109
E-15. Load vs. Deflection Curve for 14C01, 14C02, 14C04, and 14C05	110
E-16 Load vs. Deflection Curve for 14C06, 14C07, 14C08, 14C09, and 14C10.....	110
E-17 Load vs. Deflection Curve for 5745, 5751, 5755, 5759, 5765, and 5769	111
E-18. Load vs. Deflection Curve for 5777, 5781, 5785, 5787, 5791, and 5797	111
E-19. Load vs. Deflection Curve for 5757, 5761, 5767, and 5771	112
E-20. Load vs. Deflection Curve for 5779, 5783, 5789, and 5793	112
F-1. 356 mm I-Joist Tension Test: Load vs. Exposure Days	114
F-2. 356 mm I-Joist Tension Test: Deflection vs. Exposure Days	115
G-1. Building shear wall frames	117
G-2. Drilling holes in framing members	117
G-3. Sheathing Construction.....	118
G-4. Building Paper Configuration	118
G-5. Completed Shear Walls.....	119
G-6. Moisture Content Measurements	119
G-7. Shear Wall Test Installation.....	120
G-8. Shear Wall Test Setup.....	120
H-1. Moisture Content Contour Plots of SW9, SW10, SW11, and SW12	122

LIST OF APPENDIX FIGURES (Continued)

<u>Figure</u>	<u>Page</u>
H-2. Moisture Content Contour Plots of SW13, SW14, SW15, and SW16	123
H-3. Moisture Content Contour Plots of SW17, SW18, SW19, and SW20	124
H-4. Moisture Content Contour Plots of SW21, SW22, SW23, and SW24	125
H-5. Moisture Content Contour Plots of SW25, SW26, SW27, and SW28	126
H-6. Moisture Content Contour Plots of SW29, SW30, SW31, and SW32	127
H-7. Moisture Content Contour Plots of SW33, SW34, SW35, and SW36	128
H-8. Moisture Content Contour Plots of SW37, SW38, SW39, and SW40	129
H-9. Moisture Content Contour Plots of SW41, SW42, SW43, and SW44	130
H-10. Moisture Content Contour Plots of SW45, SW46, SW47, and SW48	131
H-11. Moisture Content Contour Plots of WC9, WC10, WC11, and WC12	132
H-12. Moisture Content Contour Plots of WC13, WC14, WC15, and WC16	133
H-13. Moisture Content Contour Plots of WC17, WC18, WC19, and WC20	134
H-14. Moisture Content Contour Plots of WC21, WC22, WC23, and WC24	135
H-15. Moisture Content Contour Plots of WC25, WC26, WC27, and WC28	136
H-16. Moisture Content Contour Plots of WC29, WC30, WC31, and WC32	137
H-17. Moisture Content Contour Plots of WC33, WC34, WC35, and WC36	138
H-18. Moisture Content Contour Plots of WC37, WC38, WC39, and WC40	139
H-19. Moisture Content Contour Plots of WC41, WC42, WC43, and WC44	140
H-20. Moisture Content Contour Plots of WC45, WC46, WC47, and WC48	141
I-1. Pilodyn Corner Contour Plots of C01, C02, C03, and C04.....	143
I-2. Pilodyn Corner Contour Plots of C05, C06, C07, and C08.....	144

LIST OF APPENDIX FIGURES (Continued)

<u>Figure</u>	<u>Page</u>
I-3. Pilodyn Corner Contour Plots of SW13, SW14, SW15, and SW16	145
I-4. Pilodyn Corner Contour Plots of SW25, SW26, SW27, and SW28	146
I-5. Pilodyn Corner Contour Plots of SW29, SW30, SW31, and SW32	147
I-6. Pilodyn Corner Contour Plots of SW33, SW34, SW35, and SW36	148
I-7. Pilodyn Corner Contour Plots of SW37, SW38, SW39, and SW40	149
I-8. Pilodyn Corner Contour Plots of WC21, WC22, WC23, and WC24	150
I-9. Pilodyn Corner Contour Plots of WC25, WC26, WC27, and WC28	151
I-10. Pilodyn Corner Contour Plots of WC29, WC30, WC31, and WC32	152
I-11. Pilodyn Corner Contour Plots of WC33, WC34, WC35, and WC36	153
I-12. Pilodyn Corner Contour Plots of WC37, WC38, WC39, and WC40	154
I-1. Dry Control for DC01R, DC02R, DC03R, and DC04R	156
I-2. Shear Wall Load and Deflection Curve for DC05R, DC06R, DC07R, and DC08R	156
I-3. Shear Wall Load and Deflection Curve for corn01, corn02, corn03, and corn04	157
I-4. Shear Wall Load and Deflection Curve for corn06, corn07, and corn08.....	157
I-5. Shear Wall Load and Deflection Curve for WC41, WC42, WC43, and WC44 .	158
I-6. Shear Wall Load and Deflection Curve for WC45, WC46, WC47, and WC48 .	158
I-7. Shear Wall Load and Deflection Curve for SW40, SW41, SW42, and SW43 ...	159
I-8. Shear Wall Load and Deflection Curve for SW44, SW45, SW46, SW47, and SW48.....	159
K-1. Strain at Maximum Load for DC01, DC02, DC03, and DC04.....	161
K-2. Strain at Maximum Load for DC05, DC06, DC07, and DC08.....	162

LIST OF APPENDIX FIGURES (Continued)

<u>Figure</u>	<u>Page</u>
K-3. Strain at Maximum Load for SW09, SW10, SW11, and SW12.....	163
K-4. Strain at Maximum Load for SW13, SW14, SW15, and SW16.....	164
K-5. Strain at Maximum Load for SW17, SW18, SW19, and SW20.....	165
K-6. Strain at Maximum Load for SW21, SW22, SW23, and SW24.....	166
K-7. Strain at Maximum Load for SW25, SW26, SW27, and SW28.....	167
K-8. Strain at Maximum Load for SW29, SW30, SW31, and SW32.....	168
K-9. Strain at Maximum Load for SW33, SW34, SW35, and SW36.....	169
K-10. Strain at Maximum Load for SW37, SW38, SW39, and SW40.....	170

LIST OF APPENDIX TABLES

<u>Table</u>	<u>Page</u>
D-1. Effects of exterior exposure on moisture content and physical properties of I-joists	100
F-1. Tension Test Data.....	114

1. INTRODUCTION

Average tree size has been decreasing as forest resources have changed with time, causing wood quality to also change. The once frequent large and long lumber needed for most roof and floor framing in low-rise structures has become more costly and less available (Leichti *et al.* 1990). The development of engineered wood products has filled this void and given builders many choices for job-specific tasks. In recent decades, concerns about forest management and sustainability have grown in popularity. The use of renewable materials in building practices has gained widespread acceptance as a viable way to reduce the environmental impacts of construction. Wood is one of the most prevalent, renewable resources in the world; thus, wood based composites are an excellent choice for enhancing sustainability metric of the project and have many benefits for construction. Wood as a renewable material has many advantages and a long history of performance under adverse conditions (Meyer 1982). However, there are little data regarding the durability and service life of many wood-based composites, which often puts these materials at a disadvantage against other materials. Wood composites are biological in nature and, as a result, their long-term performance can be affected by a variety of factors, including extreme wind events, seismic activity, or environmental conditions. Environmental factors could easily have the broadest impact on long-term performance of structural systems and the largest potential for economic consequence (Mankowski and Morrell 2000, Sanchez-Silvia and Rosowsky 2008).

Engineered wood composites are used in many structural applications and are generally designed for dry use. The presence of moisture often produces irreversible effects on the material properties of these composites (McNatt and Laufenberg 1989, River 1994, Okkonen and River 1996, Wu 1997, Hayashi *et al.* 2005, Garay *et al.* 2009, Kojima *et al.* 2011); thus, manufacturers typically specify that these materials be protected from wetting. There are times, although infrequent, that these composites encounter significant amounts of wetting while in service. Wetting not only affects wood composite material properties, but can also provide an environment favorable to the growth of decay fungi. Wetting alters structural capacity and, as a result, structural integrity could become jeopardized. Therefore, inspectors need more tools to properly assess damage once wetting is discovered.

The durability of wood-based products is one of the most important properties considered in housing construction (Norita *et al.* 2008). An estimation of how long these products maintain their required performance attributes under actual environmental conditions has been a goal of many studies. Methods for evaluating the durability of wood-based composites include short-term and long-term tests. Short-term evaluations assess changes in mechanical properties after accelerated aging treatments, such as water immersion, boiling, steaming, drying, or freezing. Compared to long-term test, these treatments are quicker to perform, more standardized, and less variable. In contrast, long-term exposure tests often use elapsed time as a primary independent variable to evaluate deterioration. Fungal decay is usually a main focus for these tests given that tests are frequently conducted outdoors in a natural

environment. Several long-term studies have been conducted with a variety of wood-based panels, laminates, and connections (Hayashi *et al.* 2002, Wu 1997, Kent *et al.* 2004, Hayashi *et al.* 2005, Kent *et al.* 2005, Kojima *et al.* 2011). These studies have broadened our understanding of wood-based composites and have given us tools to predict longevity. Although these studies are useful, they cannot represent wetting or fungal decay effects on material properties of combined wood composite interfaces such as I-joists and shear walls. Studies on these materials would help ensure confidence in long-term performance. Herein lays the opportunity for this work.

Although many engineered wood composites are intended for dry use, there are occasions where these materials experience wetting while in service. In this study, we combined aspects of wood science, mechanics, structural engineering, and mycology to assess changes in material properties of I-joists and small-scale, wood-composite shear walls over extended periods of wetting. The goal of this study was to gain a better understanding of structural damage caused by combinations of wetting and fungal decay on I-joists and wood-composite shear walls. More specifically, the objectives of the study were:

- To evaluate the effects of exposure time on I-joist ultimate flexural strength and stiffness
- To develop predictive models of ultimate flexural failure subjected to long-term exposure
- To evaluate progressive bending test failure modes of I-joists

- To evaluate the effects of exposure time on I-joist web-flange tensile strength
- To track shear wall capacity loss as it relates to exposure time
- To differentiate the effects of fungal decay from those of wetting on shear wall capacity
- To analyze the failure progression of shear walls

In order to fulfill these objectives, two studies were undertaken which resulted in two manuscripts. Supporting data and figures not included in the manuscripts are included in the appendix. The first manuscript (Chapter 3) titled “Effects of Outdoor Exposure on Properties of I-joists” presents a long-term outdoor exposure test of I-joists. Sets of I-joists were periodically removed from exposure and subjected to flexural and tensile tests. The second manuscript (Chapter 4) titled “Moisture and Fungal Effects on Wood Composite Shear Walls” presents a long-term exposure test of small-scale wood-composite shear walls inoculated with a brown rot decay fungi in a conditioning room. Sets of shear walls were periodically removed from exposure and subjected to lateral bearing and density tests. Fulfillment of these objectives will lead to a better understanding of long term performance for I-joists and shear walls. This information will allow us to give inspectors better knowledge for proper damage assessment.

2. LITERATURE REVIEW

Forest management practices in the United States have been continually changing over time. Old growth timber that was once the most common forest export now has become limited and is rarely harvested (Leichti *et al.* 1990). Many mills no longer accept logs larger than 30 inches in diameter. The shift towards second growth timber has brought new challenges followed by creative thinking. Processing second growth produces a higher volume of secondary materials (wood chips, sawdust, bark, etc.). Looking for solutions to minimize loss, entrepreneurs have developed engineered wood products (particle board, glulam beams, oriented strand board, laminated veneer lumber, etc.) that utilize these low value materials to make value added products. These engineered wood products have many advantages such as uniform material properties, high reliability, efficient wood use, and because they are dry when installed, they have reduced in-use shrinkage. However, there is little data regarding the service life of many of these products, which often puts these at a disadvantage against other materials. Wood composites are biological in nature and, as a result, their long-term performance can be affected by a variety of factors, including extreme wind events, seismic activity, or environmental conditions. Environmental factors could easily have the broadest impact on long-term performance of structural systems and the largest potential for economic consequence (Mankowski and Morrell 2000, Sanchez-Silvia and Rosowsky 2008). Perhaps two of the most detrimental environmental factors that can affect wood-based composites are moisture and fungal

decay, since evidence can be hidden for months behind gypsum board or exterior cladding (Morrell 2002). Unfortunately there is little information on the effects of these factors on many wood-based composites such as I-joists and shear walls. However, the components used to create these composites (oriented strand board, laminated veneer lumber, and solid wood) have been researched.

2.1 ORIENTED STRAND BOARD

Like most other engineered wood products, oriented strand board (OSB) is designed for use under dry service conditions. OSB is produced by taking a low value material, such as aspen flakes, and transforming it into a higher value product. OSB is designed to evenly distribute wood defects such as knots, checks, and worm holes; thus, giving the builder greater confidence in wood as a building material. The physical and mechanical properties of the board are enhanced by the layering and alignment of wood flakes (Wu 1999). OSB strand is aligned in a $0^{\circ}/90^{\circ}/0^{\circ}$ layup pattern which produces a strong and weak axis.

OSB has been highly successful in modern construction, and as a result, accounts for approximately 43.6 percent of the construction material used in new homes in 2012 (UN 2013). OSB can be useful in many applications, but most are usually focused around wall and diaphragm structures. The manufacturing processes of OSB are continuously being improved, which has significantly boosted the production rates and reduced costs of this building material (Lin *et al.* 2013).

OSB is not extremely sensitive to small amounts of moisture since it has some inherent moisture resistance due to the resins which hold together the strands, along with some waxes that are added to the product specifically for this purpose. Consequently, OSB can accommodate exposure to some water without swelling; however, panel edges are especially vulnerable to moisture. Thus, most panels are coated with a sealant on the panel edges to retard moisture penetration. Although OSB absorbs water slowly, it is also slow to dry out. This can jeopardize the material properties of this product.

The durability of wood-based panels is one of the most important properties considered in housing construction and has been the subject of many studies (Lehmann 1978, River 1994, Okkonen and River 1996, Wu and Suchsland 1997, Norita *et al.* 2008, Kojima and Suzuki 2011, Meza *et al.* 2013). OSB panels are commonly composed of nondurable wood species such as aspen, and are thus susceptible to fungal attack when wetted. Aspen is the predominant wood used for OSB in North America (Bergman *et al.* 2010). Kojima and Suzuki (2011) found that aspen OSB retained just 35 percent MOR after only one year of outdoor exposure in Shizuoka, Japan. Meza *et al.* (2013) observed a 30 percent decrease in MOR of OSB after just 100 days of exposure in the Willamette Valley of Oregon. Some naturally durable wood species, such as white cedar, have also been used for making composite panels that are resistant against decay and termites (Haataja and Laks 1995). However, limited research has been conducted on using biological treatment to improve panel durability (Mai *et al.* 2004).

Waferboard is similar to OSB, but waferboard strands are randomly aligned, causing strength to be equal in all directions. Mechanical properties including edge crushing and static bending of treated aspen waferboards exposed to mold and decay fungi were evaluated using soil block and soil-pan tests (Schmidt *et al.* 1983). Models for weight loss and mechanical property reductions when materials were exposed to *Gloeophyllum trabeum* or *Postia placenta* were developed using linear regression. The equations were considered to have good fit with correlation coefficients ranging from 0.82 to 0.93. This study indicated that specific gravity may be a suitable explanatory variable for mechanical property loss in wood composites.

Wood-based composites are known to swell significantly in thickness when exposed to high relative humidity. Thus, most degradation studies of OSB incorporate thickness swell (TS) tests to determine losses in material properties (Liu and McNatt 1991, Suchsland and Xu 1991, River 1994, Okkonen and River 1996, Wu and Lee 2002, Garay *et al.* 2009, Kojima 2011). Total-thickness swelling is comprised of two components: recoverable TS and non-recoverable TS. Recoverable TS is the swelling of the wood caused by change in relative humidity in the hygroscopic range. Non-recoverable TS is a result of the combined effect of the compression stress release from the pressing operation and differential swelling potential due to inherent in-plane density variation. The latter results in normal swelling stress between high and low density areas in the plane of a panel. These stresses are often large enough to break the adhesive bonds, leading to significant non-recoverable TS (Liu and McNatt 1991, Suchsland and Xu 1991). OSB also has much less resistance to fungal attack than solid

wood or plywood of the same species due to the network of internal voids. These networks become more prevalent as the panel swells at high moisture contents. As a result, the surface area available for fungal colonization increases significantly, which then facilitates fungal attack throughout the panel. Wu and Lee (2002) found that the non-recoverable component of TS occurred with moisture content increases above 11 percent. Panels with moisture content between 11 and 23 percent experienced non-recoverable TS ranging from 1 to 20 percent which was associated with reductions in bending MOR ranging from 20 to 65 percent.

Research on connections as they relate to OSB degradation has been limited. Kent *et al.* (2004) investigated the effect of fungal decay by *Postia placenta* (brown rot) on properties of aspen OSB sheathing including weight loss, dowel bearing strength, and single fastener shear connection behavior. Weight loss of each OSB sample was determined using the oven-dry method. Dowel bearing was performed as a sub-sample analysis to test the national design specification for wood construction (NDS) yield models. Dowel bearing and single fastener shear connections, which were evaluated parallel to the strong axis of the panel, were sensitive to small initial weight losses. A weight loss of five percent was associated with reductions in mean dowel bearing strength and single fastener shear connections of 15 and 18 percent, respectively. Fungal growth was observed in the network of internal voids throughout the thickness of the samples. Kent *et al.* (2005) also researched the effects of decay on cyclic properties of nailed connections. Nail fatigue and nail withdrawal failure modes

were common in connections with none to moderate decay, whereas an OSB sheathing failure mode occurred in the more heavily decayed connections.

2.2 LAMINATED VENEER LUMBER

Laminated veneer lumber (LVL) was developed in the 1970s. One advantage of LVL is that it can be manufactured to nearly any size, and thus is only restricted by transportation. Compared with similar size solid-sawn lumber, structural composite lumber (SCL) often provides a more reliable structural member that can often span greater distances and with less dimensional change (Bergman *et al.* 2010). For this reason, LVL is the primary flange material in I-joist manufacture (Bowyer *et al.* 2003).

The use of LVL in outdoor applications is limited by several durability issues including dimensional stability and biological degradation (Nzokou *et al.* 2005). Nzokou *et al.* (2005) found that the durability of LVL manufactured with non-decay resistant species was improved with the addition of decay resistant species for both face veneers and one core veneer. Douglas-fir is a moderately durable wood species and is often used in LVL. Long-term outdoor exposure tests of LVL showed that modulus of elasticity (MOE) decreased linearly to about 77 percent over a six year period in Tsukuba, Ibaraki Prefecture, Japan (Hayashi *et al.* 2002).

Yang *et al.* (2001) examined weight losses of OSB, southern yellow pine LVL composites, and solid wood exposed to the brown rot fungus *Gloeophyllum trabeum* and the white rot fungus *Trametes versicolor*. The brown rot fungus degraded the solid

wood samples approximately three times faster than the LVL over a 12-week exposure, whereas the degradation rate caused by the white rot fungus was the same for the composite and solid wood samples. LVL samples exposed to the brown rot fungus had a four-week delay prior to experiencing any significant weight loss. No delay was observed for either the solid wood or LVL samples exposed to the white rot fungus.

2.3 I-JOISTS

The average tree size has been decreasing as forest resources have changed with time, causing wood quality to also change. This has created a demand for products that can fulfill the needs of long span loads while offering a competitive price in the building market. I-joists have found a home in this market with their unique ability to compete with, and many times outperform, traditional solid sawn lumber.

The development of I-joists has a disjointed history, including numerous experiments on strength, stiffness, composite structural shapes, adhesives, assembly methods, and moisture effects. Composite I-joists have been in use since as early as the 1920s, where I-sections were used in aeronautics technology with wooden woodcraft assemblies (Robins 1975). By the mid-1930s, composite I-joists with hardboard webs were used in various structures in Europe (McNatt 1980). Researchers at the U.S. Forest Products Laboratory studied web buckling in composite assemblies and found that I-shaped sections were very efficient (Lewis and Dawley 1943). Combining lumber and plywood into beams with an I-section design provided a high

degree of structural efficiency by placing more appropriate material in the flange where high-strength demands occurred and less material in the web where low-strength demands were present. Other research concluded that the flexural stiffness of I-joists equaled that of solid wood beams of an equal weight (Lehmann 1973). Jokerst (1981) found that strength losses caused by the joint of an I-joist had less effect on flange material as compared to the presence of a knot or knothole. Polocoser *et al.* (2012) studied the effects of circular cut-outs of web material of I-joists at $L/10$ from the support and evaluated remediation techniques. The manufacturer hole charts do not permit modification at this location. Polocoser *et al.* (2012) concluded that holes in this zone were associated with significant reductions in I-joist flexural capacity, but an OSB collar patch could restore ultimate capacity statistically equivalent to the condition of “No Hole” 80 percent of the time.

Decades of research have shown the utility of I-joists, but these products were not competitive until the early 1970's when technology and facilities developed that allowed for mass production of prefabricated wood composite I-joists (Leichti *et al.* 1990). In their early stages of mass production, I-joists were most commonly found in roof support beams, but have since been used for floor joists, garage door headers and other framing mechanisms (McNatt 1980). I-joists are designed for long span loading and are used as an alternative to sawn lumber. In many cases, I-joists have superior performance as compared with solid sawn lumber, and for this reason, have become a popular choice for builders.

I-joists have become important components in both residential and low rise commercial buildings. I-joists can be constructed using a number of materials including solid sawn or structural composite lumber (SCL) for the flange and plywood or oriented strand board for the web. The advantages of these products include more uniform material properties, the ability to use smaller diameter timber in manufacturing and, because they are dry when installed, a reduced tendency to shrink or deform during use.

Like nearly all wood-based composites, I-joists are intended for dry use applications because water absorption can lead to swelling, deformation, and losses in material properties. These environments expose many engineered wood materials that are already sensitive to decay and moisture uptake to conditions above their acceptable limits (Baileys *et al.* 2003). Manufacturers make efforts to protect I-joists from wetting and caution users to do the same, but there is little in the way of guidance concerning how much wetting can take place before adverse effects occur.

Limited work has been done on the effects of moisture and creep on the functioning of I-joists. Chen *et al.* (1989) evaluated the flexural performance of I-joists under three short-term environmental conditions and found that high moisture contents (MC) decreased the load-deflection ratio for OSB and plywood webbed beams as well as decreasing the ultimate load capacity. Chen *et al.* (1989) also found that MC had a non-linear load-deflection function.

2.4 SHEAR WALLS

Shear walls are a primary element of the lateral force resisting system responsible for transferring lateral loads caused by wind and seismic events. Shear wall behavior is often considered analogous to a deep cantilever beam with the end framing members acting as “chords” to resist overturning moment forces and the panels acting as a “web” to resist shear (Johnson 1997). Shear walls rely upon the rigidity of sheathing to minimize deflections. Lateral forces are primarily resisted by sheathing and transferred to framing members via nailed connections, which are then transferred to the foundation. This system relies on properly designed connections between sheathing and framing members to provide anchorage to the foundation. Connections near the perimeter have been found to be the largest contributor to strength and stiffness (McCutcheon 1985, Johnson 1997, Durham *et al.* 2001, van de Lindt 2004, Sinha and Gupta 2009). Exterior shear wall designs containing openings for doors and windows traditionally involve the use of multiple shear wall segments. The design capacity of shear walls is assumed to equal the sum of capacities for each shear wall segment. Sheathing above and below openings is not considered to contribute to the overall shear wall performance (NDS 2012). Openings disrupt sheathing continuity and have been found to be vulnerable to moisture intrusion (Nanami *et al.* 2000).

The effects of moisture intrusion and subsequent fungal decay are perhaps two of the greatest unknowns in the overall performance of wood structures. Careful

decisions in design, construction, and maintenance are critical for shielding a building envelope from moisture intrusion. Proper rainwater management in building construction includes four basic principles: deflection of water away from the building envelope, drainage of water that does not penetrate the cladding, drying of the wall cavity, and the use of durable materials in areas where exposure to moisture cannot be avoided (Hazleden and Morris 1999). This approach is effective against moisture related degradation when these principles are used in conjunction with proper maintenance. However, architectural vision often abandons these ideas, creating opportunity for moisture intrusion. An example would be the West Coast style house which uses complex roof lines and short eaves for aesthetic appeal. This style depends on sealants around perforations in the building envelope rather than roof overhangs to direct rain away from the structure. This style has become popular throughout portions of North America, even in areas with harsh climates that include wind driven rain.

In recent decades, the push for energy efficient structures has also created changes in building practice that altered moisture levels in structures (Smulski 2000). New construction makes use of house wrap or building paper and insulation under exterior cladding. As a result, building envelopes are much tighter, restricting air flow through the exterior wall cavity. The lack of air flow limits drying, providing an opportunity for moisture to accumulate and for decay fungi to become established and may lead to significant structural damage (Smulski 2000).

The use of durable materials becomes a premium in locations susceptible to moisture intrusion and is perhaps one of the most important properties in housing construction (Norita *et al.* 2008). Many studies focused on estimating how long wood-based composites maintain their required performance under actual environmental conditions. Long-term tests are useful in evaluating the durability of these products. Several studies have been conducted with a variety of wood-based panels, laminates, and connections (Hayashi *et al.* 2002, Wu 2002, Kent *et al.* 2004, Hayashi *et al.* 2005, Kent *et al.* 2005, Kojima *et al.* 2011). These studies help enhance our understanding of wood-based composite performance and give us a better grasp on the service life of these materials. However, these studies alone do not give a complete picture of wetting and fungal effects on material properties of combined wood composite interfaces such as I-joists and shear walls. This provides a great opportunity for further research.

2.5 LITERATURE CITED

- Garay M, Marie R, Poblete W, Karsulovic C, Tomás J (2009) Evaluation of oriented strandboard and plywood subjected to severe relative humidity and temperature conditions. *Forest Products Journal* 59(3): 84-90.
- Haataja BA, Laks PE (1995) Properties of flakeboard made from northern white-cedar. *Forest Products Journal* 45(1): 68-70.
- Hayashi T, Miyatake A, Harada M (2002) Outdoor exposure tests of structural laminated veneer lumber I: evaluation of the physical properties after six years. *Journal of Wood Science* 48(1): 69-74.
- Hayashi T, Miyatake A, Fu F, Kato H, Karube M, Harada M (2005) Outdoor exposure tests of structural laminated veneer lumber (II): evaluation of the strength properties after nine years. *Journal of Wood Science* 51(5): 486-491.

- Hazleden D, Morris P (1999) Designing for durable wood construction: the 4 D's. Durability of Building Materials and Components 8, Volume 2. Institute for Research in Construction, Ottawa, ON. 734-745.
- Johnson AC (1997) Monotonic and cyclic performance of long shear walls with openings MS thesis, Virginia Polytechnic Institute and State University, Blacksburg, VA.
- Jokerst R W (1981) Finger-Jointed Wood Products (No. FSRP-FPL-382). Forest Products Lab, Madison, WI. 24 pp.
- Kent SM, Leichti RJ, Rosowsky DV, Morrell JJ (2004) Effects of decay by *Postia placenta* on the lateral capacity of nailed oriented strandboard sheathing and Douglas-fir framing members. Wood and Fiber Science 36: 560-572.
- Kent SM, Leichti RJ, Rosowsky DV, Morrell JJ (2005) Effects of decay on cyclic properties of nailed connections. Journal of Materials in Civil Engineering 17(5): 579-585.
- Kojima Y, Shimoda T, Suzuki S (2011) Evaluation of the weathering intensity of wood-based panels under outdoor exposure. Journal of Wood Science 57(5): 408-414.
- Leichti RJ, Falk RH, Laufenberg TL (1990) Prefabricated wood composite I-joists: a literature review. Wood and Fiber Science 22(1): 62-79.
- Lin CH, Yang TH, Lai WJ, Lin FC (2013) Anisotropic Physical and Mechanical Performance of PF-impregnated Oriented Strand Board. BioResources, 8(2): 1933-1945
- Liu JY, McNatt JD (1991) Thickness swelling and density variation in aspen flakeboards. Wood Science and Technology 25(1): 73-82.
- Mankowski ME, Morrell JJ (2000) Incidence of wood-destroying organisms in Oregon residential structures. Forest Products Journal 50(1): 49-52.
- Mai C, Kües U, Militz H (2004) Biotechnology in the wood industry. Applied Microbiology and Biotechnology 63(5): 477-494.
- Meyer RW (1982) Structural use of wood in adverse environments, Van Nostrand Reinhold, NY, 510 pp.
- Morrell JJ (2002) Wood-based building components: what have we learned? International Biodeterioration & Biodegradation 49(4): 253-258.

- Nanami N, Shibusawa T, Sato M, Arima T, Kawai M (2000) Durability assessment of wood-framed walls and mechanical properties of plywood in use. 6-5-3. In: Proc. World Conference on Timber Engineering. July 31-August 3, Whistler, British Columbia. University of British Columbia, Vancouver, British Columbia. 9 pp.
- NDS (2012). National design specification for wood construction. American Forest and Paper Association Inc, Washington, DC.
- Okkonen EA, River BH (1996) Outdoor aging of wood-based panels and correlation with laboratory aging: Part 2. *Forest Products Journal* 46(3): 68-74.
- River BH (1994) Outdoor aging of wood-based panels and correlation with laboratory aging. *Forest Products Journal* 44(11/12): 55-65.
- Sanchez-Silva M, Rosowsky DV (2008) Biodeterioration of Construction Materials: State of the Art and Future Challenges. *Journal of Materials in Civil Engineering* 20(5): 352–365.
- Schmidt E, Hall H, Gertjeansen R, Carll C, DeGroot R (1983) Biodeterioration and strength reductions in preservative treated aspen waferboard. *Forest Products Journal* 33(11/12): 45-53.
- Smulski S (2000) Durability of energy-efficient wood-frame houses. 4-2-4. In: Proc. World Conference on Timber Engineering. Jul 31-Aug 3, Whistler, British Columbia. University of British Columbia, Vancouver, British Columbia. 8 pp.
- Suchsland O, Hong X (1991) Model analysis of flakeboard variables. *Forest Products Journal* 41(11-12): 55-60.
- Wu Q, Suchsland O (1997) Effect of moisture on the flexural properties of commercial oriented strandboards. *Wood and Fiber Science* 29(1): 47-57.
- Wu Q, Lee JN (2002) Thickness swelling of oriented strandboard under long-term cyclic humidity exposure condition. *Wood and Fiber Science* 34(1): 125-139.
- Yang V, Illman B, Ferge L, Ross R (2001) Wood-based composites exposed to fungal degradation: laboratory results. IRG/WP 01- 40215. In: Proc. 32nd Annual Meeting International Research Group on Wood Preservation. May 20-25, Nara, Japan. International Research Group on Wood Preservation. 5 pp.

MANUSCRIPT

3. EFFECTS OF OUTDOOR EXPOSURE ON PROPERTIES OF I-JOISTS

David King, Jeffery J. Morrell, Arijit Sinha

Society of Wood and Technology
Wood and Fiber Science Journal

Society of Wood Science and Technology
P.O. Box 6155
Monona, WI 53716-6155

Summited 2014

3.1 ABSTRACT

Wood I-joists are important components for floor systems. These materials are often left uncovered and exposed to the weather during construction. Since the oriented strand board (OSB) and laminated veneer lumber (LVL) in these systems can be adversely affected by water absorption, manufacturers typically specify that these materials be protected from wetting. This can be difficult in wetter climates such as those in the Pacific Northwest. Determining the effects of exterior exposure and the results of wetting on mechanical properties of I-joists could help encourage builders to better protect these materials during construction. The flexural properties and ultimate tensile strength of I-joists exposed to the weather for extended periods of time were studied by exposure of I-joists on elevated racks during the rainy winter months in the Willamette Valley of Western Oregon. Sets of eight to ten I-joists were removed from the field each month, dried, and then tested in static bending (flexure) using a six-point bending test. I-joist strength decreased as a function of exposure time and rainfall. Twenty-seven days of external exposure was associated with a significant increase in flexural variability. Further exposure was associated with significant decreases in I-joist strength (MOR). Changes in exposure time, rainfall, and rain days were regressed against maximum load or deflection at maximum load. While most I-joists never experience this degree of wetting, they can when construction is delayed. The results illustrate the detrimental effects of exposure to wetting during construction and support improved efforts to limit wetting.

3.2 KEYWORDS

Weathering; wetting; outdoor exposure; degradation; oriented strand board; laminated veneer lumber; engineered wood

3.3 INTRODUCTION

Wood composite I-joists were first designed for and used in aircraft during the 1920s (Robins 1975). By the mid-1930s, composite I-joists with hardboard webs were used in various structures in Europe (McNatt 1980). I-joists became more widely used in the early 1970's, when technology and facilities were developed to allow mass production of prefabricated I-joists (Leichti *et al.* 1990). I-joists were most commonly found as roof support beams, but have since been used for floor joists, garage door headers and other framing applications (McNatt 1980). I-joists are designed for long span loading and are used as an alternative to sawn lumber. In many cases, I-joists have superior properties and low variability when compared with solid sawn lumber and, for this reason, have become a popular choice for builders. The advantages of these products include more uniform material properties, the ability to use smaller diameter timber in manufacturing and, because they are dry when installed, a reduced tendency to shrink or deform during use. Like nearly all wood based composites, I-joists are intended for dry use applications because water absorption can lead to swelling, deformation, and losses in material properties. Manufacturers make efforts to protect I-joists from wetting and caution users to do the same, but there is little in the

way of guidance concerning how much wetting can take place before adverse effects occur.

The most common materials used in I-joist assemblies are laminated veneer lumber (LVL) and oriented strand board (OSB). The use of LVL in outdoor applications is limited by several durability issues, such as dimensional stability and biological degradation (Nzokou *et al.* 2005). Long term outdoor exposures of LVL in Japan showed that modulus of elasticity (MOE) decreased 23% over a six year period (Hayashi *et al.* 2002). The durability of wood-based panels is one of the most important properties considered in housing construction (Norita *et al.* 2008), thus many studies have been done involving moisture effects on OSB (Lehmann 1978, River 1994, Okkonen and River 1996, Wu and Suchsland 1997, Norita *et al.* 2008, Kojima and Suzuki 2011, Meza *et al.* 2013). Kojima and Suzuki (2011) found that aspen OSB retained only 35% of its original modulus of rupture (MOR) after one year of outdoor exposure in Shizuoka Japan. On the other hand, Meza *et al.* (2013) observed a 30% decrease in MOR of aspen OSB after 100 days of exposure in similar weather conditions encountered in this study. Very little has been done to study the effects of wetting on I-joists. Chen *et al.* (1989) tested I-joists in a wetted state and found that moisture produced a non-linear load deflection function. High moisture levels decreased the load deflection ratio for OSB and plywood webbed beams and reduced ultimate load capacity.

While builders generally attempt to finish construction as quickly as possible, delays can be critical when I-joists are installed during rainy periods. In this study, we examined the effects of 138 days of exterior exposure of I-joists on moisture uptake, flexural properties and ultimate tensile strength.

3.4 MATERIALS AND METHODS

Specimens

I-joists in this study were 406 mm deep by 2.59 m long and consisted of 59 mm wide by 35 mm deep Douglas-fir laminated veneer lumber flanges and a 10 mm thick aspen oriented strand board web. I-joists were stored outdoors under cover for one year prior to exposure. While changes in relative humidity could have affected strength and stiffness properties as compared to the fresh condition, the I-joists could still be used to assess the effects of external exposure on properties. Although ASTM Standard E105 and Section 3.3 of ASTM Standard D2915-10 call for 20-30 replicates per variable in order to delineate treatment differences, only eight to ten units were tested during each interval due to limited quantities of I-joist stock (ASTM, 2010a, b).

I-joists were cut to 2.59 m in length which allowed for short span bending tests. The web and flanges of each I-joist had web-to-web and flange-to-flange finger joints at 1220 mm on center. The finger joints of the web and the flanges alternated at 610 mm on center. A set of smaller I-joists (356 mm deep) were also tested and produced similar results in comparison to the large I-joists (Appendix E).

Exposure

I-joists were weighed before being exposed at an open field located near Corvallis, Oregon. The site receives approximately 1.2 m of rainfall per year, mostly between November and May. Each I-Joist was weighed (nearest g) before being exposed on a test fence (two 3.6 m long boards) that suspended the units approximately 450 mm above ground where they were exposed to regular rainfall over a 138-day period. Rainfall data were collected from the Oregon State University Hyslop Farm, located approximately 5 km from the test site.

Eight to ten I-joists were removed after 0, 27, 65, 95, or 138 days of exposure. Eight units were initially tested, but the sample size was increased as the test proceeded and individual unit variation began to increase.

Units removed from exposure were immediately weighed and then conditioned to approximately 12% moisture content. Uniformity in moisture content allowed for characterization of permanent degradation that resulted from exposure by separating the reversible effects of moisture from the irreversible ones. The differences between initial and final mass were used to calculate moisture content.

Test setup

I-joists were evaluated in a bending test similar to that described by Polocoser *et al.* (2013) (Fig. 3-1). Briefly, web stiffeners were attached at the ends of each unit before the I-joist was placed on an apparatus that applied loads at four equal points

along the top flange, spaced at a distance of $2L/10$, where L is the span length. Web stiffeners were 50 x 100 mm wide lumber pieces that spanned the distance between the flanges. Typically a 3 – point bending test is used in flexural analysis because it creates the largest moment. Section 6.2.6 of ASTM Standard D5055 requires a 3 – or 4 – point bending test (ASTM, 2013). The test set-up in this experiment used a 6 – point bending test to represent a distributed load since this is the most common loading in real-world I-joist applications. The advantages of a 6 – point bending test include constant values of shear between loading points and increased lateral restraint due to shorter buckling lengths. The set-up was designed for short span testing that forced shear failures through the web as opposed to bending failures that are more common in long span testing. Lateral bracing was used to keep the I-joist from bending out of plane. Load cells under the bearing plates transmitted data to a computer software package designed by National Instruments named LabView 2010 as two hydraulic cylinders applied force. A linear variable differential transformer (LVDT) was positioned at mid span on the top flange to collect deflection data. Each I-joist was loaded at a rate of 5 mm/minute. Load and deflection were continuously monitored and these values were used to determine the maximum load and mode of failure.

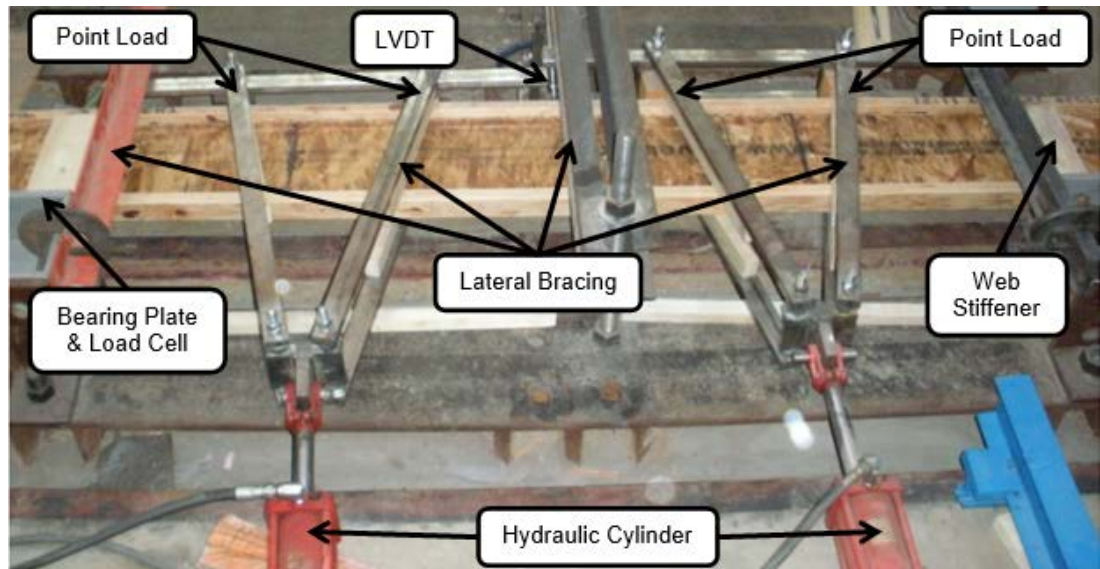


Fig. 3-1. I-joist bending test setup

Failure mode was classified in accordance with failure codes listed in ASTM Standard D5055-13. Additionally, a 150 mm long sample was cut from a site away from the failure area to be tested in tension. Clamps were attached to each flange of this sample and the top clamp was pulled at a rate of 5 mm/minute until the I-joist failed. Load and deflection were continuously recorded to determine tensile strength. The failure zone was then examined to determine if the failure occurred in the wood or the resin.

Statistics

The data were subjected to an analysis of variance ($\alpha = 0.05$) and individual treatments were then compared using unpaired t-tests at $\alpha = 0.05$. Assumptions of the regression, such as normality and homogeneity of variance, were evaluated using Shapiro-Wilk and Levene's tests, respectively (Ramsey and Schafer, 2002). Linear

regression models were developed for the I-joist data comparing maximum load and deflection at maximum load versus exposure time, rainfall, and rain days. Best fit models were determined using backwards stepwise selection and evaluating extra sum of square F test at each level.

3.5 RESULTS AND DISCUSSION

Rainfall and moisture content

I-joists were exposed to 85 days of measureable rainfall over the 138 day test period. Most rainfall events were small (<10 mm); however, two events in the first 27 days delivered 40 mm and 101 mm of precipitation, respectively (Fig. 3-2). Six rainfall events over the remainder of the exposure delivered 20 to 40 mm of rainfall. The samples were subjected to repeated wetting with limited opportunities for drying. Moisture contents of the I-joists increased steadily from 12% to approximately 50% within the first 27 days of exposure and then increased only slightly thereafter. As we had a limited number of test pieces, it was not possible to destructively sample units to determine moisture distribution in the web and flange, but the data show that one month of rainfall exposure resulted in dramatic increases in moisture content (Table 3-1).

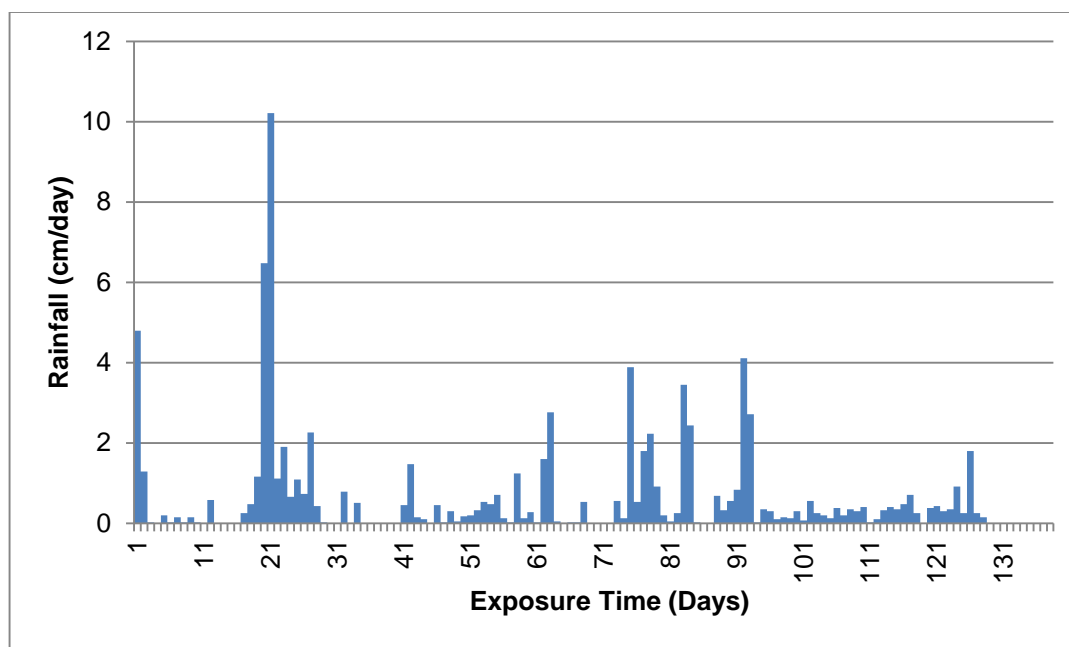


Fig. 3-2. Daily rainfall amounts over the 138 day period when I-joists were exposed in Western Oregon

Table 3-1. Effect of exterior exposure on moisture content and physical properties of I-joists

I-Joist (type)	Exposure (days)	Replicates (n)	Statistics	Max Load (kN)	Deflection ^a (mm)	MC ^b (%)	Predominate Failure	Rainfall (cm)	Rain Days (days)
406.4 mm	Control	8	Mean	54.63	14.92	12.4	ZW	0.00	0
			SD ^c	2.92	1.48	0.5			
	27	8	Mean	53.29	12.99	49.7	ZJ	33.66	20
			SD	5.82	1.39	1.2			
	65	8	Mean	49.54	12.91	50.1	ZJ	47.12	48
			SD	5.87	2.28	2.3			
	95	8	Mean	45.03	12.91	51.7	WB	73.81	71
			SD	7.09	2.17	2.5			
	138	10	Mean	44.58	12.99	52.3	WB	85.19	104
			SD	5.75	1.18	2.4			

^a Deflection at maximum load ^b MC = moisture content measured directly after exposure ^c SD = standard deviation

Bending test

Bending tests showed that maximum load did not differ significantly between non-wetted samples and those exposed for 27 days: however, standard deviations (SD) increased sharply after exposure (Table 3-1). One of the attributes of I-joists is

material uniformity and these results show that even relatively short exposures increased variability. Continued exposure led to steadily lower maximum loads that were significantly lower than the controls after 65 days (t-test, p-value = 0.027) (Fig. 3-3). I-joists lost 9% of their original strength after 65 days of exposure and 18% strength after 138 days of exposure (Fig. 3-4). Centerline deflection decreased significantly for the I-joists, but only showed small changes in SD compared to the control (t-test, p-value < 0.05). Deflection decreased, but not significantly after 27, 65, 95, or 138 of exposure, and this suggests that the I-joists were becoming less stiff (Fig. 3-4). Similar results were obtained with smaller I-joists (356 mm deep) exposed under the same condition for 566 days (data not shown).

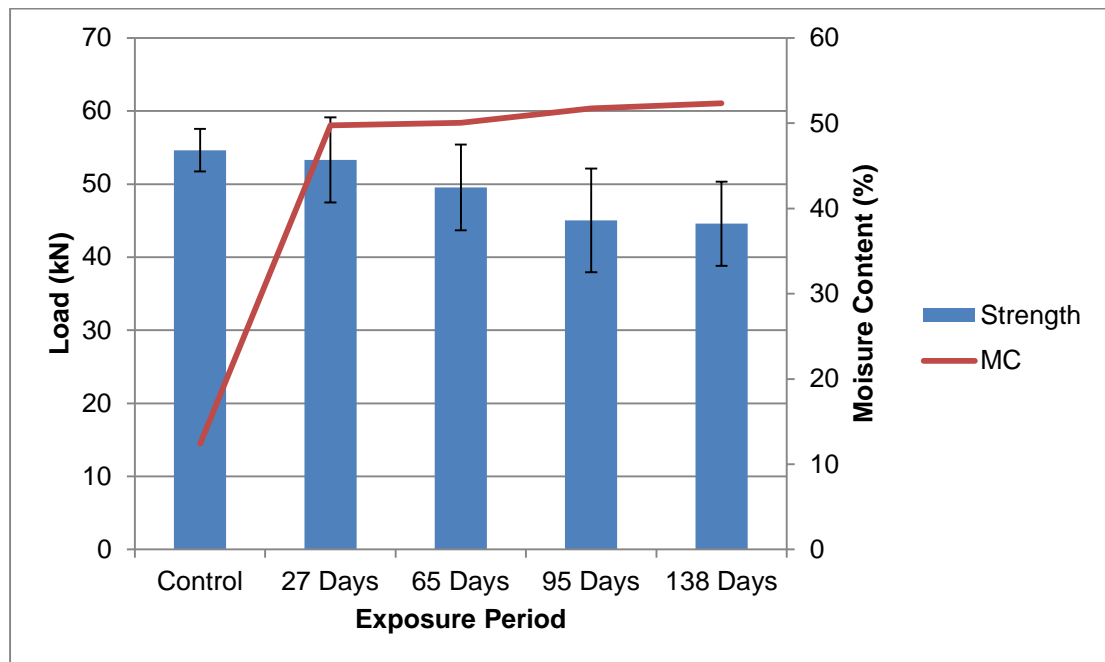


Fig. 3-3. Moisture content and maximum loads of I-joists exposed outdoors in an above ground test for 0 to 138 days in Western Oregon.

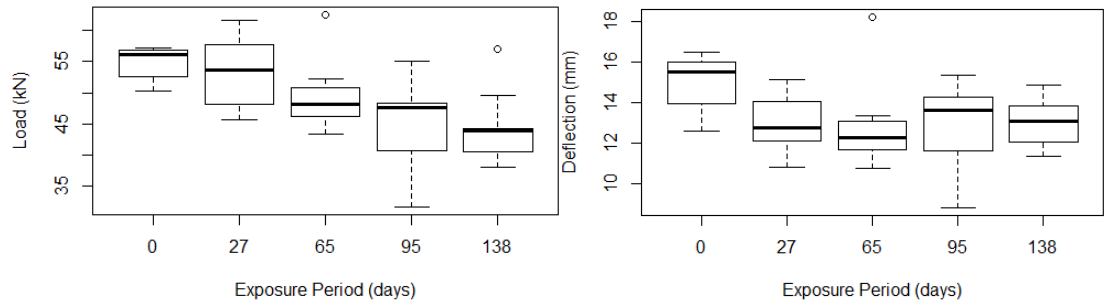


Fig. 3-4. Box and whisker plots of capacity (load) and deflection at maximum load of I-joists exposed to wetting over a 138 day period.

Regression

Two linear regression models were developed using maximum load or deflection at maximum load (dependent variables) and exposure time, total rainfall, and number of rain days (explanatory variables). The best fit models are presented below.

$$\text{Load} = 52.93 - 0.0870 \text{ Rainfall (kN)} \quad [1]$$

$$\text{Deflection} = 11.23 - 0.016 \text{ Rainfall (mm)} \quad [2]$$

There was significant evidence that I-joist maximum load was dependent on the amount of rainfall received during the exposure period (p-value = << 0.001). Deflection at maximum load as compared with rainfall performed the best as per extra sum of squares F-test and is presented as eq. [2]. There was significant evidence that I-joist deflection at maximum load was correlated with rainfall (p-value = 0.0018). Although, maximum load and deflection at maximum load were regressed against rainfall, exposure days, and rain days, the final model that explained most of the

variability in the data did not use exposure and rain day terms. Rainfall was highly correlated with exposure days and similarly, rain days are highly correlated with rainfall. Hence, only one of these variables was sufficient to capture the essence of variability in maximum load (or deflection) contained within the experimental data through a regression.

Bending test failure modes

In addition to declining maximum load, exterior exposure also affected the mode of failure. All units not exposed to wetting failed in shear, while failures were caused by a mix of shear, web buckling, and bond failure in samples exposed for 27 or 65 days. Web buckling became more frequent in samples exposed for 95 or 138 days. Wetting should induce swelling and permanent deformation and these effects are more likely to occur in the OSB web. The shift in failure mode supports the premise for a weakened web.

The failure codes used to define failures of I-joists are outlined in ASTM D5055-13 (ASTM, 2013). Shear failures can be classified as ZJ, ZW and IJ type failures. FTJ type failures are considered bond failures and can be classified as GB (good bond), PB (poor bond), or BB (bad bond), indicating how well the adhesive performed. Z type failures appeared in each group of I-joist tests, but became progressively less frequent as exposure increased.

Shear type failures occurred for the control I-joists. The most common failure mode for the control test was a ZW type failure in which the bottom flange at the end

of the beam developed a crack that propagated horizontally, and then ran through the web at an approximately 45 degree angle, then horizontally through the top flange (Fig. 3-5a). The other, less frequent, shear failure observed was a ZJ type failure (Fig. 3-5b). A ZJ failure is similar to the ZW failure except that the failure through the web follows the web – web finger joint vertically as opposed to the 45 degree angle. Polocoser *et al.* (2013) also found that the most frequent failure in short span bending tests were of the Z type classification.

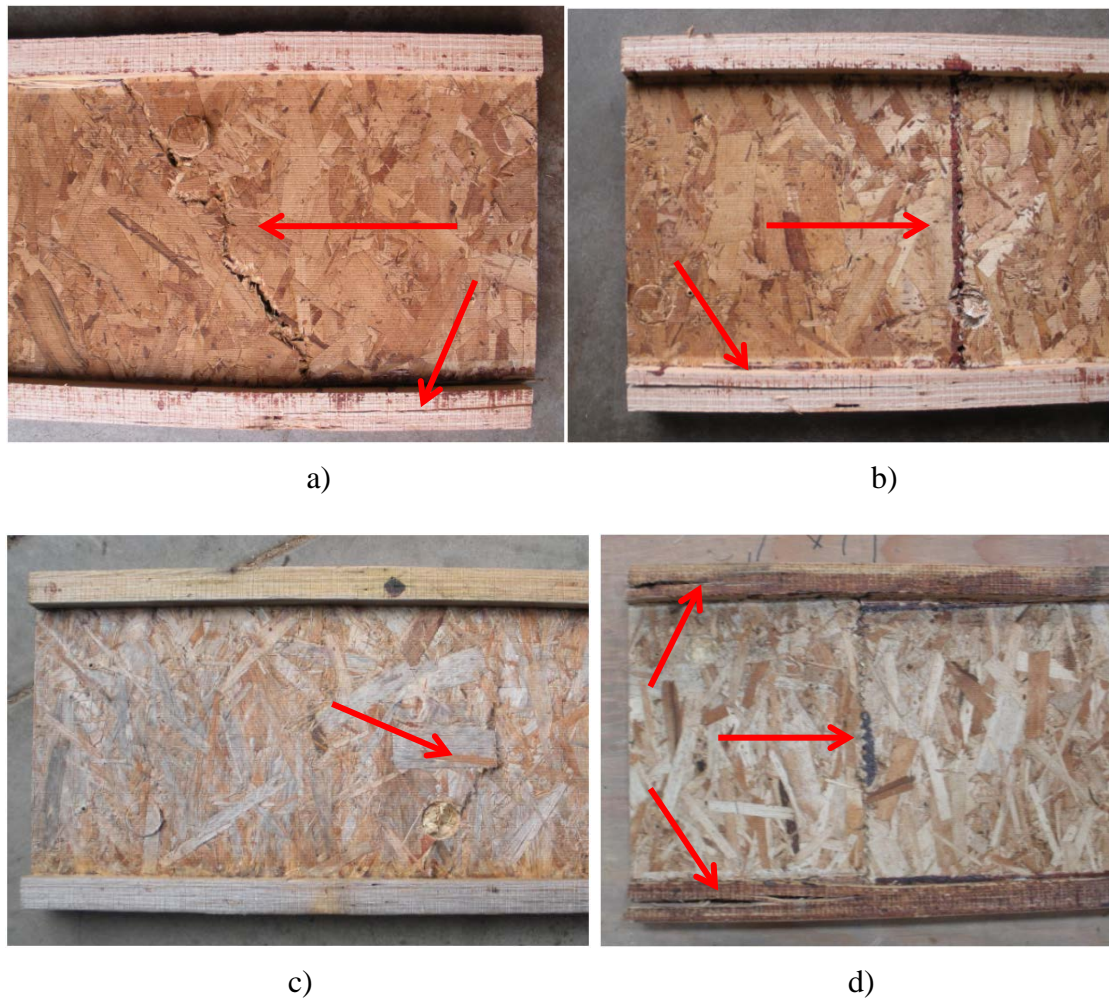


Fig. 3-5. Various failure modes of I-joist: a) ZW, b) ZJ, c) WB, and d) IJ

I-joist failure modes began to diversify after 27 days of exposure. The most frequent failure mode was again the Z type failure, but FTJ and WB type failures were also observed. Z type failures accounted for fifty percent of the failures observed. The FTJ failures occurred in the middle section of the I-joists with seventy to one-hundred percent wood failure along the glue joint. Another, less frequent, failure mode for the 27 day exposure samples was web buckling classified as WB (Fig. 3-5c). Web buckling was caused by a weakened web due to moisture swelling of the OSB. Web buckling after exposure to moisture is consistent with findings by Chang *et al.* (1989), although those I-joists were tested at much higher moisture contents.

The failure modes for the 65 day exposure period were again composed of ZJ, FTJ, and WB failure types with the dominate failure mode being Z type failures (sixty-three percent of failures). FTJ type failures were the second most frequent mode while WB type failures were least frequent. The FTJ type failures had seventy to one-hundred percent wood failure along the glue joint.

I-joists exposed for 95 and 138 days primarily experienced WB type failures and some Z type failures. The increase in WB type failures further supports the notion of a weakened web due to OSB swelling. An IJ type failure occurred in the 95 day exposure test (Fig. 3-5d). IJ failures were in the Z type failure class, but had a horizontal flange-web joint failure that extended both ways from the web-web failure

line. Both the 95 and 138 day exposure tests had WB type failures that accounted for sixty-three percent of the failures.

Tension test failure modes

Tension tests on sections removed from the I-joists showed that rainfall exposure had no negative effect on ultimate load nor did it alter the location of the failure (Fig. 3-6). These results appear to be at odds with the bending test results. The moisture induced changes primarily occurred in the web and away from the joint. The bottom flange should be most affected by this effect since water can collect at this location, resulting in greater moisture uptake in the OSB. This should lead to increased swelling and greater effects on the OSB/flange bond. The data do not support this process and suggest that the web/flange bond was less affected by wetting than the OSB. Results suggest that I-joists could be made more weather resistant by using more moisture resistance OSB, such as the materials offered for sub-flooring; however, the best practice would still be to protect these materials from wetting during storage and to cover them as soon as possible when they are installed in a structure.

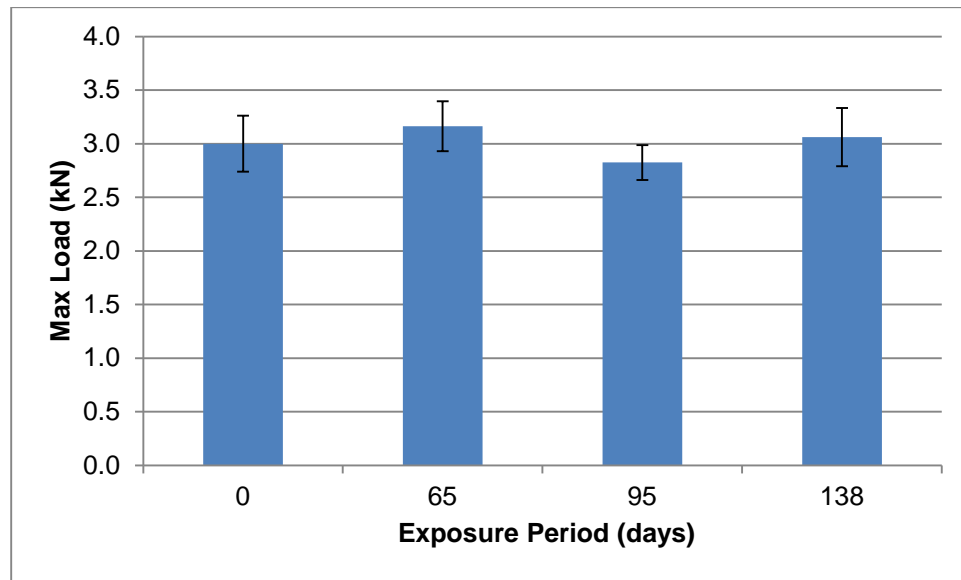


Fig. 3-6. Maximum load in tension of sections cut from I-joists exposed for 0 to 138 days outdoors in an above ground test in Western Oregon

3.6 CONCLUSIONS

I-joists exposed outdoors during the winter in Western Oregon experienced increased moisture contents coupled with losses in flexural properties over the test period. Variance in flexural strength nearly doubled after 27 days of exposure. One of the main advantages of I-joists is uniformity in properties and the data show the drastic effect wetting can have on this attribute in a very short time. The effects of exterior exposure on flexural properties were significant after 65 days of exposure. Progressive changes in failure mode supported the view that swelling of the OSB web due to wetting was the primary cause of strength loss. Exterior exposure had no negative effect on tension properties. The results illustrate the negative effects

associated with wetting of I-joists and demonstrate why these materials need to be protected from moisture.

3.7 REFERENCES

- ASTM (2010a) D2915. Standard practice for sampling and data-analysis for structural wood and wood-based products. American Society for Testing and Materials, West Conshohocken, PA.
- ASTM (2010b) E105. Standard practice for probability sampling of material. American Society for Testing and Materials, West Conshohocken, PA.
- ASTM (2013) D5055. Standard specification for establishing and monitoring structural capacities of prefabricated wood I-joists. American Society for Testing and Materials, West Conshohocken, PA.
- Chen GH, Tang RC, Price EW (1989) Effect of environmental conditions on the flexural properties of wood composite I-beams and lumber. *Forest Products Journal* 39(2): 17-22.
- Hayashi T, Miyatake A, Harada M (2002) Outdoor exposure tests of structural laminated veneer lumber I: evaluation of the physical properties after six years. *Journal of Wood Science* 48(1): 69-74.
- Kojima Y, Suzuki S (2011) Evaluation of wood-based panel durability using bending properties after accelerated aging treatments. *Journal of Wood Science* 57(2): 126-133.
- Lehmann WF (1978) Cyclic moisture conditions and their effect on strength and stability of structural flakeboards [wood-base composite panels]. *Forest Products Journal* 28(6): 23-31.
- Leichti RJ, Falk RH, Laufenberg TL (1990) Prefabricated wood composite I-beams: a literature review. *Wood and Fiber Science* 22(1): 62-79.
- Meza L, Sinha A, Morrell JJ (2013) Effect of wetting during construction on properties of Douglas-fir plywood and oriented strandboard flooring. *Forest Products Journal* 63(5/6):199-201.
- McNatt JD (1980) Hardboard-webbed beams: research and application. *Forest Products Journal* 30(10): 57-64.

- Norita H, Kojima Y, Suzuki S (2008) The aging effects of water immersion treatments in wet-bending for standardized testing of wood panels. *Journal of Wood Science* 54(2): 121-127.
- Nzokou P, Zyskowski J, Boury S, Kamdem DP (2005) Natural decay resistance of LVL made of veneers from durable and non-durable wood species. *Holz als Roh-und Werkstoff* 63(3): 173-178.
- Okkonen EA, River BH (1996) Outdoor aging of wood-based panels and correlation with laboratory aging: part 2. *Forest Products Journal* 46(3): 68-74.
- Polocoser T, Miller T, Gupta R (2013) Evaluation of remediation techniques for circular holes in the webs of wood I-joists. *Journal of Materials in Civil Engineering* 25(12): 1898–1909.
- Ramsey FL, Schafer DW (2002) *The statistical sleuth: a course in methods of data analysis*. Cengage Learning, Kentucky. 768 pp.
- River BH (1994) Outdoor aging of wood-based panels and correlation with laboratory aging. *Forest Products Journal* 44(11/12): 55-65.
- Robins JG (1975) *The wooden wonder: a short history of the wooden aeroplane*. J. Bartholomew and Sons Ltd., Edinburg. 55 pp.
- Wu Q, Suchsland O (1997) Effect of moisture on the flexural properties of commercial oriented strandboards. *Wood and Fiber Science* 29(1): 47-57.

MANUSCRIPT

**4. MOISTURE AND FUNGAL EFFECTS ON WOOD COMPOSITE
SHEAR WALLS**

David King, Jeffery J. Morrell, Arijit Sinha

Society of Wood and Technology
Wood and Fiber Science Journal

Society of Wood Science and Technology
P.O. Box 6155
Monona, WI 53716-6155

Summited 2014

4.1 ABSTRACT

Moisture intrusion can affect the performance of materials commonly used in shear wall construction. Weakened components could lead to shear wall failure in high wind or seismic events, resulting in structural collapse. This study investigates the effects of moisture exposure and fungal inoculate on small scale shear walls constructed with Douglas-fir studs and aspen oriented strand board sheeting. Shear walls were inoculated with *Postia placenta* (a brown rot decay fungi) and subjected to cyclic wetting over six incubation periods. Ultimate shear wall strength and stiffness were evaluated during shear wall loading. Wetting distributions were tracked and compared with changes in density. Shear wall capacity initially increased by 37% as the fasteners corroded, producing better withdrawal resistance. Moisture distributions tended to vary widely in the assemblies over time. Shear wall assemblies with visual decay developed strain concentrations at an early stage of loading and ultimately experienced reductions in capacity ranging from 13 to 61%. Small quantities of shear wall assemblies were colonized which limited the scope of conclusions that were drawn.

4.2 KEYWORDS

Biodegradation; wood decay; deterioration; brown rot; fungi; strength; mechanical properties; wetting; oriented strand board; engineered wood

4.3 INTRODUCTION

Wood is a primary building material for low rise structures in the United States. Wooden structures must be able to withstand forces from wind and seismic events throughout their lifespan; thus, lateral resistance is an important component in structural design. Most wooden structures utilize shear walls as the principal lateral force resisting system for these forces. Shear walls are typically made of 38 x 89 mm or 38 x 140mm (nominal 2x4 or 2x6) framing lumber and structural sheathing (oriented strand board or plywood) held together with dowel-type fasteners (nails, screws or staples). Shear walls experience large stress concentrations in the uplift corner during loading (Sinha and Gupta 2009); thus, nailed connections between framing and sheathing members have been determined to be the primary source of strength, stiffness, and energy dissipation in wind and seismic events (Polensek and Bastendorff 1987, Chui *et al* 1998). The push for energy efficient structures has created changes in building practice that altered moisture levels in structures. Building paper or house wrap is used in conjunction with siding to seal off cracks and create a nearly air tight building envelope. This limits the ability of moisture to escape from within the building, but problems can occur when moisture levels become excessive. Poor construction, roof deterioration, or plumbing problems can lead to significant moisture intrusion that may go unnoticed for months. This trapped moisture creates conditions conducive for colonization of decay fungi and may lead to significant

structural damage. Although wood composite shear wall behavior has been well documented (McCutcheon 1985, Johnson 1997, Durham *et al.* 2001, van de Lindt 2004, Sinha and Gupta 2009), there is little information on the effects of wetting and fungal decay.

Brown rot, white rot, and soft rot are wood degrading fungi classified by their effects on wood. White rot fungi generally consume all wood structural components at nearly the same rate they are degraded, while brown rot fungi consume the holocellulose and are considered the most destructive to wood structures because they depolymerize cellulose and hemicellulose faster than they are consumed. Structural lumber in the United States is primarily softwood and decay of softwoods in service is accomplished primarily by brown-rot fungi (Wilcox 1978). One of the most common problems in assessing wood decay is determining how much strength has been lost. Early stages of brown rot decay are associated with significant reductions in mechanical properties, but changes in observable physical properties are nearly undetectable (Clausen and Kartal 2003). For example, modulus of rupture of solid wood can decrease 13-50% with only 2% weight loss. (Wilcox 1978).

Connections are a very important part in structural behavior. Merrill and French (1964) studied the effect of nail head pull-through strength at various levels of fungal damage and found that a 12 – 15% weight loss caused an approximate 50% reduction in pull-through strength. Kent *et al.* (2004) found similar results as lateral

capacity of connections declined at an increasing rate after OSB sheathing weight loss exceeded 12%. Nailed OSB connections experience significant losses in tensile and compression properties over time when colonized by brown rot decay (Kent *et al.* 2005). Decay around connections could have a significant impact on shear wall behavior.

Moisture intrusion is a common problem for many structures. Decay fungi cannot survive without access to free water in wood cell lumens. Therefore, wood must retain moisture above the fiber saturation point prior to colonization. In this study, we investigated the effects of moisture and brown rot fungi (*Postia placenta*) on small-scale shear wall capacity over six incubation periods. The goal of this study was to gain a better understanding of decay fungi and shear wall interactions which will allow us to give inspectors better knowledge for proper damage assessment.

4.4 MATERIALS AND METHODS

Assemblies

The shear walls in this study were analyzed using procedures described in ASTM E564 – 06 (ASTM, 2012) except that the dimensions were reduced to square frames measuring 610 mm by 610 mm. The shear walls were made of 38 mm x 89 mm (2x4 nominal) select structural, kiln dried Douglas-fir lumber and 11mm thick exposure 1 aspen oriented strand board (OSB). Each shear wall consisted of one top

plate (610 mm long), one bottom plate (610 mm long), two studs (530 mm long), and a 610 mm by 610 mm OSB panel. Two 3 mm diameter holes were drilled at 15 mm edge spacing in each end of the top and bottom plate. The pre-drilled holes kept the ends of the lumber from splitting during frame assembly. Eight 90 mm x 3.3 mm full round head nails (Senco, Cincinnati, OH) were driven into the pre drilled holes in the top and bottom plate by hand to assemble the shear wall frame. The OSB was nailed to the shear wall frame with a pneumatic gun using 60 mm x 2.9 mm Senco full round head nails at 102 mm spacing which is common edge spacing in light frame construction (NDS, 2012). This spacing resulted in twenty-four sheathing nails per panel. Squares of building paper (610 mm by 610 mm) were fastened to the OSB on the sheathing side of each shear wall with 10 mm x 3 mm x 2 mm staples (Duo-Fast, Vernon Hills, IL). Clear polyethylene sheeting was used to cover the open side of each shear wall. The polyethylene sheeting acted as a vapor barrier, restricting evaporation but allowed for observation of the panel interior during incubation. Each sample was weighed after assembly. Ninety-six shear walls were constructed including eight dry controls, eight with the lower corner of OSB removed, 48 samples that were subjected to wetting only, and 48 samples that were subjected to both wetting and fungal inoculation.

Uplift corner

Shear walls are primarily designed to restrain shear, compression, and tensile forces. The most problematic location on wood frame constructed shear walls is the uplift corner. Shear wall damage can occur when air pressure below a roofing system is greater than the air pressure above the roofing system. The pressure directly above the surface of the roof decreases as wind flows over the structure. At the same time, internal air pressure increases due to air infiltration through openings, cracks, and other pathways. Vertical forces from the roof above are transferred through connections to the shear wall and create uplift. Cross wind and earthquakes also contribute to shear wall uplift. These lateral forces are transposed into vertical forces as the shear wall undergoes an overturning moment and causes uplift on one end of the wall and compression on the other. Large concentrated stresses occur around the connections in the uplift corner. The lumber, paneling, and fasteners must be able to carry these loads or the wall will tear apart.

The location of interest in this study was the uplift corner of the shear wall because this was where large stress concentrations would develop around the connections as shown by Sinha and Gupta (2009). The experimental design focused on wetting and decay development around the uplift corner. An irrigation system was designed to produce a wetting pattern in this part of the shear walls.

Treatments

The experiment was developed as a completely randomized design with incubation time at five different levels as the primary effect. Four different treatments were incorporated in this experiment (Fig. 4-1): 1) Assembly constructed and tested without exposure to water or fungi (dry control), 2) Assembly with the OSB in the uplift corner removed, tested without exposure to water or fungi (no corner control), 3) Assembly constructed and exposed to wetting prior to testing (wetting only), and 4) Assembly constructed and exposed to both fungi and wetting prior to testing (wetting and fungal exposure). The dry control shear walls represented a shear wall under normal loading conditions (no exposure to moisture) and served as a baseline for material properties. The no corner control treatment was similar to the dry control in that the walls were built and tested in a dry state. The OSB paneling (the $\frac{1}{4}$ corner) on the uplift corner of these assemblies was removed to simulate fungal decay in the panel that was so severe that this section did not contribute to the assembly properties. The no corner control treatment was compared with shear wall material properties on panels exposed to both wetting and fungal attack.

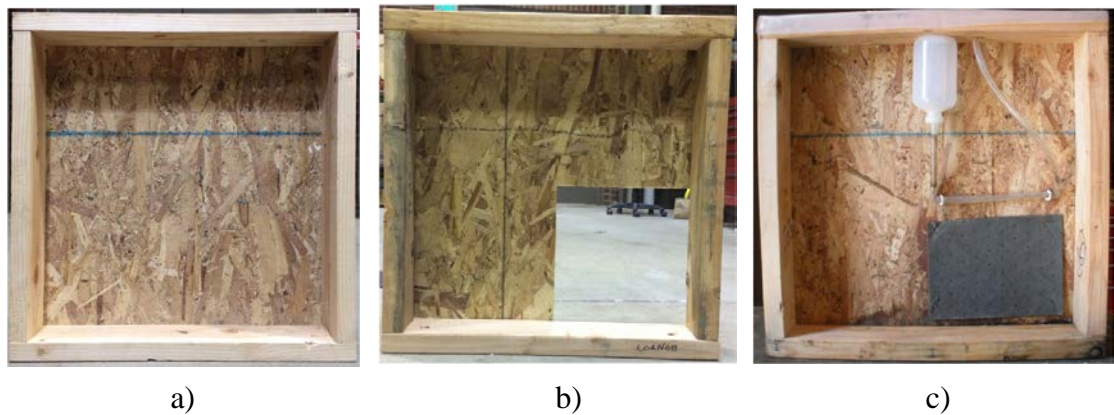


Fig. 4-1. Shear wall assembly configurations a) dry control, b) no corner control, c) wetting only or wetting and fungal exposure

The wetting only and wetting/fungal inoculated assemblies were placed on a three tiered rack in a conditioning room at 30° C and 90% relative humidity. Assemblies were exposed to cyclic wetting using an irrigation system. Fifty mL of water was added to the irrigation system every three days over the duration of the experiment to achieve target moisture content in the wetted zone of 60%. Randomly selected assemblies were weighed at the start and then at regular intervals to monitor moisture uptake. The wetted and wetted/fungal assemblies were separated from each other to reduce the chance of contamination. Each assembly was inoculated with a brown rot fungus nine days after the wetting pattern was established. The wetting only and wetting/fungal inoculated assemblies were incubated for 32, 112, 177, 234, 258, and 402 days.

Irrigation system

Fungal decay can begin when wood reaches the fiber saturation point (27-30% moisture content), but decay proceeds more quickly at moisture levels between 60 and 80%. A drip irrigation system, targeting the uplift corner of each shear wall, was installed on the OSB of each assembly to provide controlled wetting (Fig. 4-2). One 13 mm diameter hole was drilled in the top plate at mid span and a second 13 mm diameter hole was at a 50 mm offset from mid span. These holes provided fill and vent locations for the irrigation system. A 250mL bottle was attached to the bottom side of the top plate beneath the hole at mid span using screws and a 13 mm diameter hole was drilled into the bottom of the bottle. 13 mm diameter tubing was cut to size and fitted with elbows. There were three pieces of tubing used for each shear wall. The first piece of tubing was attached to the spout end of the 250mL bottle and ran vertically down to the center of the shear wall into the first elbow. The second piece of tubing was attached to the first elbow and ran horizontally to one edge of the shear wall into the second elbow. The third piece of tubing attached to the second elbow and ran diagonally before attaching to the vent hole in the top sill plate. The third piece of tubing acted as an air vent for the irrigation system and minimized air bubble build up in the tubing. An awl was used to poke five evenly spaced holes along the bottom edge of the second piece of tubing facing the OSB paneling so that the water exiting the tubing would contact the shear wall. The tubing was secured to the wall with two 44.5

mm x 9.5 mm x 3.8 mm diamond point staples. The staples wrapped around the horizontal piece of tubing near the elbows and were secured to the OSB using a hammer. A pneumatic staple gun was used to attach a 250 mm x 190 mm sheet of absorbent mat to the OSB directly beneath the irrigation system in the bottom right corner of each shear wall. The placement of the absorbent mat was designed to collect water as it dripped down the OSB, keeping water near the target area and supporting fungal growth.

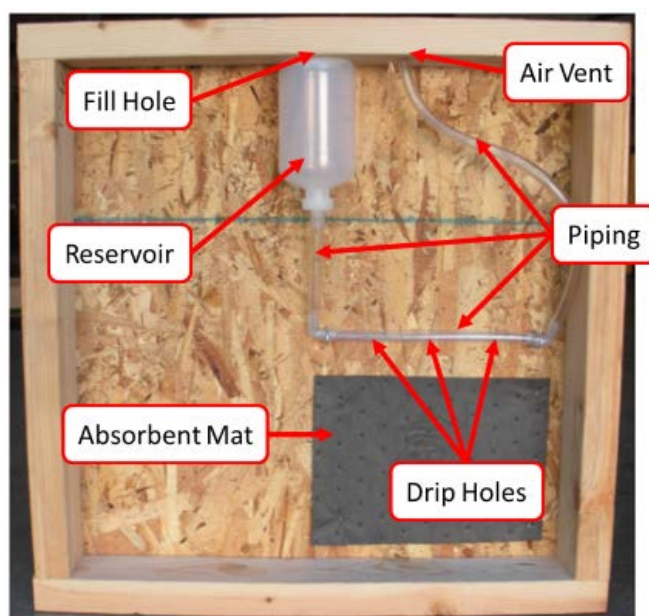


Fig. 4-2. Shear wall irrigation system

Inoculum

Postia placenta (Fries) M Larsen et Lombard (Isolate # Madison 698)

inoculum was prepared by inoculating 200 mL of 1% malt extract with an agar plug

cut from the edge an actively growing culture of the test fungus. The malt extract and inoculum were incubated for two weeks at 20-23° C. The resulting mycelium was then collected by filtration and suspended in deionized water. The mixture was then shredded in a blender for 20 seconds and collected in 50 mL test tubes. Shear wall inoculation was then performed by pouring 50 mL of the mixture into the irrigation system of each designated wetting/fungal inoculated assembly. Samples received fungal inoculation 9, 26, 31, 70, 76, 83, 122, 129, and 137 days after wetting began.

Moisture content mapping

At the end of each incubation time, sets of eight wetted and eight wetted/fungal inoculated shear walls were removed from the conditioning room. The walls were immediately weighed and then a series of measurements was taken with a resistance type moisture meter. Moisture meter readings were taken in a grid with 100 mm or 67 mm between each reading location. A total of 35 readings were taken per panel. The data were used to develop moisture content contour plots in SigmaPlot using a 5 by 7 grid pattern of the inner face of the OSB paneling. Wetting patterns varied between shear walls and a coding system was developed to characterize the patterns.

Shear wall tests

After moisture content mapping, the samples were air dried at an equilibrium moisture content of approximately 12%. Conditioning allowed for separation of the

effects of permanent degradation that resulted from the exposure and the reversible effects of moisture uptake. The dried samples were weighed and the building paper and polyethylene sheeting were removed from each shear wall. Digital image correlation was used as a supplemental part of the testing procedure and required that special steps be taken in preparing the outer OSB surface. The outer side of the OSB paneling of each sample was coated with black paint and then a paint gun was used to overlay a white speckle pattern on the surface. This speckle pattern was important for the image recognition in the digital image correlation software. Once the paint was dry, four 13 mm diameter holes (two in the top plate and two in the bottom plate) were drilled in the shear wall frames and the samples were secured with bolts to a computer-controlled hydraulic-actuated testing device (Fig. 4-3). The loading geometry and test set up incorporated a fixed platform and a kinetic swing arm actuated by a hydraulic ram that induced force on the top plate of each sample. The samples were loaded at a controlled rate of 5 mm per minute. The load cell on the hydraulic ram produced force outputs during the loading cycle. A linear variable differential transformer was used to measure relative deflection as each sample was loaded. Failure modes were documented as each sample was loaded until failure.

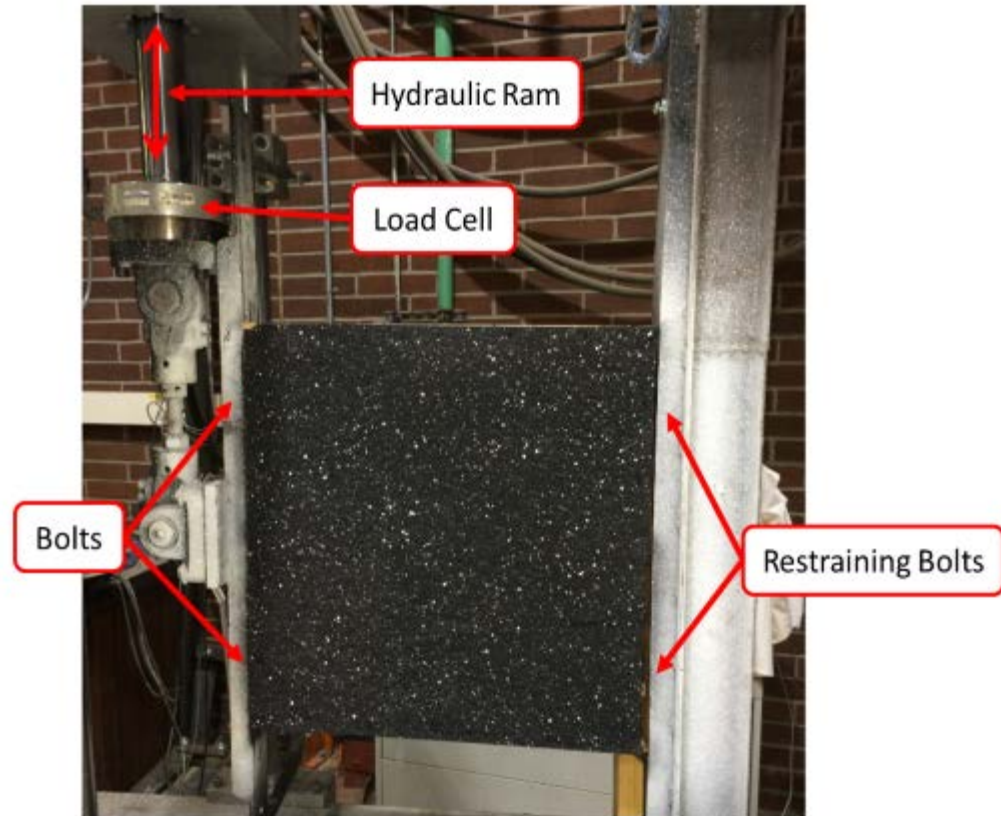


Fig. 4-3. Shear wall testing apparatus

Digital image correlation

A non-contact strain measurement system based on the principles of digital image correlation (DIC) was used to track surface deformation during loading. Two stereo-mounted cameras were focused on the assembly during testing. The cameras imaged the black and white speckle pattern to track speckle movement in space. These cameras first recorded a reference image and then a series of images were captured every second during testing. These data were used to create a three dimensional model

of pixel movement with respect to the reference image. An MTS 407 hydraulic controller was used in conjunction with the DIC software and each image was tagged with specific load and deflection data. The DIC software uses the cache of images and maps the surface of interest by correlating the movement of each pixel to calculate strain. Shear strain (ϵ_{xy}) is one of many outputs that can be extracted from the acquired data. Shear strain maps were produced from the DIC outputs and used to compare localized strains on each shear wall. DIC is only capable of making surface measurements, but the strain of the OSB was assumed to be representative of the strain through the thickness because of strain compatibility (Lookman, 2003).

Density mapping

It is difficult to determine spatial changes in panel integrity without testing numerous small samples. The Pilodyn has the potential to evaluate panel integrity indirectly and provides a simple, reproducible measurement of density. After the assemblies were loaded to failure, they were removed from the test set-up and a series of measurements was taken using a 70 mm – 18 Nm Pilodyn. The Pilodyn is a hand held, spring driven, pin penetrating device that uses penetration depth as an indirect measure of density that is useful in determining wood condition. Measurements were made at a much tighter spacing in a more focused area as compared to the moisture content maps in order to obtain a better representation of moisture effects in the uplift corner. Measurements were made every 60 mm apart in a 5 by 5 grid pattern in the

uplift corner of the assembly. These data were used to develop contour plots in SigmaPlot and the plots were compared with the moisture distribution data.

Culturing

The final step in this experiment was to determine if the fungus had successfully colonized the assembly. Three plugs were removed along the bottom edge of each OSB panel for culturing. The plugs were sterilized with an open flame to limit the presence of contaminating surface spores and placed in petri dishes containing malt benlate media. The petri dishes were incubated at room temperature for four weeks, and then examined for evidence of fungal growth. Any growth was examined under a light microscope for characteristics typical of *Postia placenta*.

Statistics

The data were subjected to an analysis of variance ($\alpha = 0.05$) and individual treatments were then compared using unpaired t-tests at $\alpha = 0.05$. Assumptions of the regression, such as normality and homogeneity of variance, were evaluated using Tukey's and Levene's tests, respectively (Ramsey and Schafer, 2002).

4.5 RESULTS AND DISCUSSION

Moisture content mapping

The moisture meter used for moisture content mapping had a range from 5-60% with an accuracy ranging from $\pm 0.25\%$ in the 5-12% moisture content range to $\pm 1\%$ in the 20-30% moisture content range. This moisture content range was useful since it covered the fiber saturation point (27-30%) and our target moisture content (60%). Six different wetting patterns were established by the drip system (Fig. 4-4): 1) Full wetting in the absorbent mat location and full wetting along the top edge of the bottom plate (Type B), 2) Two wetted columns in the absorbent mat location (one beneath either end of the horizontal tubing) and full wetting along the top edge of the bottom plate (Type F), 3) One wetted column beneath the water reservoir in the absorbent mat location and full wetting along the top edge of the bottom plate (Type T), 4) One wetted column beneath the right end of the horizontal tubing in the absorbent mat location and full wetting along the top edge of the bottom plate (Type L), 5) Wetting along the top edge of the bottom plate (Type I), and 6) Minimal wetting on and beneath the absorbent mat location (Type X). The program (SigmaPlot) used to develop the contour plots estimates the gradient change in between data points resulting in approximations across the field. These contour approximations corresponded with visual evidence of wetting during moisture content mapping. These

estimates were sufficient to determine relative wetting pattern in a graphical display (Fig. 4-4).

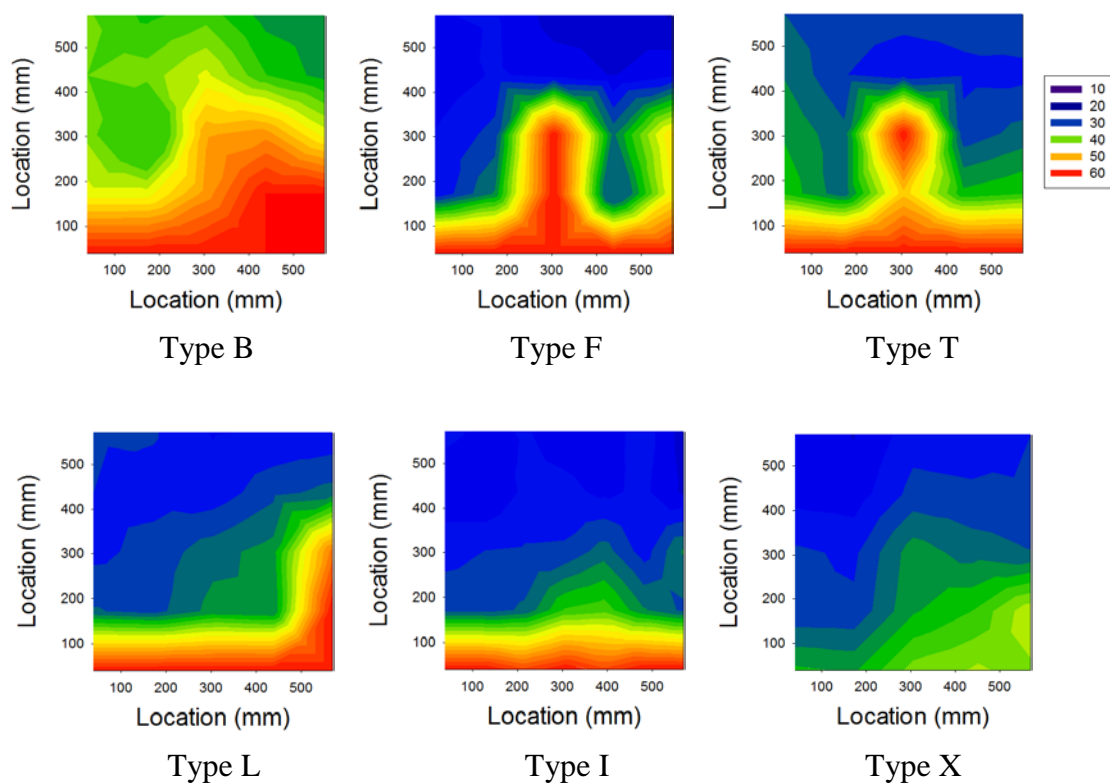


Fig. 4-4. Typical shear wall wetting patterns Type B, Type F, Type T, Type L, Type I, and Type X

Location on conditioning rack and irrigation system effectiveness contributed to wetting pattern development. Rack location affected moisture retention with samples on the top shelf in the incubation chamber developing lower moisture levels than those on the middle and bottom shelves (p-value = $\ll 0.001$). Both the middle and bottom shelves had a covered top whereas the top shelf was uncovered. An air

circulation fan in the ceiling led to drying that contributed to the moisture differences. The irrigation system had problems creating water droplet contact on the OSB panel that produced variations in wetting patterns (Table 4-1). Hence, a particular wetting pattern is a function of panel location in the incubation room as well as the efficiency of the irrigation system. A tilted rack and protection from direct air flow contact would help to alleviate these problems.

Table 4-1: Frequencies of the six moisture content distributions in assemblies exposed for different incubation periods

Assembly (type)	Incubation (days)	Statistics (n = 8)	Max Load (kN)	Wt Gain (%)	Quantities of Moisture Content Map Type					
					B	F	T	L	I	X
W	32	Mean	3.45(0.70)	11.98(2.48)	1	3	0	0	2	2
W	112	Mean	3.29(0.76)	16.02(5.35)	3	0	2	2	0	1
W	177	Mean	2.88(0.36)	14.10(3.63)	2	2	2	1	0	1
W	244	Mean	2.89(0.32)	16.84(4.11)	2	2	1	0	3	0
W	258	Mean	2.95(0.47)	14.43(5.33)	2	0	0	0	5	1
W	402	Mean	2.98(0.44)	14.46(3.71)	4	0	0	0	1	3
I	32	Mean	3.20(0.54)	12.69(2.60)	1	1	3	0	3	0
I	112	Mean	3.33(0.71)	16.19(4.47)	2	2	1	2	1	0
I	177	Mean	3.05(0.44)	16.06(2.74)	3	3	0	1	1	0
I	244	Mean	2.68(0.28)	15.59(5.28)	3	0	1	0	3	1
I	258	Mean	3.23(0.51)	16.27(6.91)	4	0	0	0	3	1
I	402	Mean	2.92(0.61)	15.90(4.12)	3	2	0	0	2	1

W = wetted only assemblies and I = Wetted/Inoculated Assemblies. Values represent means of 8 replicates and figures.

Parentheses represent one standard deviation.

The Type B wetting pattern produced the ideal moisture distribution for the wetting only and wetting/fungal assemblies since it produced nearly uniform 60% moisture content in the target region (uplift corner). These high moisture contents should have allowed for accelerated fungal growth throughout the uplift corner region.

The irrigation system used in Type B wetting patterns performed as designed and led to high moisture retention in the target zone. Type B wetting patterns accounted for 31% of the observed moisture distributions.

The Type F wetting pattern produced the next best moisture distribution. This wetting pattern covered the majority of the uplift corner region. The horizontal tubing near the tube fasteners was held tight to the OSB and allowed for vertical columns of wetting. The mid-span of the horizontal tubing had separated from the OSB allowing water droplets to fall onto the bottom plate before contacting the lower region of the OSB. Type F wetting patterns accounted for 15% of the observed moisture distributions.

The third best moisture distribution covered roughly two thirds of the uplift corner region and was produced by the Type T wetting pattern. The horizontal tubing near the middle panel tube fastener was held tight to the OSB and resulted in a vertical column of wetting. The mid-span and right side of the horizontal tubing separated from the OSB, allowing water droplets to fall onto the bottom plate before contacting the lower region of the OSB. Type T wetting patterns accounted for 10% of the observed moisture distributions.

The Type L wetting pattern produced the fourth best moisture distribution. This wetting pattern was similar to Type T in that it covered roughly two thirds of the uplift corner region. The horizontal tubing near the edge panel tube fastener was held

tight to the OSB and resulted in a vertical column of wetting. The mid-span and left side of the horizontal tubing separated from the OSB, allowing water droplets to fall onto the bottom plate before contacting the lower region of the OSB. Type L wetting patterns accounted for 6% of the observed moisture distributions.

The Type I wetting pattern produced the fifth best moisture distribution as it covered roughly one third of the uplift corner region. The drip-holes in the horizontal tubing in the assemblies failed to produce water droplet contact with the OSB, allowing water droplets to fall onto the bottom plate before contacting the lower region of the OSB. Type I wetting patterns accounted for 25% of the observed moisture distributions.

The Type X wetting pattern had minimal wetting and produced the poorest moisture distributions in the uplift corner region. This wetting pattern was similar to Type I in that it covered roughly one third of the uplift corner region, however, the moisture content in this region was very low compared to all other wetting pattern types. The low moisture content was caused by rack location. Type X wetting patterns were found on the top shelf of the conditioning rack where shear walls experienced accelerated drying caused by the air circulation fan. Type X wetting patterns accounted for 11% of the observed moisture distributions.

Moisture uptake can have irreversible effects on the mechanical properties of OSB (Wu *et al.* 2002). The shear walls were sorted by group types in order to compare

mechanical properties. A one way analysis of variance ($\alpha = 0.05$) showed that moisture uptake differed significantly between types B, F, and T compared with types L and X shear wall assemblies. Tukey's 'Honest Significant Difference' test showed that wetting patterns type B, F, and T corresponded with high shear wall weight gain and were considered optimal wetting patterns (Fig. 4-5) (Ramsey and Schafer, 2002). These data were expected since larger wetting patterns should lead to greater moisture retention. Type B, F, and T wetting patterns produced the largest target zone moisture retention. Data from the assemblies with these patterns were segregated from those with Types L, I, and X to evaluate material properties developed using the digital image correlation and uplift tests.

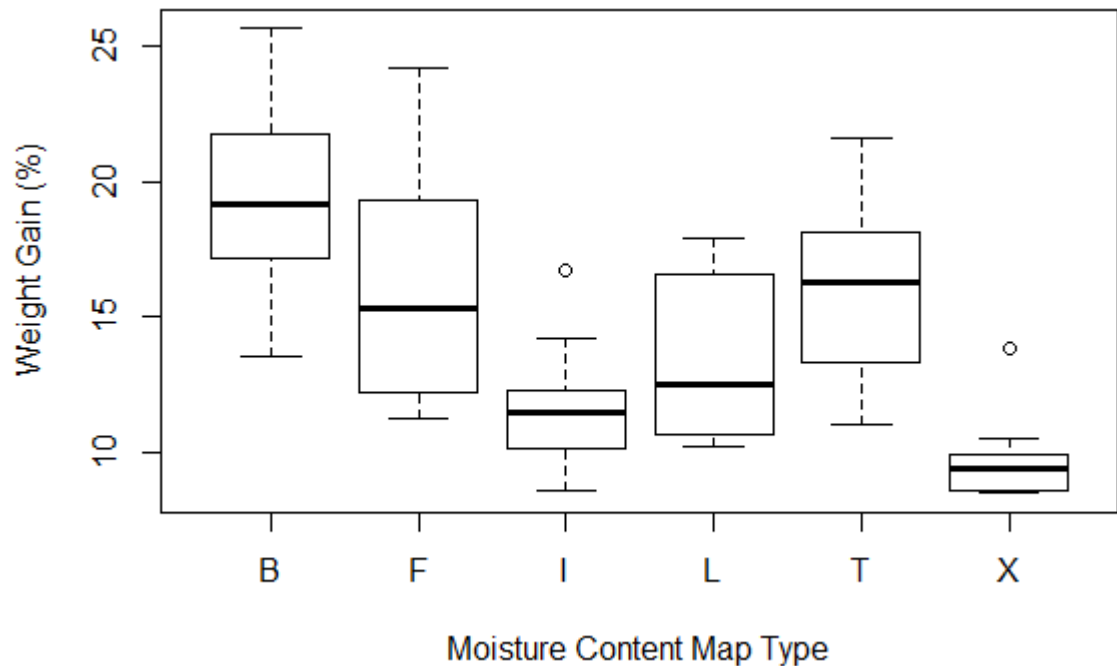


Fig. 4-5. Box and whisker plots of shear wall percent weight gain with respect to wetting patterns (moisture content map type)

Shear wall tests

Failure modes

Tensile forces in the uplift corner of the shear walls governed failure modes. Nail withdrawal, nail pull-through, flake debonding, and cross grain tension were the main failure modes produced by the uplift test (Fig. 4-6). Nail withdrawal occurred when applied axial force exceeded the side friction holding capacity of the nail shaft; the nail then progressively extracted as loads were amplified during tested (Figs. 4-6a and 4-6b). Wetting affected OSB rigidity and led to nail pull-through. This failure mode occurred as shear wall loading induced lateral forces on sheathing nails causing

the nail heads to bend and simultaneously crush the OSB (Fig. 4-6c). Flake debonding was a subsequent failure of nail pull-through and occurred as the sheathing nail heads crushed the OSB forcing some fragments to separate from the paneling (Fig. 4-6c). Cross grain tension failures were observed when framing nail side friction forces exceeded the radial tension capacity of the dimensional lumber in the sill plate (Fig. 4-6d). Nail withdrawal occurred in the framing nails in the uplift corner (Fig. 4-6a) and in the sheathing nails along the bottom edge of the OSB paneling in the uplift corner (Fig. 4-6b). This was also observed by Alldritt *et al* (2014). The sheathing nails along the OSB paneling experienced a combination of bending and side friction failure during loading. This failure mode was also documented by Foshchi (1974). Uplift forces were exerted on the stud and OSB paneling as an increasing amount of load was applied developing a bending moment on the shafts of the sheathing nails. The sheathing nails failed simultaneously in bending and withdrawal. Nail heads sunk into the OSB paneling as the shafts of the sheathing nails bent. The OSB was able to withstand the sinking force of the nail head in dry control assembly tests, but was unable to withstand the sinking force of the nail head in wetted only and wetted/inoculated assembly tests. Strain was greatest in the uplift corner; thus, sheathing nails closest to the uplift corner experienced the greatest withdrawal and deformation, which was expected.

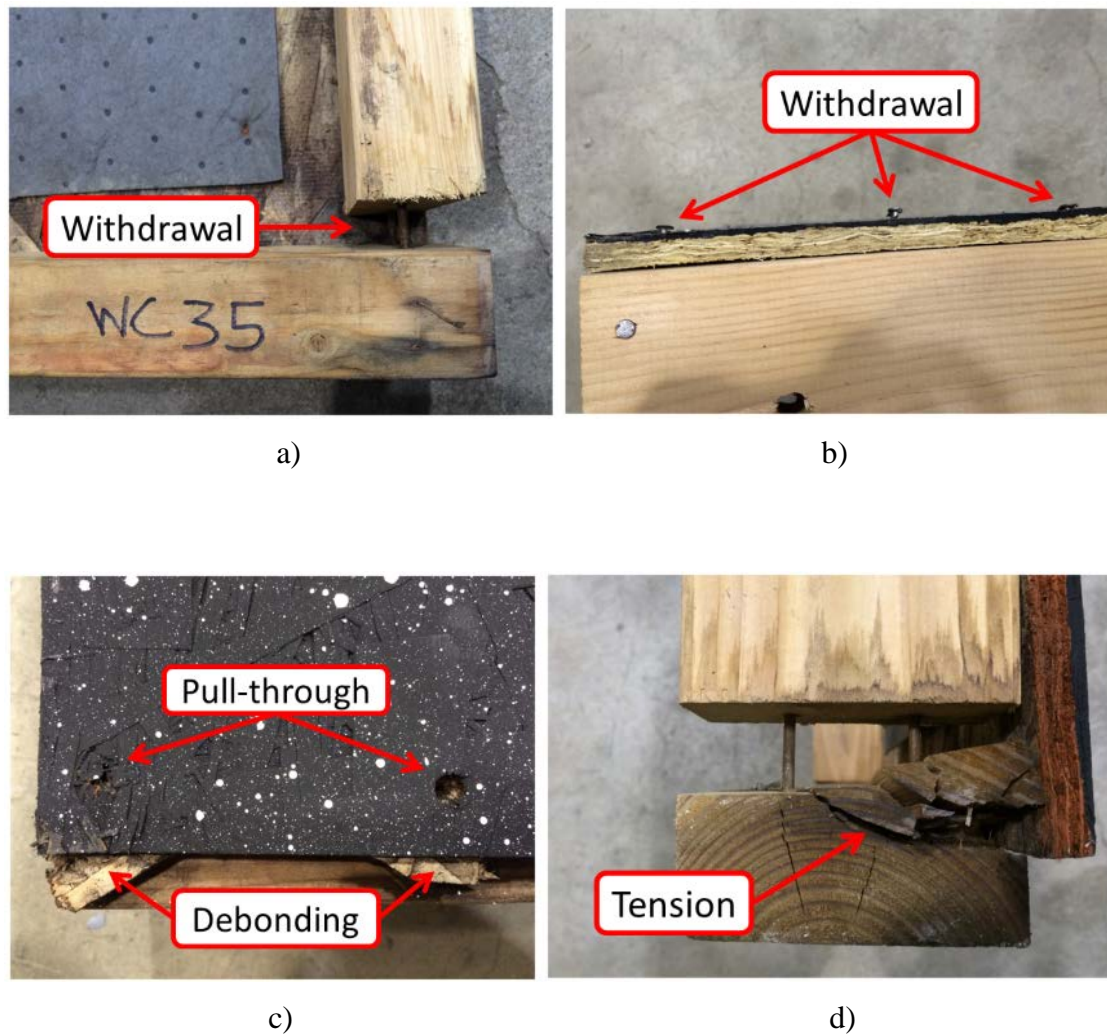


Fig. 4-6. Photographs show a) nail withdrawal on frame in uplift corner, b) nail withdrawal on paneling in uplift corner, c) nail pull-through and flake debonding on paneling in uplift corner, and d) cross grain tension on the sill plate in uplift corner of small scale shear wall assemblies

The initial failure mode for all shear walls tested came through the connections. In some cases, subsequent failures occurred in the OSB and sill plate. Every shear wall tested failed in nail withdrawal. The principal failure mode of the dry

control assemblies was nail withdrawal with an occasional cross grain tensile failure. The principal failure mode for the no corner control assemblies was also nail withdrawal. Failure modes in the wetted only and wetted/inoculated assemblies were governed by nail withdrawal with subsequent failures in nail pull-through. Many of the wetted only and wetted/inoculated assemblies also experienced failures in flake debonding occasionally coupled with cross grain tension.

The wetted only and wetted/fungal inoculated assemblies both experienced irreversible effects on OSB mechanical properties. Moisture uptake weakened the OSB and caused the heads of the sheathing nails along the bottom edge of the paneling in the uplift corner to pull through the OSB (Fig. 4-6c). In many cases, the flakes beneath the sheathing nails debonded causing wood fiber fragmentation (Fig. 4-6c). Sheathing nails along the bottom edge of the paneling in the uplift corner of the dry control assemblies did not pull through nor did flakes debond and fragment (Fig. 4-6b).

Vertical displacement of the sheathing nails in the uplift corner produced tensile failures on the sill plate (Fig. 4-6d). Sheathing nails induced force on the cross grain of the wood in the sill plate as the uplift corner lengthened during loading. In some cases, tensile stress exceeded sill plate capacity depending on grain direction, causing the end grain on the sill plate to split. Tensile failures occurred in dry control, wetted only, and wetted/fungal inoculated assemblies.

Shear wall loading

The uplift test showed that maximum load did not differ significantly between the wetted only assembly groups with increased incubation period. Maximum loads in the wetted/inoculated assemblies also did not differ significantly over the incubation period. The uplift test maximum load did not differ significantly between wetted only and wetted/fungal inoculated assemblies (Fig. 4-7). The wetted only and wetted/fungal inoculation assembly groups were combined for comparison with dry control assemblies since there were no significant differences between groups.

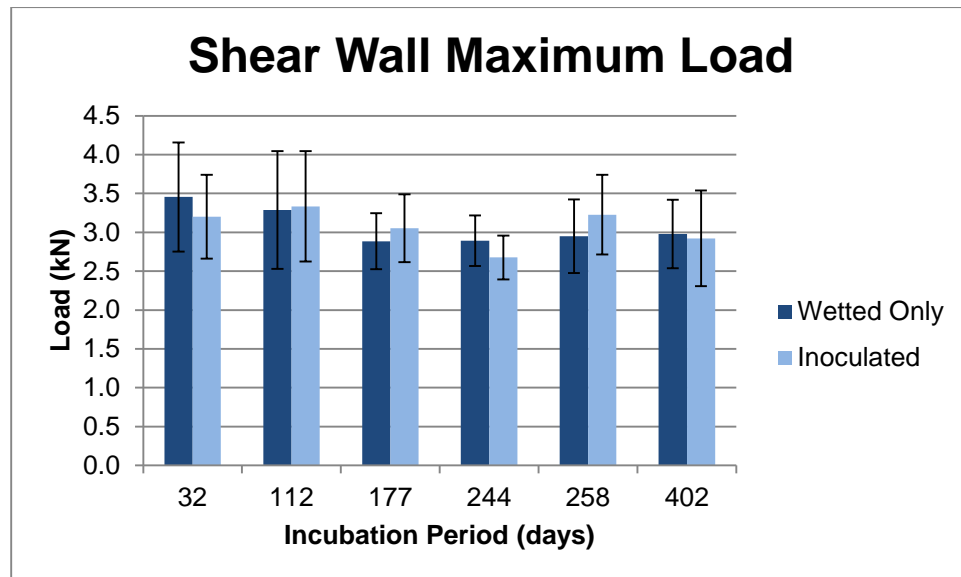


Fig. 4-7. Wetted and wetted/fungal inoculated shear wall maximum load versus incubation period

Maximum loads for the dry control assembly group were significantly different from those of the no corner control assembly group ($p\text{-value} = \ll 0.001$) (Fig. 4-8).

These data provided a good baseline for comparison between decayed shear walls versus shear walls under normal loading conditions. Shear walls in the dry control assembly group had twice the capacity of shear walls in the no corner control assembly group.

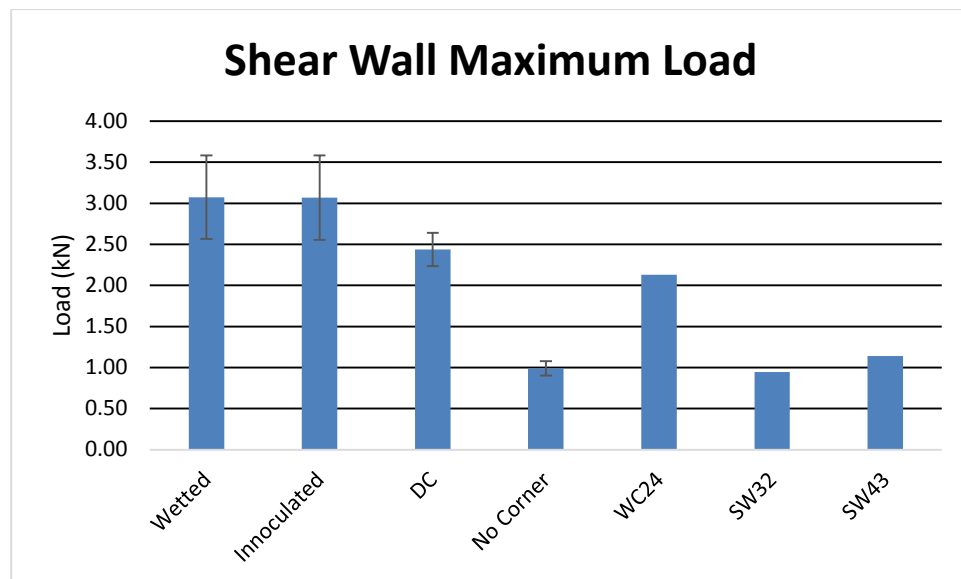


Fig. 4-8. Maximum shear wall capacity as shown by treatment groups

Maximum loads for wetted only and wetted/fungal inoculated assemblies were significantly higher than the dry control assemblies ($p\text{-value} = << 0.001$) (Fig. 4-8). Moisture uptake produced a gain in shear wall capacity possibly because moisture in the wetted assemblies caused the steel in the fasteners to oxidize (Fig. 4-9a). The ensuing fastener corrosion increased side friction and led to a stronger connection. Kang et al. (1999) observed increased resistance in nail withdrawal caused by corrosion in a study of preservative treatment on Douglas-fir and Hem-fir. The dry

control assemblies had no exposure to moisture resulting in fasteners with smooth shafts with minimal side friction (Fig. 4-9b). Alldritt *et al.* (2014) found that small scale shear wall strength and stiffness were primarily attributed to the behavior of the connection because the OSB panel strength in its original condition vastly exceeded the strength of the connection by a ratio of 15/1. In this study, the OSB in the wetted only and wetted/inoculated assemblies underwent losses in material properties caused by moisture uptake, but the strength in the OSB was still sufficient enough to overcome the strength of the connection.



Fig. 4-9. Examples of a) a) wetted assembly with corroded framing nails, b) dry control shear wall with non-corroded framing nails.

Three out of the 96 shear walls exposed to wetting (wetted only and wetted/fungal inoculated assemblies) experienced visible fungal decay. One of these

assemblies was part of the moisture control group (WC24), while the other two were inoculated with the test fungus (SW32 and SW43). The properties of all three of these shear walls differed significantly from the wetted and wetted/inoculated groups (Fig. 4-8). Assemblies SW32 and SW43 failed at loads similar to the no corner control group with losses ranging from 63 to 70% and 53 to 61% of capacity compared to the wetted and dry control groups, respectively. Assembly WC24 failed at a load similar to the dry control group with losses reaching 31% and 13% of capacity compared to the wetted and dry control groups, respectively. There were too few cases of visual decay to make any statistical conclusions on reduced shear wall capacity, but the three cases with visual decay suggest substantial loss in shear wall capacity when decay was present.

Digital Image Correlation

The DIC data were used to develop contour plots to show progressive strain development during shear wall loading (Fig. 4-11). These contour plots represent the average shear wall from the dry control assembly group (DC04) and the wetted/inoculated assembly group (WC30) as well as two of the individual shear walls that had visible decay (assemblies SW32 and WC24). The load cases investigated were 0.50 kN (Fig. 4-11a), 0.94 kN (Fig. 4-11b), 2.13 kN (Fig. 4-11c), 2.41 kN (Fig. 4-11d), or 3.23 kN (Fig. 4-11e). The contour plots shown at the bottom of each column represent strain in each shear wall just before failure. The level of strain in the

contour plots was indicated using a color scale ranging from -0.002 to 0.002. The location of the uplift corner is in lower left corner of each image (Fig. 4-11). Locations of sheathing nails along the sill plate in the uplift corner became evident by the formation of localized strain circles as load was increased (Fig. 4-11).

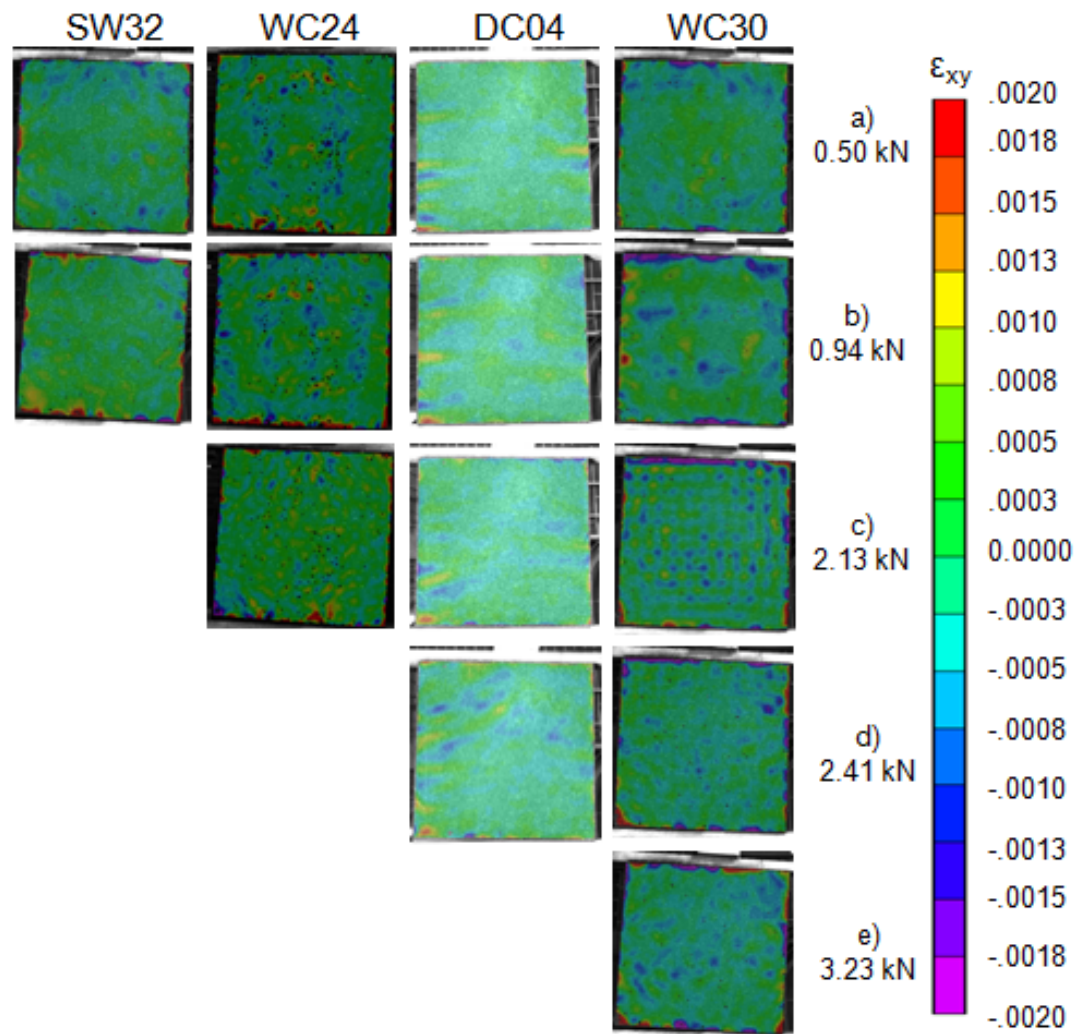


Fig. 4-11. Progressive strain contour plots showing strain in shear walls at: a) 0.50 kN, b) 0.94 kN, c) 2.13 kN, d) 2.41 kN, or e) 3.23 kN

The reference images of each shear wall showed no evidence of strain. Load was gradually applied and subsequent images were compared. Strain, albeit small in magnitude, began to develop around the corner sheathing nail in the uplift corner of each shear wall at a load of 0.50 kN (Fig. 4-11a). There were no discernible differences between shear wall groups at this load.

Strain patterns between groups began to deviate at a load of 0.94 kN. The assemblies with visible decay (SW32 and WC24) developed red strain circles (positive strains of 0.002) around multiple sheathing nail heads along the sill plate in the uplift corner (Fig. 4-11b). Assemblies in the dry control (DC04) and wetted (WC30) groups showed strain development on the corner sheathing nail in the uplift corner (Fig. 4-11b). The development of red strain circles on assemblies SW32 and WC24 suggests that the OSB had experienced stiffness losses. Fig. 4-11b shows an image of assembly SW32 just before failure.

Assemblies in the dry control (DC04) and wetted (WC30) groups developed strain circles along the sill plate in the uplift corner at a load of 2.13 kN (Fig. 4-11c). Assembly WC24 experienced a secondary failure in cross grain tension (Fig. 6d) which led to a decrease in localized strain indicated by the dark blue circle (a negative strain of -0.002) around the corner sheathing nail in the uplift corner (Fig. 4-11c). Assembly WC24 failed at a 2.13 kN load (Fig. 4-11c).

There were no discernible differences between the dry control and wetted groups as load was applied beyond 2.13kN (Fig. 4-11d and 4-11e). There were constant strain circles around the sheathing nail heads along the sill plate in the uplift corner. In some cases, the corner sheathing nail in the uplift corner would experience a drop in strain due to cross grain failure in the sill plate. Fig. 4-11d shows an image of assembly DC04 just before failure. Fig. 4-11e shows an image of assembly WC30 just before failure.

Assemblies SW32 and WC24 experience significant amounts of strain in the uplift corner at a lower load than assemblies in the dry control and wetted groups. This was expected because visible decay is associated with reduction in mechanical properties. The majority of the OSB sustained very little strain in the uplift tests. This supports the observation that failure occurred at the connections.

Density Mapping

The Pilodyn was used for indirect density mapping on the 11 mm thick OSB and measured depths of pin penetration on a scale from 0-20 mm. Pilodyn maps were developed on a 0-12 mm scale to allow for swelling of the OSB. Since density was measured by depth of pin penetration, lower numbers correspond to high densities and higher numbers correspond to low densities. The dry control assembly group yielded an average penetration depth of 7 mm. Pilodyn mapping of these assemblies was difficult because the pin would occasionally penetrate completely through the OSB;

however, these assemblies showed enough density continuity for comparison with the wetted only and wetted/inoculated assemblies (Fig. 4-12). Density variations were expected as OSB is not designed for the concentrated point loads generated by the Pilodyn. Glue seams and slight variations in strand thickness produced density differences in the dry control assemblies.

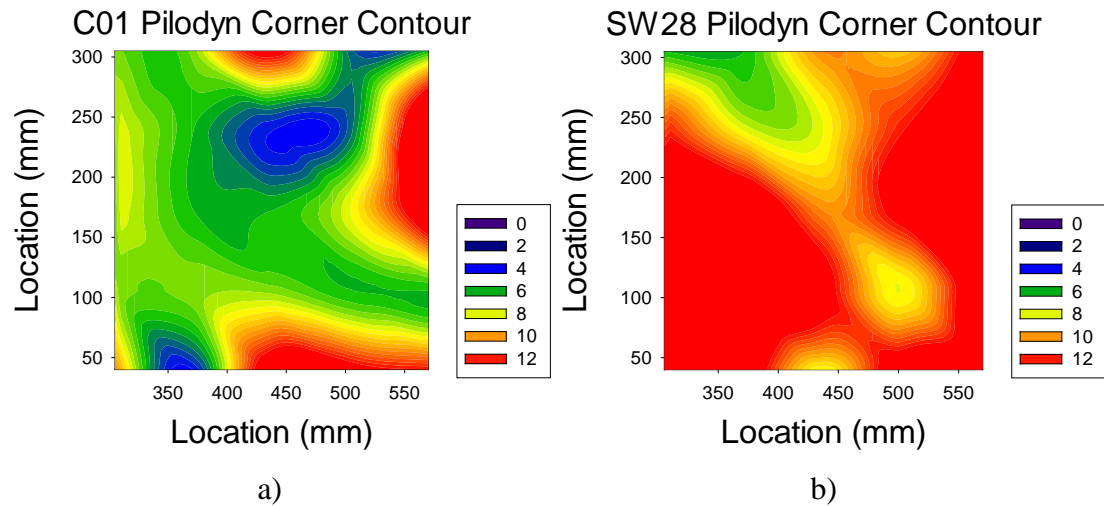


Fig. 4-12. Typical density maps of a) dry control and b) wetted/inoculated assemblies

Moisture content maps and the corresponding Pilodyn maps were compared for the exposed assemblies (wetted only and wetted/inoculated) (Fig. 4-13). Assemblies SW17 (Fig. 4-13a) and WC26 (Fig. 4-13b) represent typical moisture content versus density map comparisons and demonstrate how wetting alone affected density. Although fungal attack was present on only three assemblies, assemblies

WC24 (Fig. 4-13c) and SW32 (Fig. 4-13d) showed difference in moisture content versus Pilodyn map comparisons compared to assemblies with no visible decay.

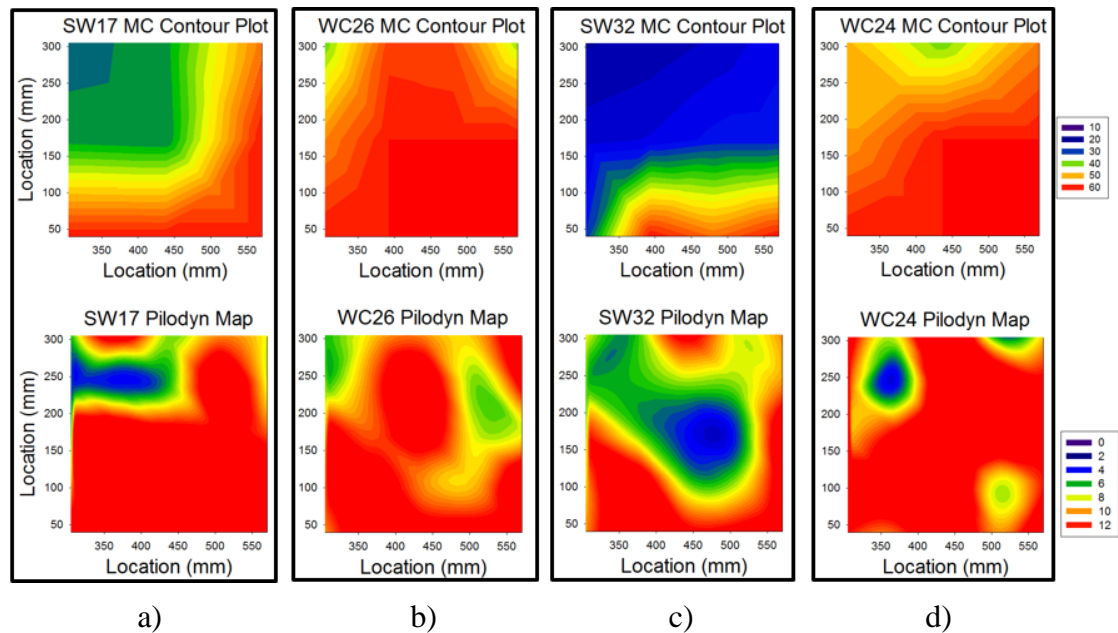


Fig. 4-13. Comparisons between moisture content and Pilodyn maps of: a) assembly SW17 b) assembly WC26 c) assembly SW32 and d) assembly WC24. Note: Moisture content contour plots were developed using data points covering the entire shear wall face, whereas Pilodyn contour plots were developed using data points covering the $\frac{1}{4}$ panel in the uplift corner resulting in a tighter grid spacing.

The Pilodyn map for a Type L moisture distribution showed density changes that reflected the wetting pattern (Fig. 4-13a). The low density bubble in the upper left hand corner of the Pilodyn map was likely caused by density variations in the original OSB as discussed earlier.

The Pilodyn map for a Type B moisture distribution showed density changes that were also very similar to the moisture content map (Fig. 4-13b). The dip in moisture levels in the upper right corner was reflected by the higher density zone at that same location. Likewise, the boundary of the wetting zone in the upper left corner was represented by the higher density observed on the Pilodyn map in that same area.

The changes in density shown by the Pilodyn in the Type I assembly SW32 were similar to the contour lines observed in the moisture content map (Fig. 4-13c). Wetted locations corresponded to lower density. The low densities on the left and right edges of the Pilodyn map could have been caused by fungal decay or variations in the original OSB.

The Type B moisture content map for assembly WC32 also corresponded well to the Pilodyn map (Fig. 4-13d). The two higher density locations (upper left and lower right corners) were likely due to more accurate data produced by the more frequent Pilodyn mapping. The high density zone in the upper left corner showed very low penetration depth which is likely due to its proximity to the edge of the wetted zone where moisture had much less effect. The high density zone in the lower right corner was associated with moderate pin penetration which was expected since it was within the wetted zone.

Density mapping was performed at a much tighter spacing as compared to the moisture content mapping. Thus, some of the variations in density did not correlate

with the wetted patterns. The Pilodyn maps coupled with their corresponding moisture content maps generally showed similar patterns suggesting that OSB density was affected by wetting.

Culturing

Attempts to isolate *Postia placenta*, the fungus originally introduced in the water, were problematic. Samples removed from assemblies SW32, WC24, and SW43 were positive for *Postia placenta*, but the fungus was not isolated from any other samples. Fungi isolated from most samples were in the genera *Trichoderma* and *Aspergillus*. Failure to isolate does not necessarily mean that a particular fungus is absent, but it suggests that the test fungus was unable to become established in the wood. The presence of molds suggests possible external influences. *Postia placenta* may have had difficulty becoming established and was likely outcompeted by *Trichoderma*, *Aspergillus*, and the other mold fungi that were already present in the conditioning room prior to shear wall exposure.

There are some steps that could be taken to improve *Postia placenta* colonization. *Postia placenta* could be inoculated onto small wood chips in an isolated environment and then these chips could be used to inoculate the shear wall assemblies. However, this method does not simulate a real world scenario since colonization by decay fungi is typically initiated from spores or hyphal fragments. Incubating the assemblies at lower temperatures would create conditions that are more favorable for

Postia placenta growth. Another option could be to use a sterilized incubation room to give the decay fungus an advantage, but this would be extremely expensive and is highly impractical in this current setting.

Conclusions

The performance of wetted only small-scale shear wall assemblies did not differ significantly from that of the wetted/inoculated assemblies. This was likely due to the inability of the decay fungus to colonize the assemblies. The wetted only and wetted/inoculated assemblies both experienced an increase in capacity which was caused by improved fastener side friction due to corrosion. Pilodyn testing used in conjunction with moisture content mapping showed that the OSB material properties were changed after wetting; however, the sheathing was not so weakened that it could not perform and shear wall capacity was still governed by connections. The primary failure mode for all shear wall assemblies was nail pull-out in the framing nails located in the uplift corner and the sheathing nails along the sill plate in the uplift corner. The wetted only and wetted/inoculated assemblies failed simultaneously in nail pull-out and nail pull-through, whereas the control groups experienced no nail pull-through. The three shear wall assemblies that had visual decay experienced substantial reductions in capacity, but the limited number of colonized samples limited the scope of conclusions that could be drawn.

4.6 REFERENCES

- Alldritt K, Sinha A, & Miller TH (2014). Designing a strand orientation pattern for improved shear properties of oriented strand board. *Journal of Materials in Civil Engineering*.
- Chui YH, Ni C, Jiang L (1998) Finite-element model for nailed wood joints under reversed cyclic load. *Journal of Structural Engineering* 124(1): 96-103.
- Clausen CA, & Kartal SN (2003) Accelerated detection of brown-rot decay: Comparison of soil block test, chemical analysis, mechanical properties, and immunodetection. *Forest Products Journal* 53(11/12): 90-94.
- Durham J, LamF, & Prion HG (2001) Seismic resistance of wood shear walls with large OSB panels. *Journal of Structural Engineering* 127(12): 1460-1466.
- Foschi RO (1974). Load-slip characteristics of nails. *J Wood Sci*, 7, 69-74.
- Johnson AC (1997) Monotonic and cyclic performance of long shear walls with openings. MS Thesis, Virginia Polytechnic Institute and State University, Blacksburg, VA.
- Kang SM, Morrell JJ, Smith D (1999) Effect of incising and preservative treatment on nail-holding capacity of Douglas-fir and hem-fir lumber. *Forest products journal* 49(3) 43-45.
- Kent SM, Leichti RJ, Rosowsky DV, Morrell JJ (2004) Effects of decay by *Postia placenta* on the lateral capacity of nailed oriented strandboard sheathing and Douglas-fir framing members. *Wood and Fiber Science* 36: 560-572.
- Kent SM, Leichti RJ, Rosowsky DV, Morrell JJ (2005) Effects of decay on cyclic properties of nailed connections. *Journal of Materials in Civil Engineering* 17(5): 579-585.
- McCutcheon WJ (1985) Racking deformations in wood shear walls. *Journal of Structural Engineering* 111(2): 257-269.
- Merrill W, French D (1964) Wood fiberboard studies: A nailhead pull-through method to determine the effects of fungi on strength. *Tappi* 47(8): 449-451.
- Polensek A, Bastendorff KM (1987) Damping in nailed joints of light-frame wood buildings. *Wood and Fiber Science* 19(2): 110-125.

- Ramsey FL, Schafer DW (2002) *The statistical sleuth: a course in methods of data analysis*. Cengage Learning, Kentucky. 768 pp.
- Sinha A, Gupta R (2009) Strain distribution in OSB and GWB in wood-frame shear walls. *Journal of Structural Engineering* 135(6): 666-675.
- van de Lindt JW (2004) Evolution of wood shear wall testing, modeling, and reliability analysis: Bibliography. *Practice Periodical on Structural Design and Construction* 9(1): 44-53.
- Wilcox WW (1978) Review of literature on the effects of early stages of decay on wood strength. *Wood and Fiber Science* 9(4): 252-257.
- Wu Q, Lee JN (2002) Thickness swelling of oriented strandboard under long-term cyclic humidity exposure condition. *Wood and Fiber Science* 34(1): 125-139.

5. CONCLUSIONS

Most engineered wood products are intended for dry use as they are susceptible to losses in material properties with long term exposure to wetting. However, these materials are occasionally subjected to moisture caused by natural disasters, construction delays, plumbing leaks and other situational events. This research integrated aspects of wood science, mechanics, structural engineering, and mycology to assess changes in material properties of I-joists and small scale wood composite shear walls over extended periods of wetting. Linear regression models were developed using exposure time, total rainfall, and rain days as dependent variables to characterize reductions in I-joist capacity. I-joists were found to nearly double in flexural strength variability after 27 days of external exposure. 65 days of external exposure was associated with a 9 percent loss in flexural capacity. Flexural test failure mode shifted from shear type failure to web buckling as exposure time increased. Exterior exposure had no negative effect on tension properties. These data can be used on jobs sites to determine quality of I-joists after construction delays.

The performance of wetted only assemblies did not differ significantly from that of the wetted/inoculated assemblies. This was likely due to the inability of the decay fungus to colonize the assemblies. The wetted only and wetted/inoculated assemblies both experienced an increase in capacity which was caused by improved fastener side

friction due to corrosion. Pilodyn testing showed that the OSB material properties were changed after wetting; however, the sheathing was not so weakened that it could not perform and shear wall capacity was still governed by connections. Pilodyn and moisture content map comparisons showed that effects of wetting and fungal decay on material properties were distinguishable and could be separated. The primary failure mode for all shear wall assemblies was nail pull-out in the framing nails located in the uplift corner and the sheathing nails along the sill plate in the uplift corner. The wetted only and wetted/inoculated assemblies failed simultaneously in nail pull-out and nail pull-through, whereas the control groups experienced no nail pull-through. The three shear wall assemblies that had visual decay experienced substantial reductions in capacity, but the limited number of colonized samples limited the scope of conclusions that could be drawn.

RECOMMENDATIONS

Continued studies on I-joists

- Long-term exposure testing on more sizes of I-joists would help solidify regression models.
- Further studies on wetting including decay fungi would simulate real life scenarios such as plumbing leaks or crawl space moisture condensation. This would help inspectors with in-use damage assessment.

- Flexural tests using variable loading configurations would add another dimension to this already complex problem.

Continued studies on shear walls and *Postia placenta* interaction:

- Further study with shear walls exposed to wetting could use galvanized nails or screws to minimize the effects of corrosion on connection capacity. However, this would not simulate a real world scenario since shear walls are typically constructed with non-galvanized nails.
- Shear walls should also be placed on a tilted rack to allow water to be in more intimate contact with the OSB and run down the paneling, creating a more consistent moisture distribution.
- The use of wood chips with established colonies of decay fungus for shear wall assembly inoculation might also produce more consistent inoculation.
- Shear walls should also be incubated in a conditioning room more favorable to growth of decay fungi (lower temperature).
- OSB thickness swell could be recorded for more comparative data analysis of the effects of moisture intrusion.
- Shear walls could be tested in the wetted state to determine in-use capacity (although this would allow moisture variations that would affect testing).

- Full-scale shear walls could be tested although conditioning room space becomes a problem and the larger samples would tend to have even higher variability in moisture distribution.
- Wetting led to increases in shear wall capacity associated with fastener oxidization. Corrosion will ultimately lead to a reduction in fastener diameter and loss of holding capacity. A long term study on the effects of wetted connections and fastener life would also be advisable.

BIBLIOGRAPHY

- Alldritt K, Sinha A, & Miller TH (2014). Designing a strand orientation pattern for improved shear properties of oriented strand board. *Journal of Materials in Civil Engineering*.
- ASTM (2010a) D2915. Standard practice for sampling and data-analysis for structural wood and wood-based products. American Society for Testing and Materials, West Conshohocken, PA.
- ASTM (2010b) E105. Standard practice for probability sampling of material. American Society for Testing and Materials, West Conshohocken, PA.
- ASTM (2013) D5055. Standard specification for establishing and monitoring structural capacities of prefabricated wood I-joists. American Society for Testing and Materials, West Conshohocken, PA.
- Chen GH, Tang RC, Price EW (1989) Effect of environmental conditions on the flexural properties of wood composite I-beams and lumber. *Forest Products Journal* 39(2): 17-22.
- Chui YH, Ni C, Jiang L (1998) Finite-element model for nailed wood joints under reversed cyclic load. *Journal of Structural Engineering* 124(1): 96-103.
- Clausen CA, & Kartal SN (2003) Accelerated detection of brown-rot decay: Comparison of soil block test, chemical analysis, mechanical properties, and immunodetection. *Forest Products Journal* 53(11/12): 90-94.
- Durham J, LamF, & Prion HG (2001) Seismic resistance of wood shear walls with large OSB panels. *Journal of Structural Engineering* 127(12): 1460-1466.
- Foschi RO (1974). Load-slip characteristics of nails. *J Wood Sci*, 7, 69-74.
- Johnson AC (1997) Monotonic and cyclic performance of long shear walls with openings. MS Thesis, Virginia Polytechnic Institute and State University, Blacksburg, VA.
- Garay M, Marie R, Poblete W, Karsulovic C, Tomás J (2009) Evaluation of oriented strandboard and plywood subjected to severe relative humidity and temperature conditions. *Forest Products Journal* 59(3): 84-90.
- Haataja BA, Laks PE (1995) Properties of flakeboard made from northern white-cedar. *Forest Products Journal* 45(1): 68-70.

- Hayashi T, Miyatake A, Harada M (2002) Outdoor exposure tests of structural laminated veneer lumber I: evaluation of the physical properties after six years. *Journal of Wood Science* 48(1): 69-74.
- Hayashi T, Miyatake A, Fu F, Kato H, Karube M, Harada M (2005) Outdoor exposure tests of structural laminated veneer lumber (II): evaluation of the strength properties after nine years. *Journal of Wood Science* 51(5): 486-491.
- Hazleden, D. and P. Morris. 1999. Designing for durable wood construction: the 4 D's. *Durability of Building Materials and Components* 8, Volume 2. Institute for Research in Construction, Ottawa, ON. 734-745.
- Johnson AC (1997) Monotonic and cyclic performance of long shear walls with openings MS thesis, Virginia Polytechnic Institute and State University, Blacksburg, VA.
- Jokerst R W (1981) Finger-Jointed Wood Products (No. FSRP-FPL-382). Forest Products Lab, Madison, WI. 24 pp.
- Kang SM, Morrell JJ, Smith D (1999) Effect of incising and preservative treatment on nail-holding capacity of Douglas-fir and hem-fir lumber. *Forest products journal* 49(3) 43-45.
- Kent SM, Leichti RJ, Rosowsky DV, Morrell JJ (2004) Effects of decay by *Postia placenta* on the lateral capacity of nailed oriented strandboard sheathing and Douglas-fir framing members. *Wood and Fiber Science* 36: 560-572.
- Kent SM, Leichti RJ, Rosowsky DV, Morrell JJ (2005) Effects of decay on cyclic properties of nailed connections. *Journal of Materials in Civil Engineering* 17(5): 579-585.
- Kojima Y, Shimoda T, Suzuki S (2011) Evaluation of the weathering intensity of wood-based panels under outdoor exposure. *Journal of Wood Science* 57(5): 408-414.
- Lehmann WF (1978) Cyclic moisture conditions and their effect on strength and stability of structural flakeboards [wood-base composite panels]. *Forest Products Journal* 28(6): 23-31.
- Leichti RJ, Falk RH, Laufenberg TL (1990) Prefabricated wood composite I-beams: a literature review. *Wood and Fiber Science* 22(1): 62-79.

- Lin CH, Yang TH, Lai WJ, Lin FC (2013) Anisotropic Physical and Mechanical Performance of PF-impregnated Oriented Strand Board. *BioResources*, 8(2): 1933-1945
- Liu JY, McNatt JD (1991) Thickness swelling and density variation in aspen flakeboards. *Wood Science and Technology* 25(1): 73-82.
- Mankowski ME, Morrell JJ (2000) Incidence of wood-destroying organisms in Oregon residential structures. *Forest Products Journal* 50(1): 49-52.
- Mai C, Kües U, Militz H (2004) Biotechnology in the wood industry. *Applied Microbiology and Biotechnology* 63(5): 477-494.
- McCutcheon WJ (1985) Racking deformations in wood shear walls. *Journal of Structural Engineering* 111(2): 257-269.
- McNatt JD (1980) Hardboard-webbed beams: research and application. *Forest Products Journal* 30(10): 57-64.
- Merrill W, French D (1964) Wood fiberboard studies: A nailhead pull-through method to determine the effects of fungi on strength. *Tappi* 47(8): 449-451.
- Meyer RW (1982) Structural use of wood in adverse environments, Van Nostrand Reinhold, NY, 510 pp.
- Meza L, Sinha A, Morrell JJ (2013) Effect of wetting during construction on properties of Douglas-fir plywood and oriented strandboard flooring. *Forest Products Journal* 63(5/6):199-201.
- Morrell JJ (2002) Wood-based building components: what have we learned? *International Biodeterioration & Biodegradation* 49(4): 253-258.
- Nanami N, Shibusawa T, Sato M, Arima T, Kawai M (2000) Durability assessment of wood-framed walls and mechanical properties of plywood in use. 6-5-3. In: *Proc. World Conference on Timber Engineering*. July 31-August 3, Whistler, British Columbia. University of British Columbia, Vancouver, British Columbia. 9 pp.
- NDS (2012). National design specification for wood construction. American Forest and Paper Association Inc, Washington, DC.
- Norita H, Kojima Y, Suzuki S (2008) The aging effects of water immersion treatments in wet-bending for standardized testing of wood panels. *Journal of Wood Science* 54(2): 121-127.

- Nzokou P, Zyskowski J, Boury S, Kamdem DP (2005) Natural decay resistance of LVL made of veneers from durable and non-durable wood species. *Holz als Roh-und Werkstoff* 63(3): 173-178.
- Okkonen EA, River BH (1996) Outdoor aging of wood-based panels and correlation with laboratory aging: Part 2. *Forest Products Journal* 46(3): 68-74.
- Polensek A, Bastendorff KM (1987) Damping in nailed joints of light-frame wood buildings. *Wood and Fiber Science* 19(2): 110-125.
- Polocoser T, Miller T, Gupta R (2013) Evaluation of remediation techniques for circular holes in the webs of wood I-joists. *Journal of Materials in Civil Engineering* 25(12): 1898–1909.
- Ramsey FL, Schafer DW (2002) *The statistical sleuth: a course in methods of data analysis*. Cengage Learning, Kentucky. 768 pp.
- River BH (1994) Outdoor aging of wood-based panels and correlation with laboratory aging. *Forest Products Journal* 44(11/12): 55-65.
- Robins JG (1975) *The wooden wonder: a short history of the wooden aeroplane*. J. Bartholomew and Sons Ltd., Edinburg. 55 pp.
- Sanchez-Silva M, Rosowsky DV (2008) Biodeterioration of Construction Materials: State of the Art and Future Challenges. *Journal of Materials in Civil Engineering* 20(5): 352–365.
- Schmidt E, Hall H, Gertjeansen R, Carll C, DeGroot R (1983) Biodeterioration and strength reductions in preservative treated aspen waferboard. *Forest Products Journal* 33(11/12): 45-53.
- Sinha A, Gupta R (2009) Strain distribution in OSB and GWB in wood-frame shear walls. *Journal of Structural Engineering* 135(6): 666-675.
- Smulski S (2000) Durability of energy-efficient wood-frame houses. 4-2-4. In: *Proc. World Conference on Timber Engineering*. Jul 31-Aug 3, Whistler, British Columbia. University of British Columbia, Vancouver, British Columbia. 8 pp.
- Suchsland O, Hong X (1991) Model analysis of flakeboard variables. *Forest Products Journal* 41(11-12): 55-60.
- van de Lindt JW (2004) Evolution of wood shear wall testing, modeling, and reliability analysis: Bibliography. *Practice Periodical on Structural Design and Construction* 9(1): 44-53.

- Wilcox WW (1978) Review of literature on the effects of early stages of decay on wood strength. *Wood and Fiber Science* 9(4): 252-257.
- Wu Q, Suchsland O (1997) Effect of moisture on the flexural properties of commercial oriented strandboards. *Wood and Fiber Science* 29(1): 47-57.
- Wu Q, Lee JN (2002) Thickness swelling of oriented strandboard under long-term cyclic humidity exposure condition. *Wood and Fiber Science* 34(1): 125-139.
- Yang V, Illman B, Ferge L, Ross R (2001) Wood-based composites exposed to fungal degradation: laboratory results. IRG/WP 01- 40215. In: Proc. 32nd Annual Meeting International Research Group on Wood Preservation. May 20-25, Nara, Japan. International Research Group on Wood Preservation. 5 pp.

APPENDICES

Appendix A - I-joist Project Photographs



Figure A-1. End View of I-joist Exposure Rack



Figure A-2. Side View of I-joist Exposure Rack



Figure A-3. Hold down Strips on I-joist Exposure Rack



Figure A-4. Flexure Test Set-up



Figure A-5. Tension Test Set-up.

Appendix B - Derivation of Beam Loading Geometry

Moment Area Method for Finding the Bending Deflection

$$\text{Area}_1 = \left(\frac{2pl}{5}\right)\left(\frac{l}{5}\right)\left(\frac{1}{2}\right) = \frac{l^2 p}{25}$$

$$\text{Area}_2 = \left(\frac{3pl}{5} - \frac{2pl}{5}\right)\left(\frac{l}{5}\right)\left(\frac{1}{2}\right) = \frac{l^2 p}{50}$$

$$\text{Area}_3 = \left(\frac{2pl}{5}\right)\left(\frac{3l}{5}\right) = \frac{6l^2 p}{25}$$

$$\text{Area}_4 = \left(\frac{3pl}{5} - \frac{2pl}{5}\right)\left(\frac{l}{5}\right) = \frac{l^2 p}{25}$$

$$\text{Area}_5 = \frac{l^2 p}{50}$$

$$\text{Area}_6 = \frac{l^2 p}{25}$$

$$\text{Total}_{\text{area}} = \text{Area}_1 + \text{Area}_2 + \text{Area}_3 + \text{Area}_4 + \text{Area}_5 + \text{Area}_6 = \frac{2l^2 p}{5}$$

$$t_{da} = \left(\frac{l}{2}\right)\left(\frac{2l^2 p}{5}\right) = \frac{l^3 p}{5}$$

$$\theta_a = \left(\frac{t_{da}}{l}\right) = \frac{l^2 p}{5}$$

$$CC' = \left(\frac{1}{2}\right) (0_a) = \frac{l^3 p}{10}$$

$$\begin{aligned} t_{ca} = \text{Area}_1 \left\{ \left(\frac{3}{2}\right) \left(\frac{1}{5}\right) + \left(\frac{1}{3}\right) \left(\frac{1}{5}\right) \right\} + \left\{ \left(\frac{\text{Area}_3}{2}\right) \left(\frac{1}{2}\right) \left(\frac{3}{2}\right) \left(\frac{1}{5}\right) \right\} \\ + \text{Area}_2 \left\{ \left(\frac{1}{5}\right) \left(\frac{1}{2}\right) + \left(\frac{1}{5}\right) \left(\frac{1}{3}\right) \right\} + \left\{ \left(\frac{\text{Area}_4}{2}\right) \left(\frac{1}{5}\right) \left(\frac{1}{2}\right) \left(\frac{1}{2}\right) \right\} = \frac{37l^3 p}{1000} \end{aligned}$$

$$\Delta C = CC' - t_{ca} = \frac{63l^3 p}{1000}$$

Superposition Method for Finding the Bending Deflection

$$\left(\frac{-P \left(\frac{4L}{5}\right) \left(\frac{L}{2}\right)}{6\Delta L} \right) \left[L^2 - \left(\frac{4L}{5}\right)^2 - \left(\frac{L}{2}\right)^2 \right] - \frac{P \left(\frac{L}{2} - \frac{L}{5}\right)^3}{6\Delta} = \frac{71L^3 P}{6000\Delta}$$

$$\left(\frac{-P \left(\frac{3L}{5}\right) \left(\frac{L}{2}\right)}{6\Delta L} \right) \left[L^2 - \left(\frac{3L}{5}\right)^2 - \left(\frac{L}{2}\right)^2 \right] - \frac{P \left(\frac{L}{2} - \frac{2L}{5}\right)^3}{6\Delta} = \frac{59L^3 P}{3000\Delta}$$

$$\left(\frac{-P \left(\frac{2L}{5}\right) \left(\frac{L}{2}\right)}{6\Delta L} \right) \left[L^2 - \left(\frac{2L}{5}\right)^2 - \left(\frac{L}{2}\right)^2 \right] = \frac{59L^3 P}{3000\Delta}$$

$$\left(\frac{-P \left(\frac{L}{5}\right) \left(\frac{L}{2}\right)}{6\Delta L} \right) \left[L^2 - \left(\frac{L}{5}\right)^2 - \left(\frac{L}{2}\right)^2 \right] = \frac{71L^3 P}{6000\Delta}$$

$$2\left(-\frac{71L^3(P)}{6000\Delta}\right) + 2\left(-\frac{59L^3(P)}{3000\Delta}\right) = -\frac{63L^3P}{1000\Delta}$$

From superposition and moment area method, the bending deflections come out the same. Where $\Delta = EI$

Shear Deflection

$$-2\left[\frac{P\left(\frac{2L}{5}\right)\left(\frac{L}{2}\right)}{\kappa L\Lambda}\right] - 2\left[\frac{P\left(\frac{L}{5}\right)\left(\frac{L}{2}\right)}{\kappa L\Lambda}\right] = -\frac{3LP}{5\kappa\Lambda}$$

Where $\Lambda = A * G$

Appendix C - LabView Programming



Figure C-1. LabView Graphical User Interface

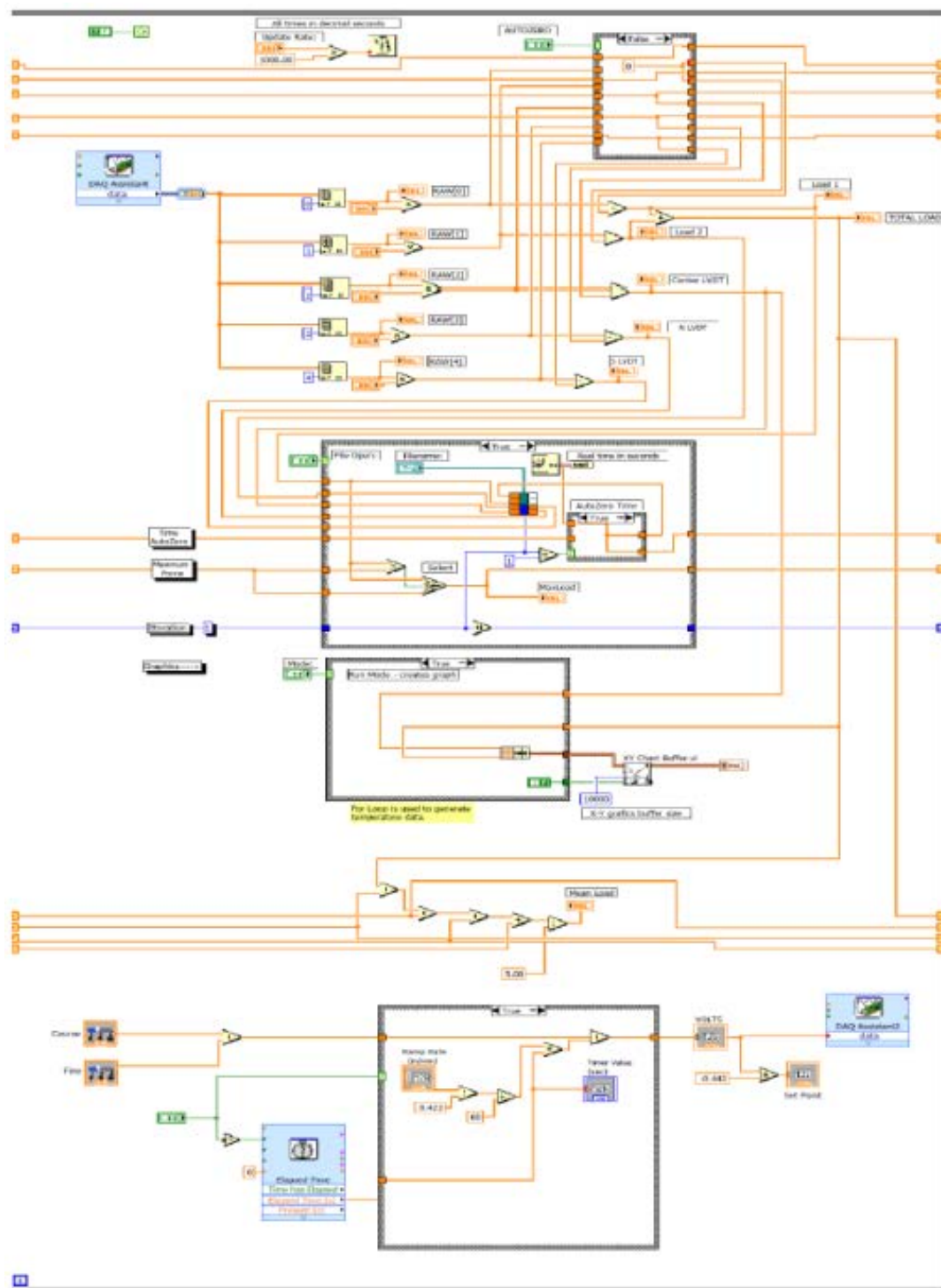


Figure C-2. LabView Programming

Appendix D - I-Joist Flexural and Tension Charts with Rain Data

Table D-1. Effects of exterior exposure on moisture content and physical properties of I-joists

I-Joist (type)	Exposure (days)	Replicates (n)	Statistics	Max Load (kN)	Deflection ^a (mm)	MC ^b (%)	Predominate Failure	Rainfall (cm)	Rain Days (days)
406.4 mm	Control	8	Mean	54.63	14.92	12.42	ZW	0.00	0
			SD ^c	2.92	1.48	0.49			
	27	8	Mean	53.29	12.99	49.74	ZJ	33.66	20
			SD	5.82	1.39	1.25			
	65	8	Mean	49.54	12.91	50.06	ZJ	47.12	48
			SD	5.87	2.28	2.31			
	95	8	Mean	45.03	12.91	51.74	WB	73.81	71
			SD	7.09	2.17	2.46			
	138	10	Mean	44.58	12.99	52.33	WB	85.19	104
			SD	5.75	1.18	2.40			
355.6 mm	Control	9	Mean	50.03	6.47	11.17	ZW	0.00	0
			SD	5.09	1.09	0.48			
	533	12	Mean	37.66	14.71	11.06	WB	181.33	275
			SD	3.84	3.13	0.64			
	566	8	Mean	36.48	12.78	11.14	WB	184.00	282
			SD	4.73	1.92	1.21			

^a Deflection at maximum load ^b MC = moisture content measured directly after exposure ^c SD = standard deviation

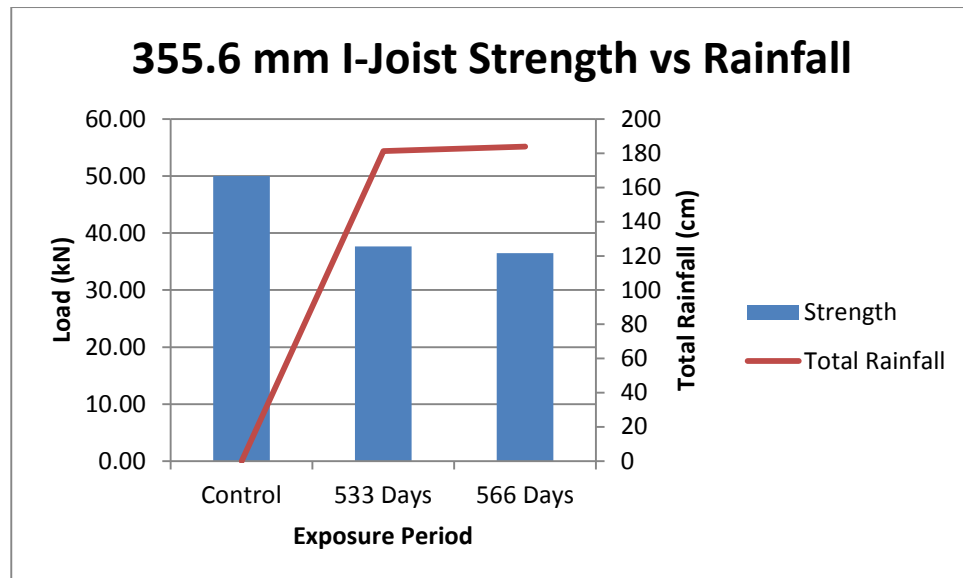


Figure D-2. Moisture content and maximum loads of 356 mm deep I-joists exposed outdoors in an above ground test for 0 to 566 days in Western Oregon.

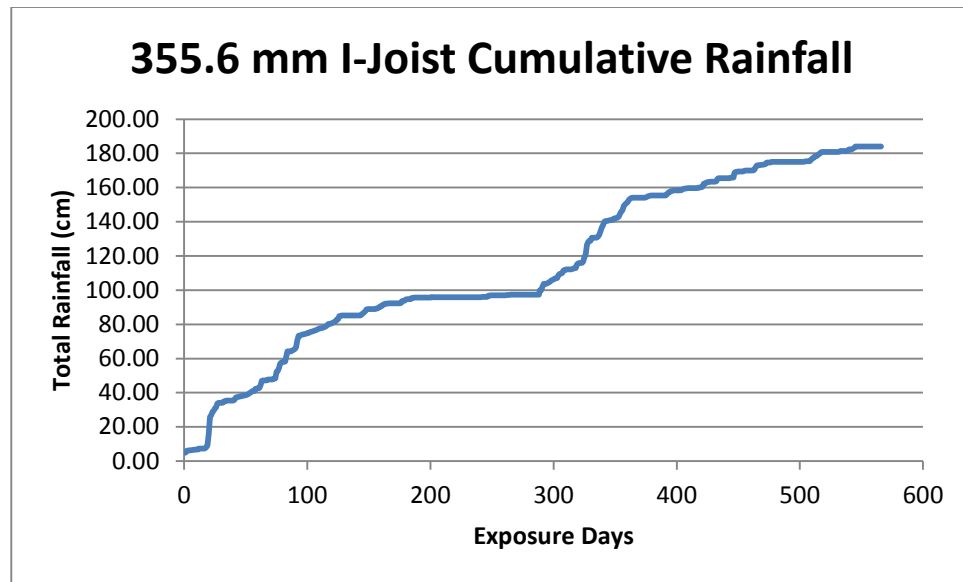


Figure D-2. Cumulative Rainfall during Exposure Period

Appendix E - I-Joist Flexural Tests Load and Deflection Data

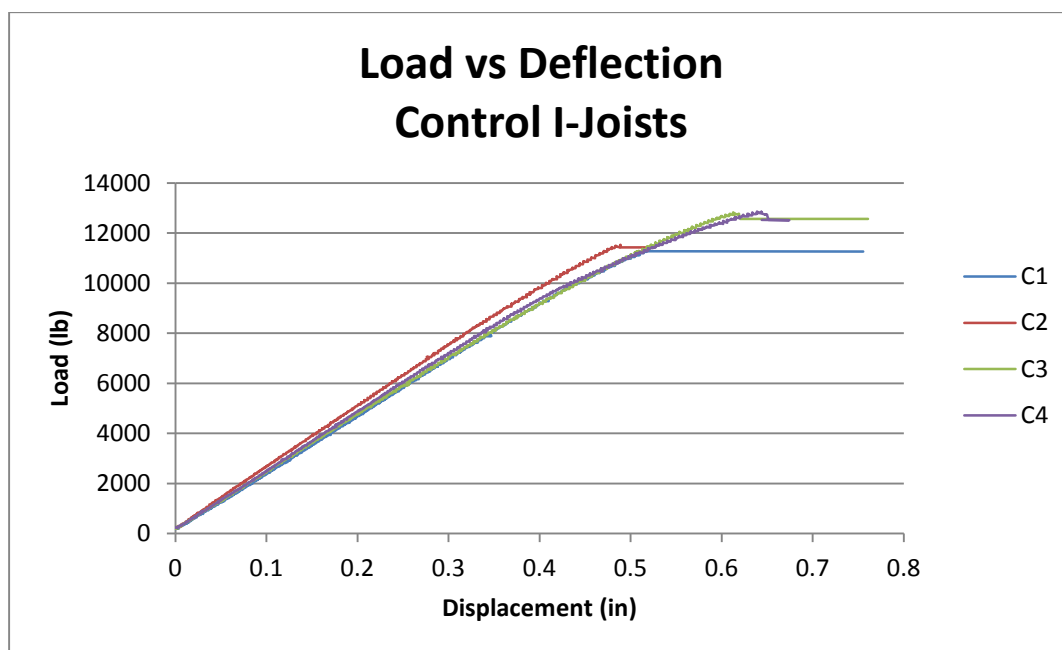


Figure E-1. Load vs. Deflection Curve for C1, C2, C3, and C4

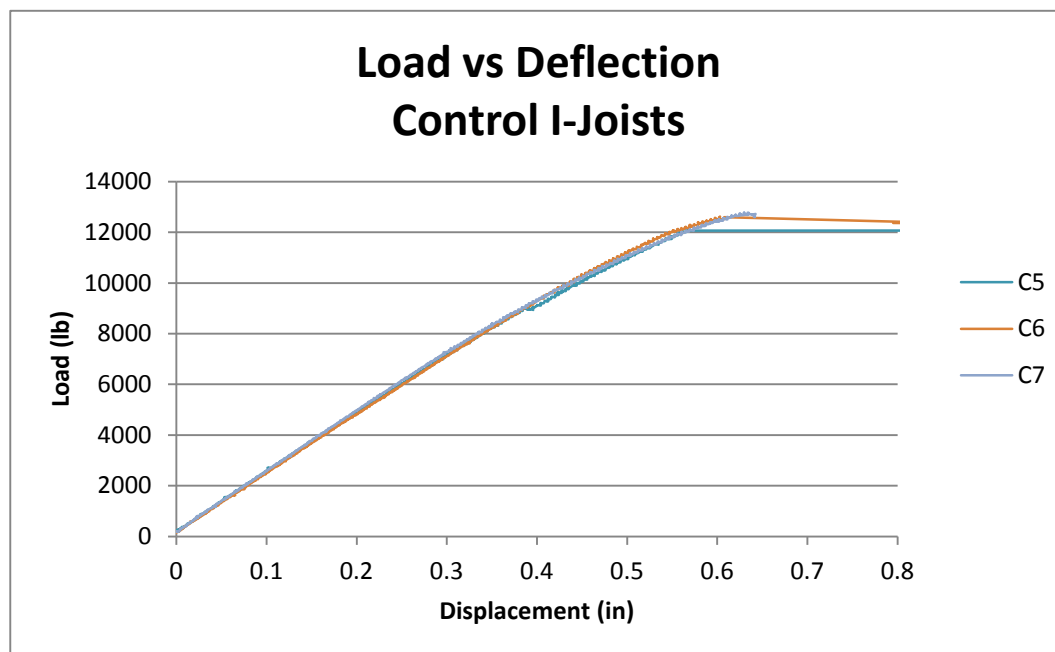


Figure E-2. Load vs. Deflection Curve for C5, C6, and C7

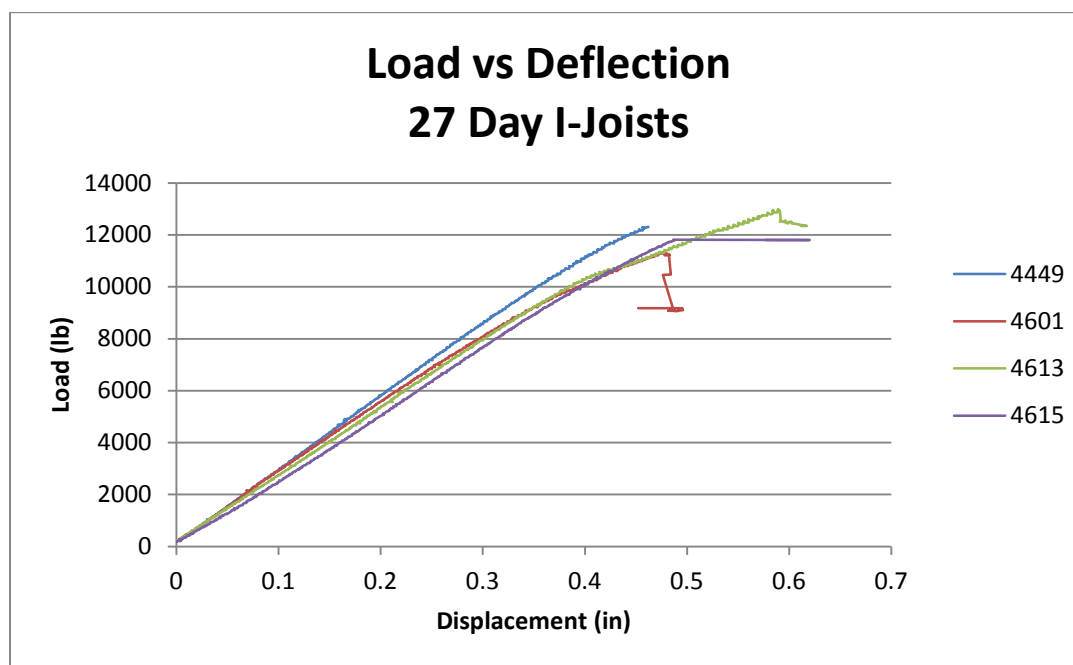


Figure E-3. Load vs. Deflection Curve for 4449, 4601, 4 613, and 4615

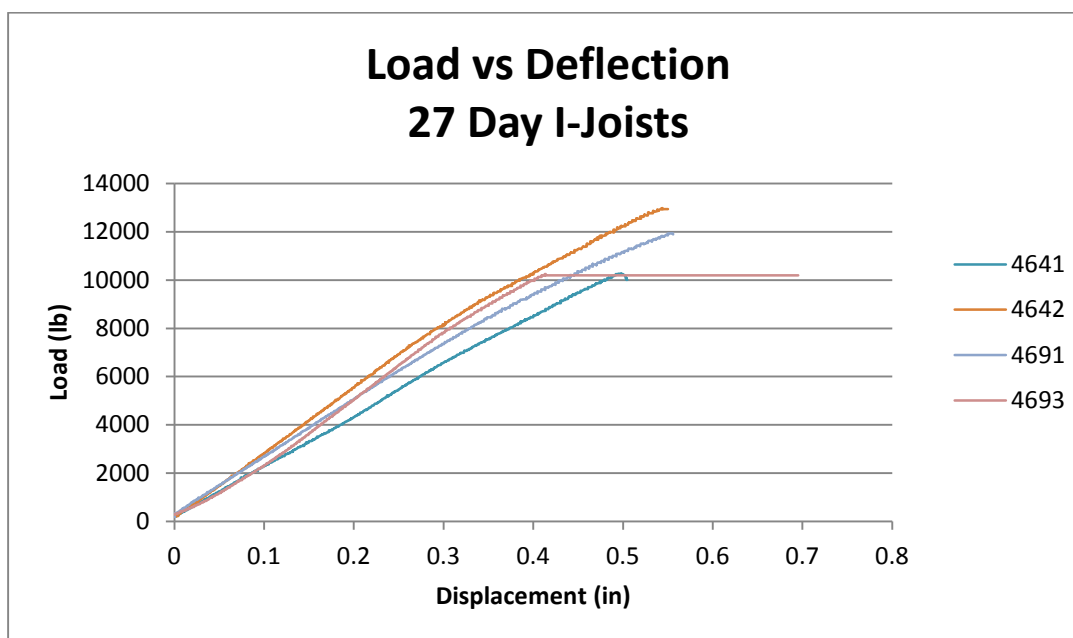


Figure E-4. Load vs. Deflection Curve for 4641, 4642, 4691, and 4693

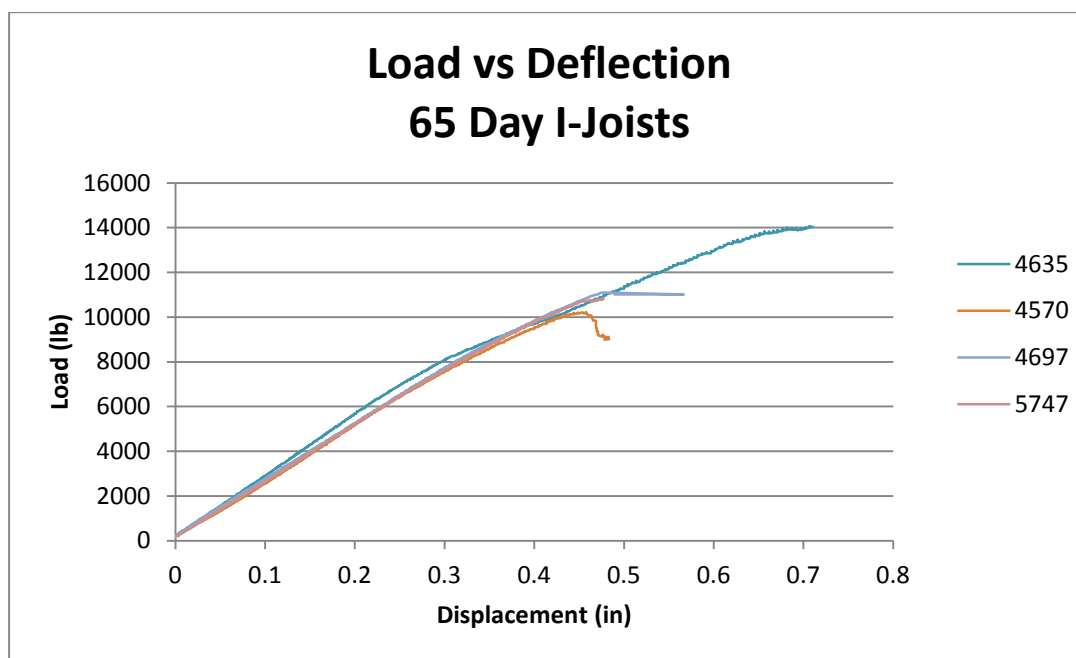


Figure E-5. Load vs. Deflection Curve for 4635, 4570, 4697, and 5747

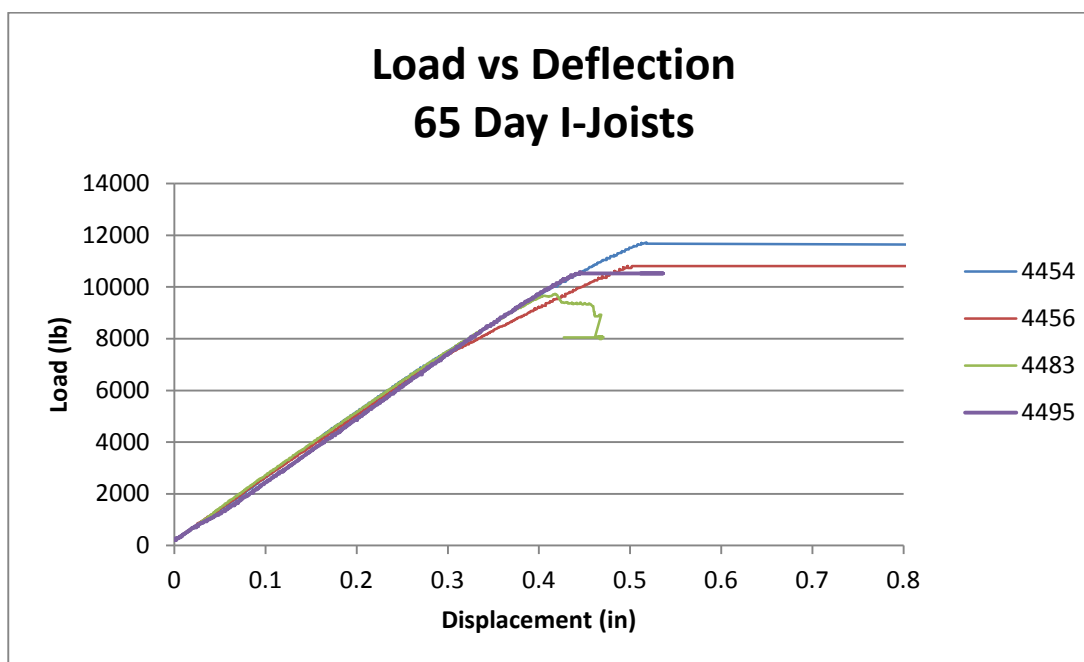


Figure E-6. Load vs. Deflection Curve for 4454, 4456, 4483, and 4495

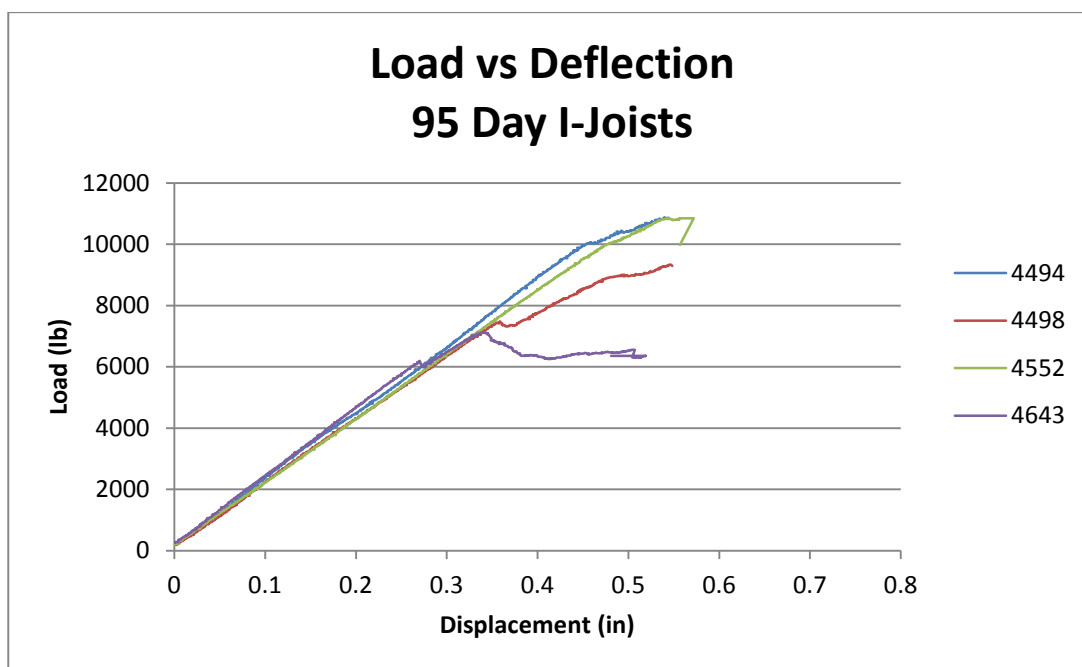


Figure E-7. Load vs. Deflection Curve for 4494, 4498, 4552, and 4643

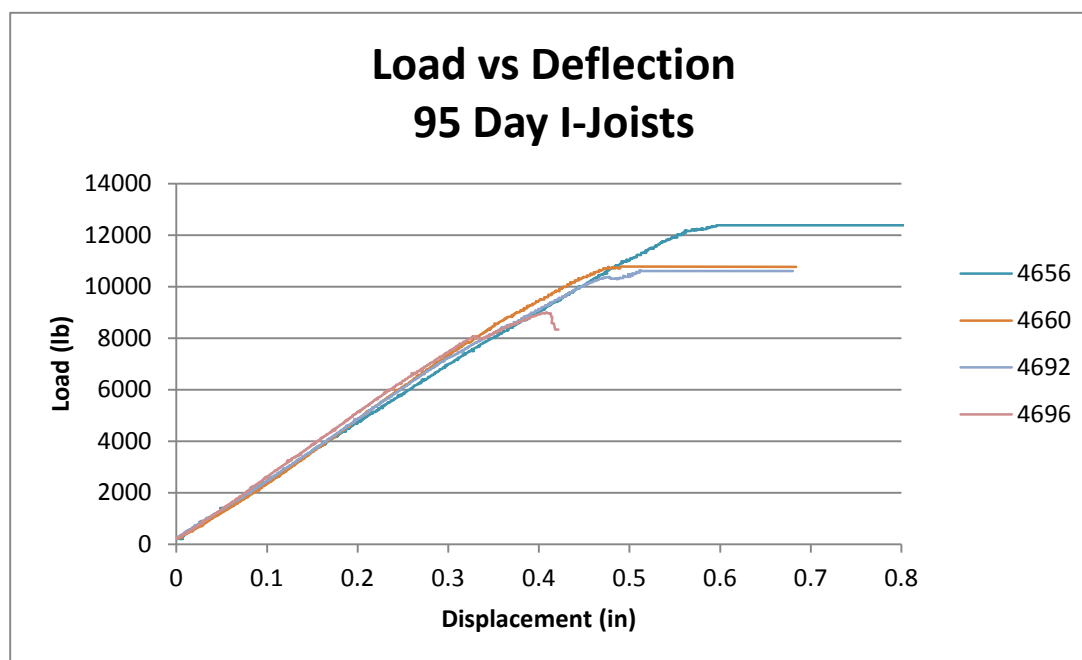


Figure E-8. Load vs. Deflection Curve for 4656, 4660, 4692, 4696

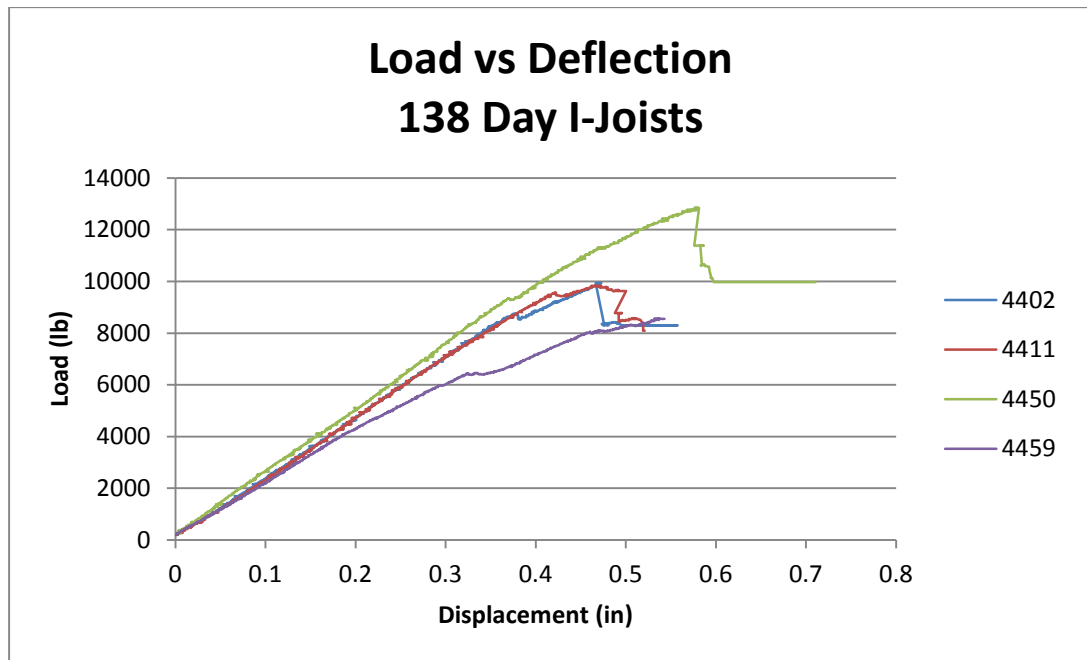


Figure E-9. Load vs. Deflection Curve for 4402, 4411, 4450, and 4459

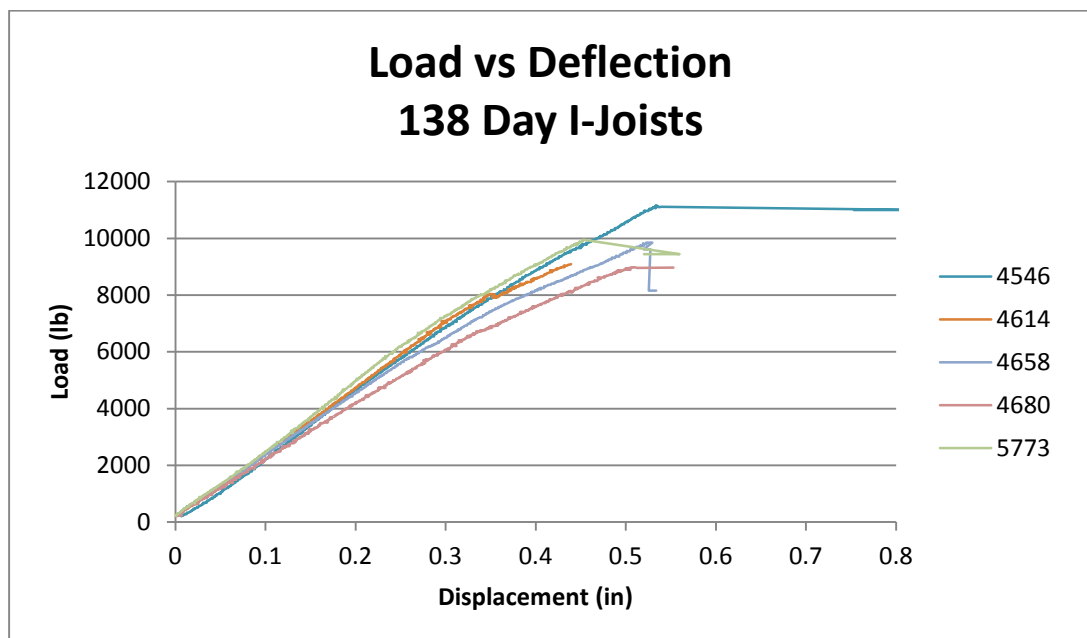


Figure E-10. Load vs. Deflection Curve for 4546, 4614, 4658, 4680, and 5773

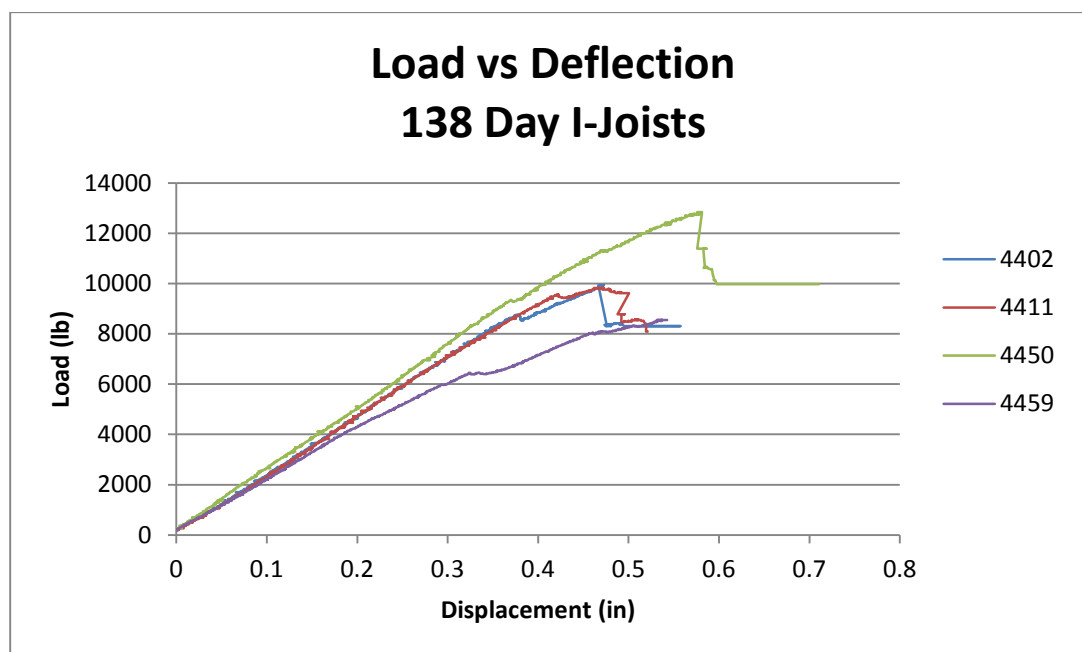


Figure E-11. Load vs. Deflection Curve for 4402, 4411, 4450, and 4459

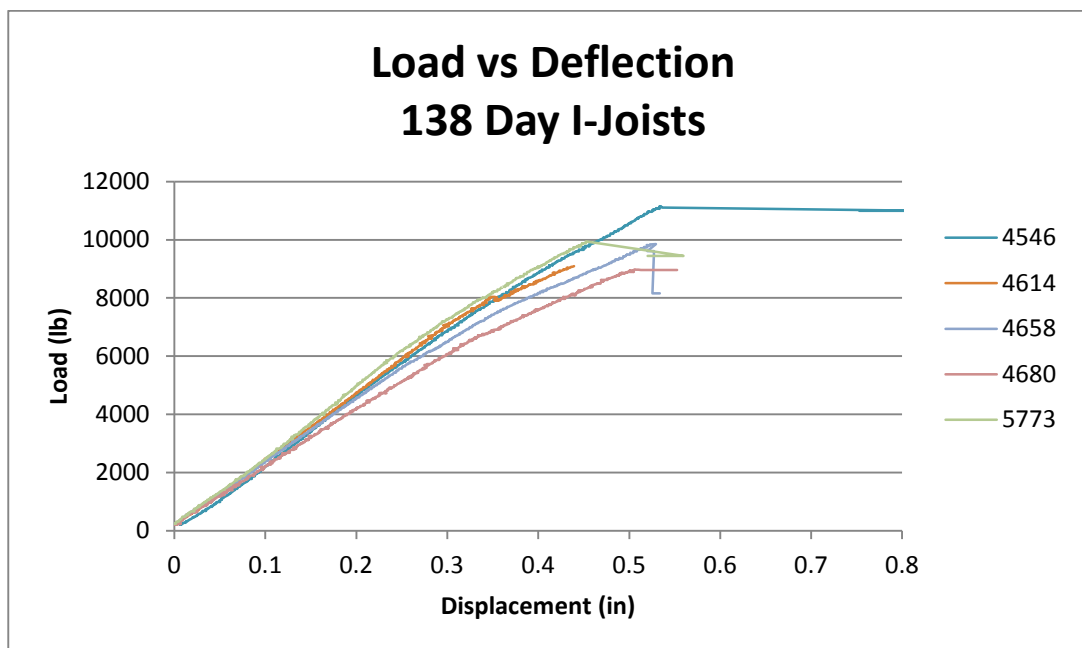


Figure E-12. Load vs. Deflection Curve for 4546, 4614, 4658, 4680, and 5773

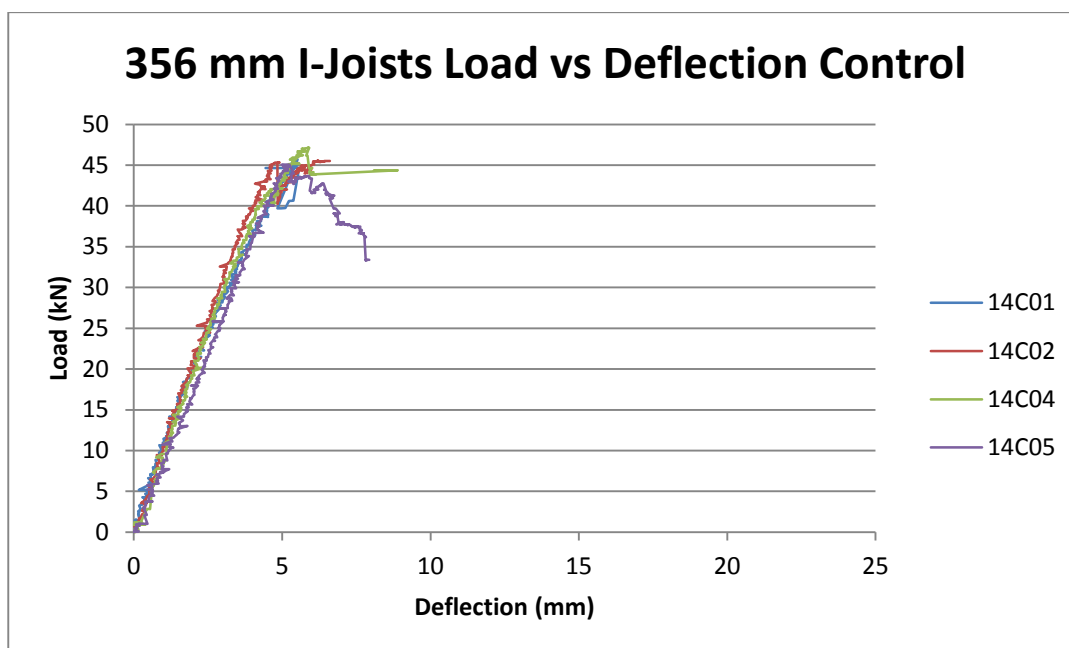


Figure E-13. Load vs. Deflection Curve for 14C01, 14C02, 14C04, and 14C05

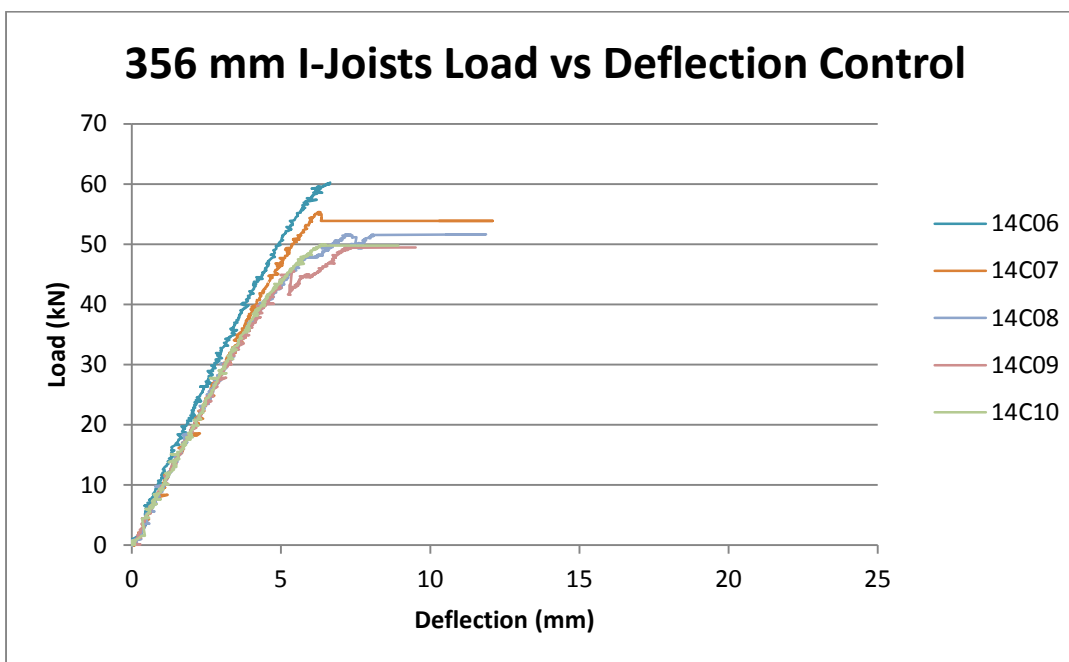


Figure E-14. Load vs. Deflection Curve for 14C06, 14C07, 14C08, 14C09, and 14C10

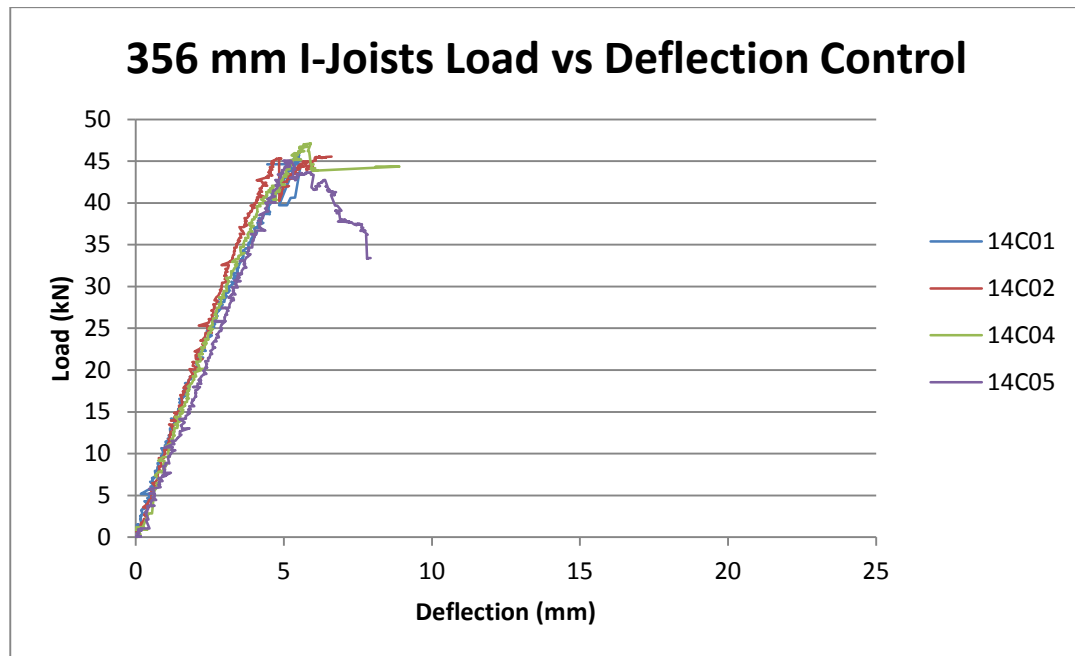


Figure E-15. Load vs. Deflection Curve for 14C01, 14C02, 14C04, and 14C05

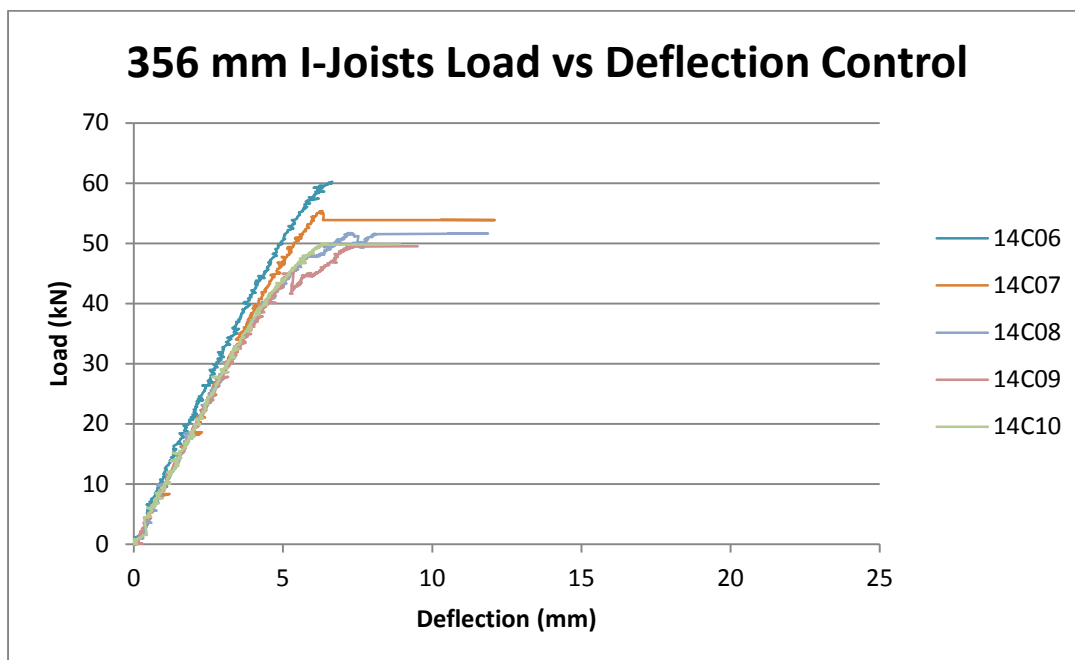


Figure E-16. Load vs. Deflection Curve for 14C06, 14C07, 14C08, 14C09, and 14C10

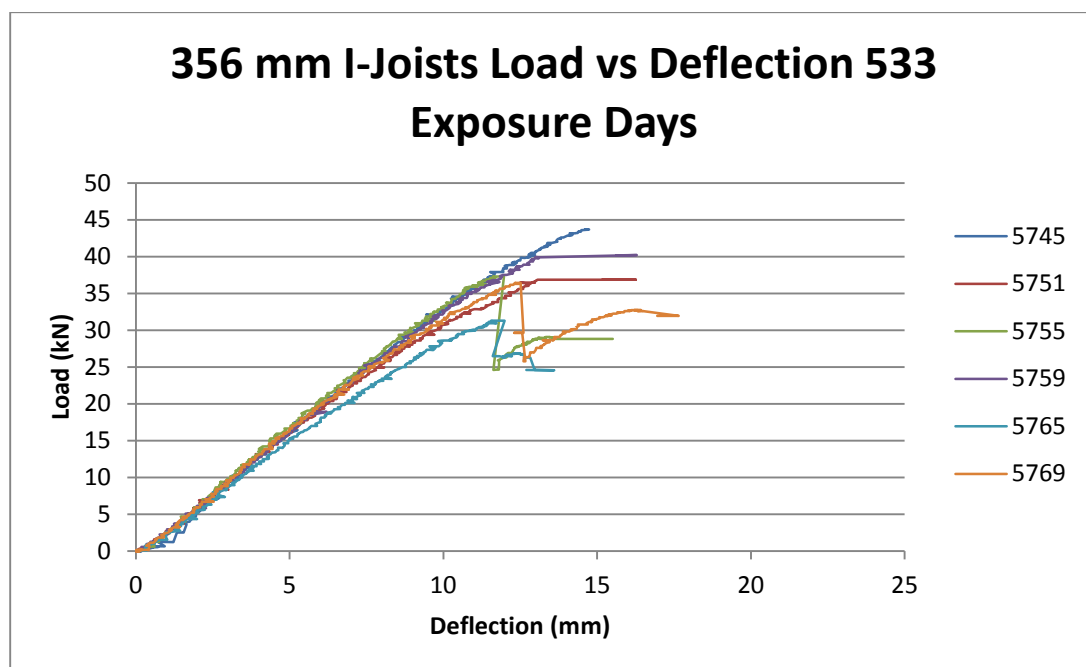


Figure E-17. Load vs. Deflection Curve for 5745, 5751, 5755, 5759, 5765, and 5769

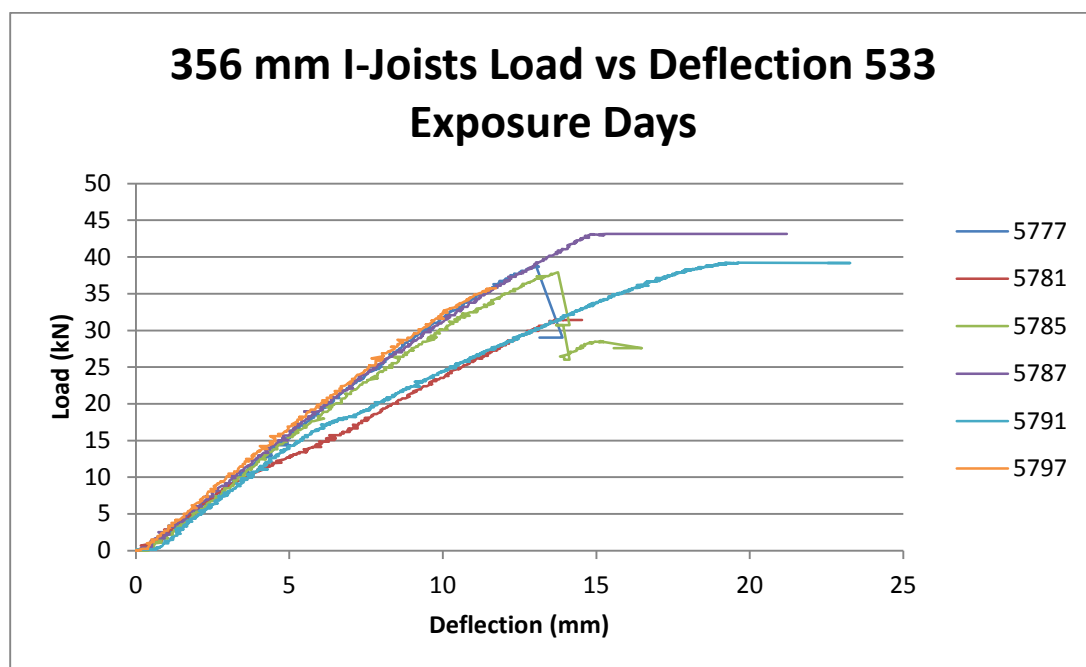


Figure E-18. Load vs. Deflection Curve for 5777, 5781, 5785, 5787, 5791, and 5797

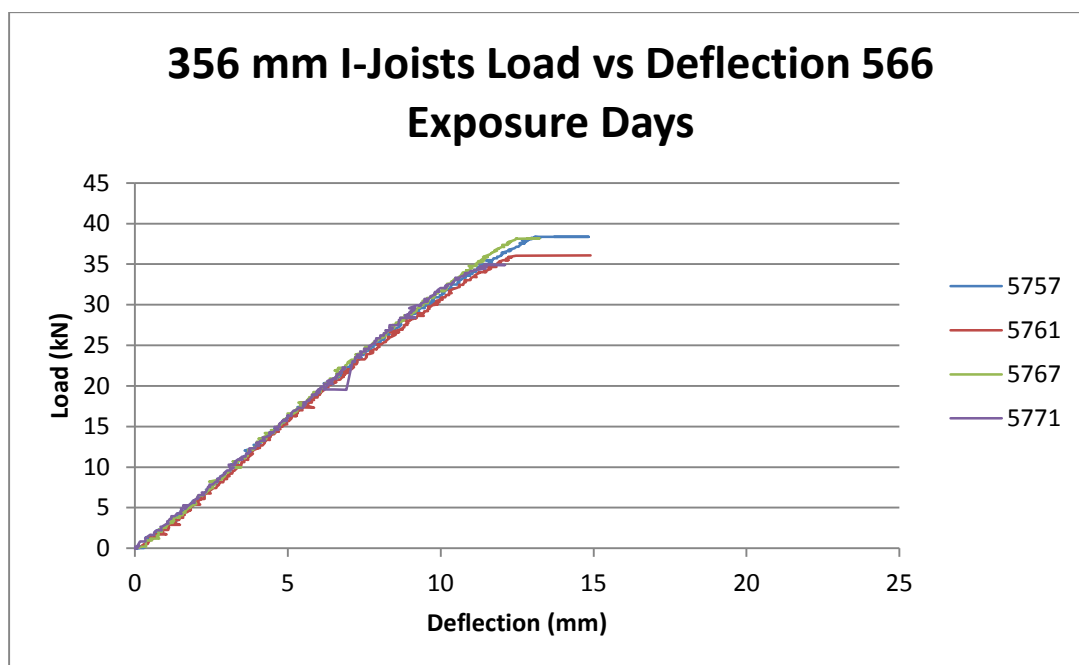


Figure E-19. Load vs. Deflection Curve for 5757, 5761, 5767, and 5771

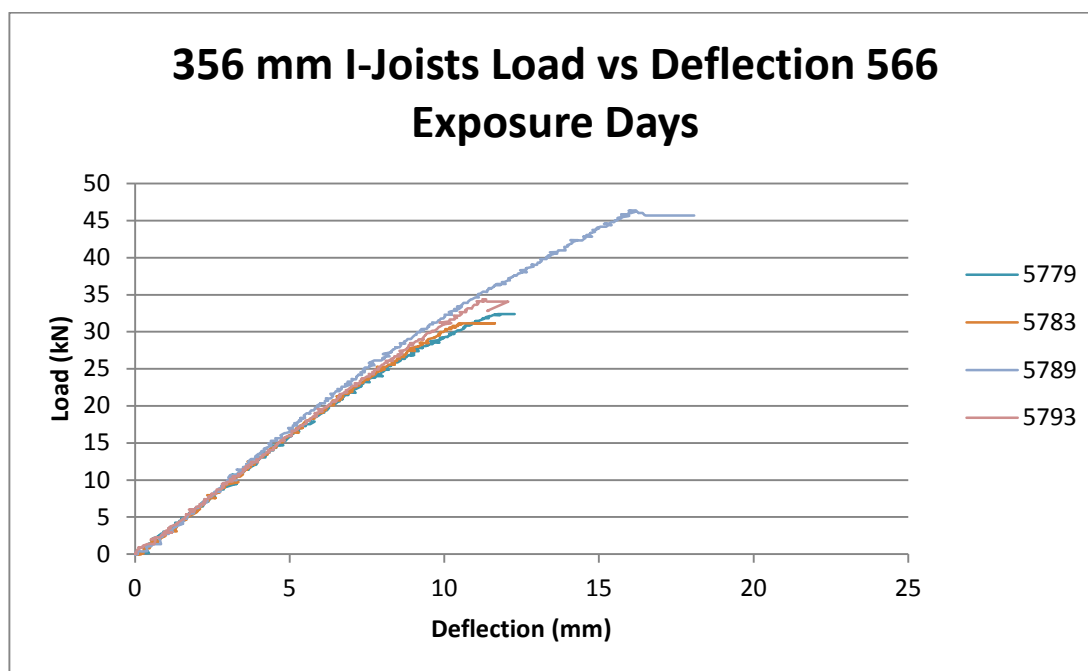


Figure E-20. Load vs. Deflection Curve for 5779, 5783, 5789, and 5793

Appendix F - I-Joist Tension Tests Load and Deflection Data

Table F-1. Tension Test Data

Exposure (days)	Type	Load _{Max} (kN)	Load _{Max} STD	Deflection _{Max} (mm)	Deflection _{Max} STD
0	406	2.98	0.52	2.91	0.32
27	406	3.97		3.28	
65	406	3.14	0.46	2.48	0.23
95	406	2.80	0.32	2.48	0.76
138	406	3.04	0.54	2.92	0.69
0	356	2.93	0.99	3.85	1.45
533	356	1.58	0.41	3.00	1.36
566	356	1.60	0.36	2.53	0.45

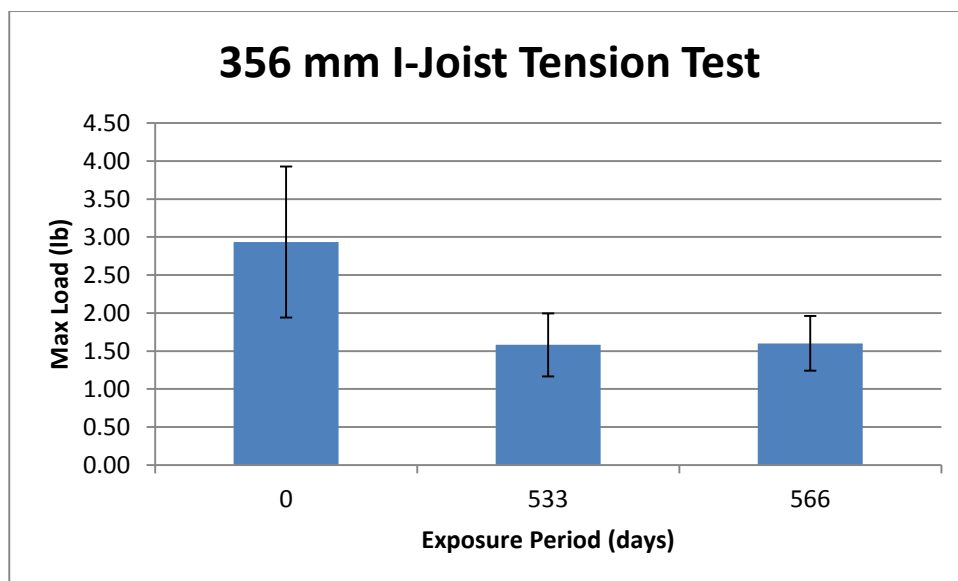


Figure F-1. 356 mm I-Joist Tension Test: Load vs. Exposure Days

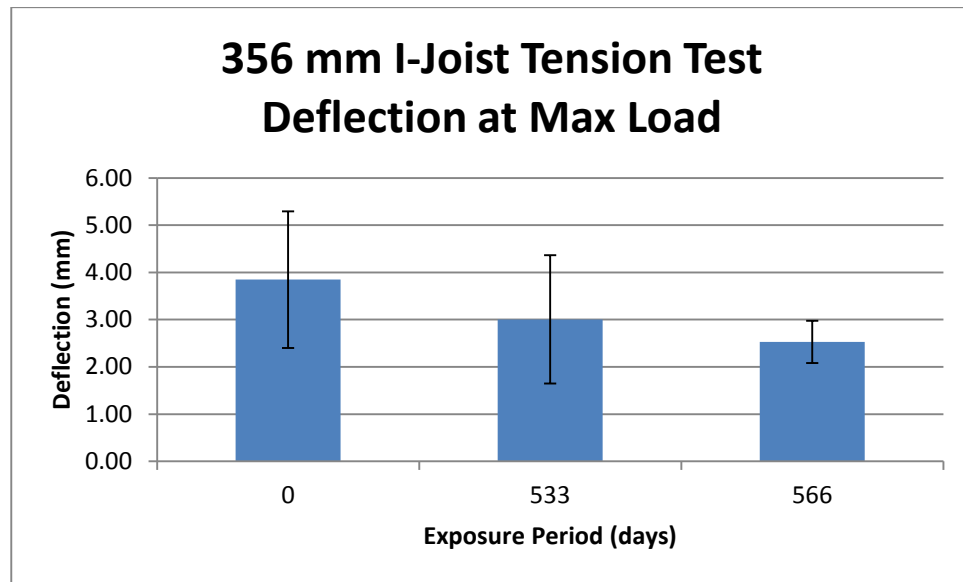


Figure F-2. 356 mm I-Joist Tension Test: Deflection vs. Exposure Days

Appendix G - Shear Wall Construction and Testing



Figure G-1. Building shear wall frames



Figure G-2. Drilling holes in framing members



Figure G-3. Sheathing Construction



Figure G-4. Building Paper Configuration



Figure G-5. Completed Shear Walls

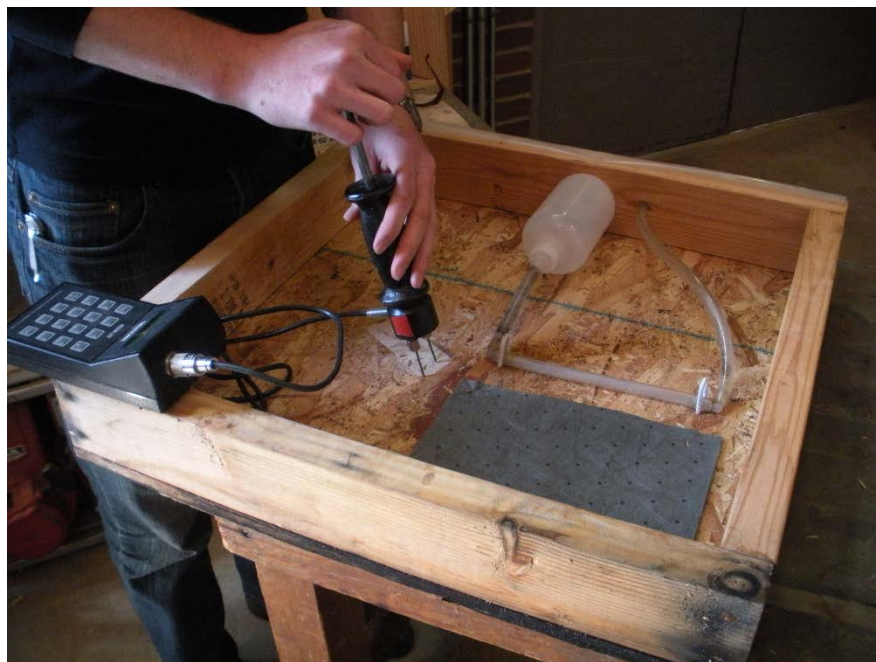


Figure G-6. Moisture Content Measurements

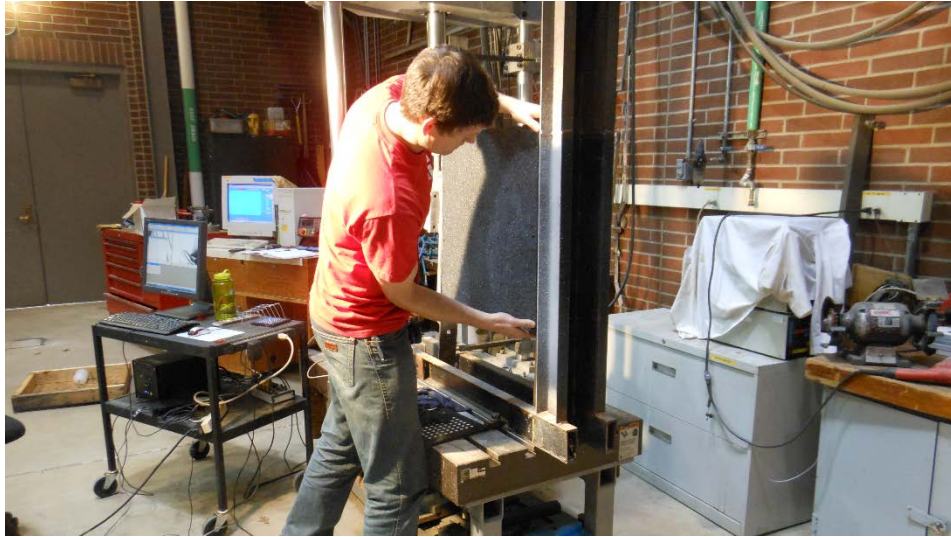


Figure G-7. Shear Wall Test Installation



Figure G-8. Shear Wall Test Setup

Appendix H - Moisture Content Maps

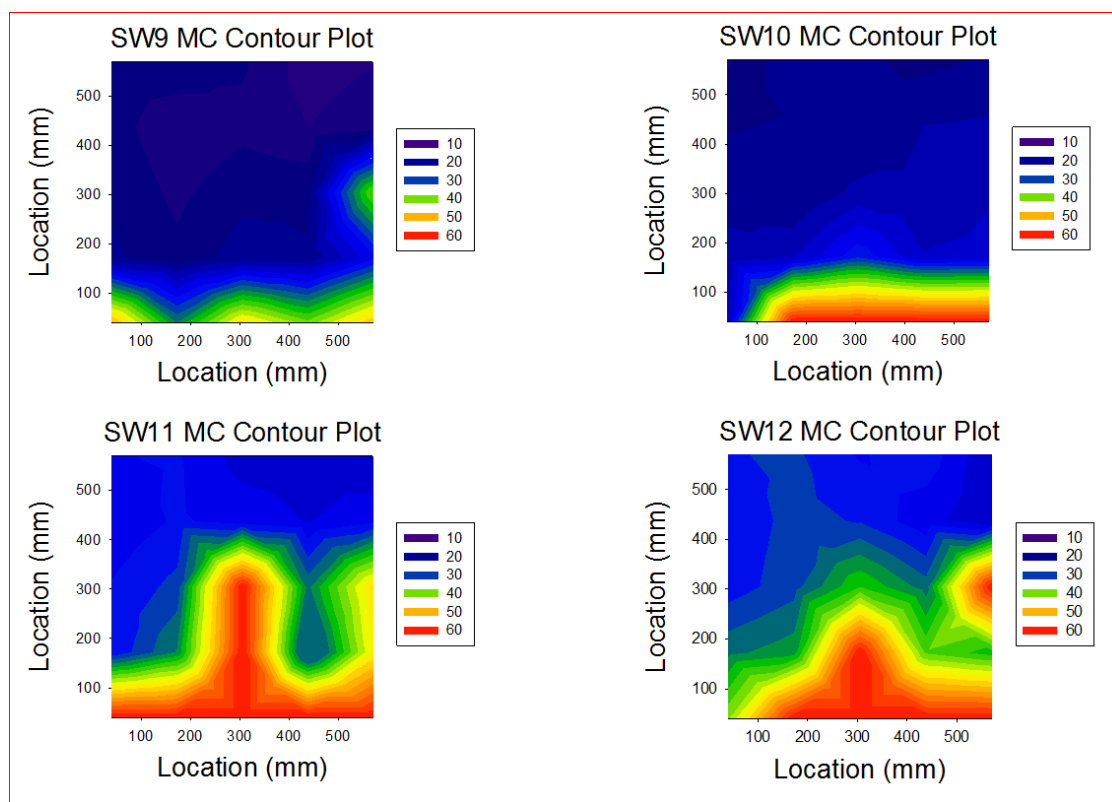


Figure H-1. Moisture Content Contour Plots of SW9, SW10, SW11, and SW12

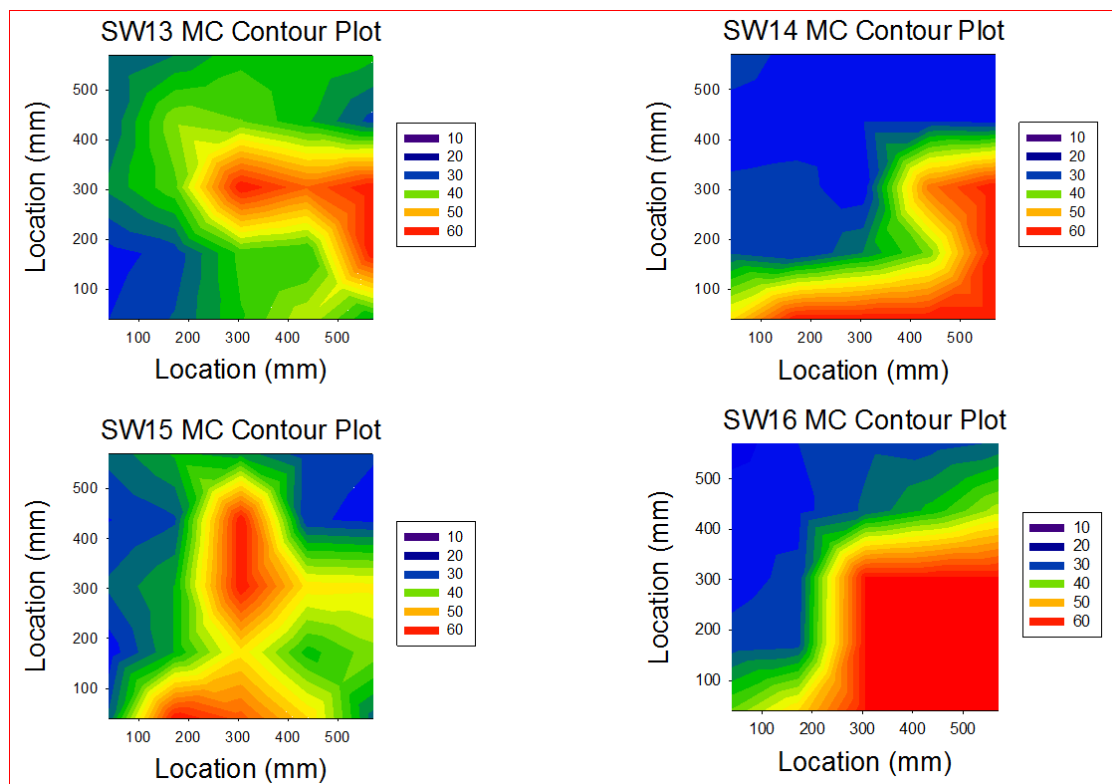


Figure H-2. Moisture Content Contour Plots of SW13, SW14, SW15, and SW16

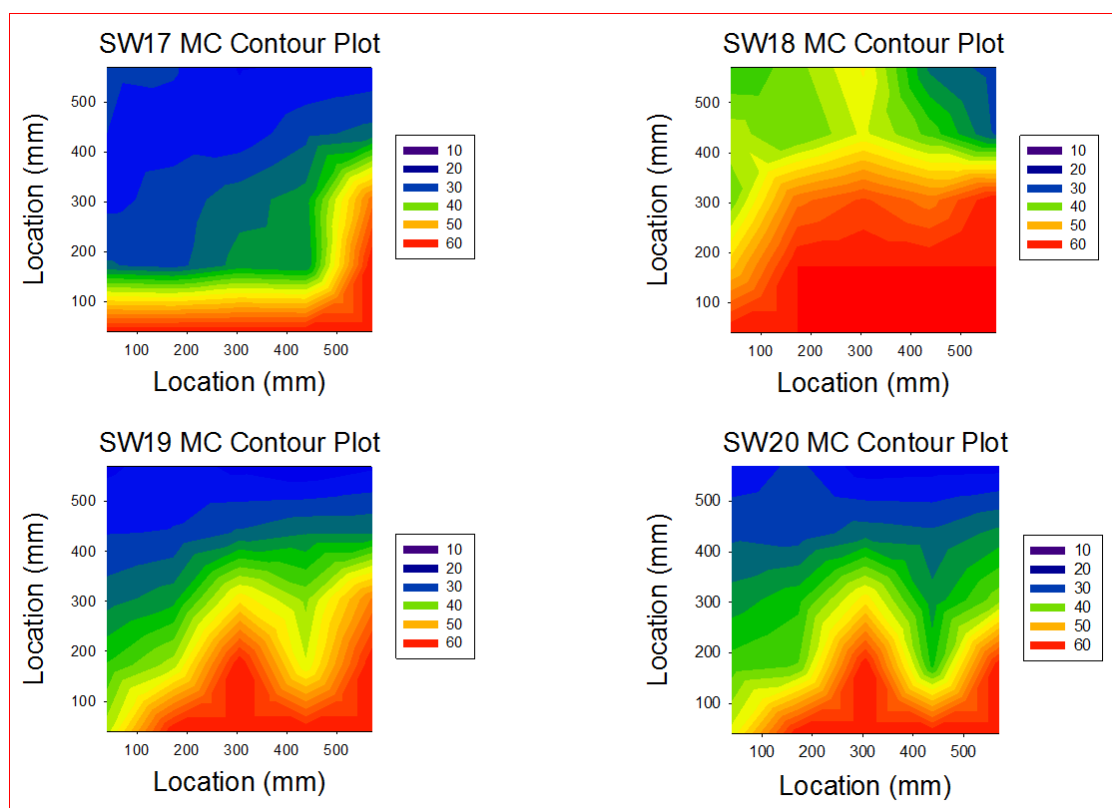


Figure H-3. Moisture Content Contour Plots of SW17, SW18, SW19, and SW20

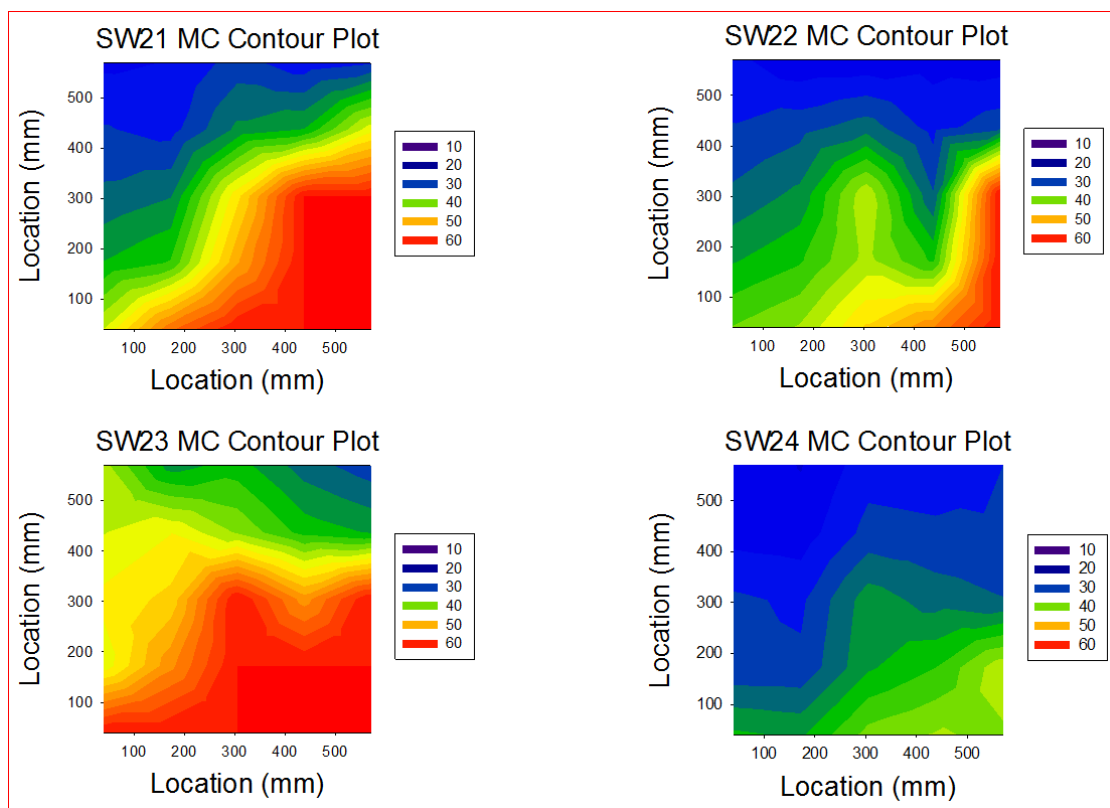


Figure H-4. Moisture Content Contour Plots of SW21, SW22, SW23, and SW24

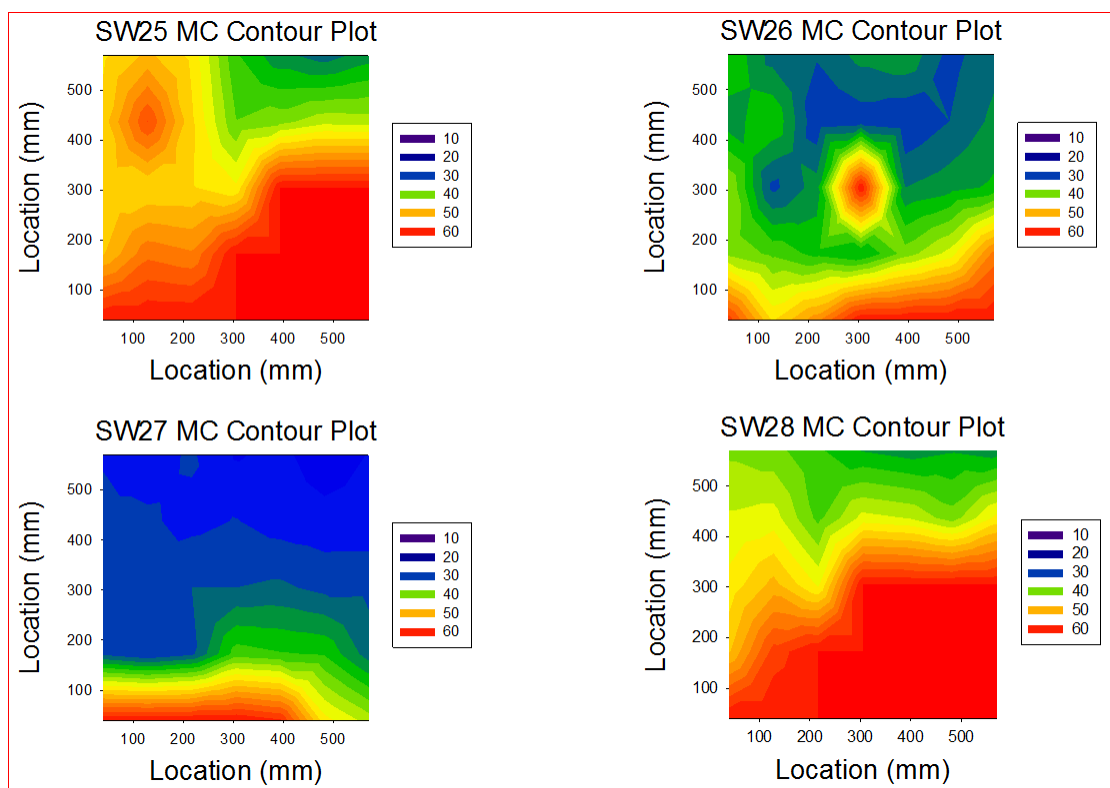


Figure H-5. Moisture Content Contour Plots of SW25, SW26, SW27, and SW28

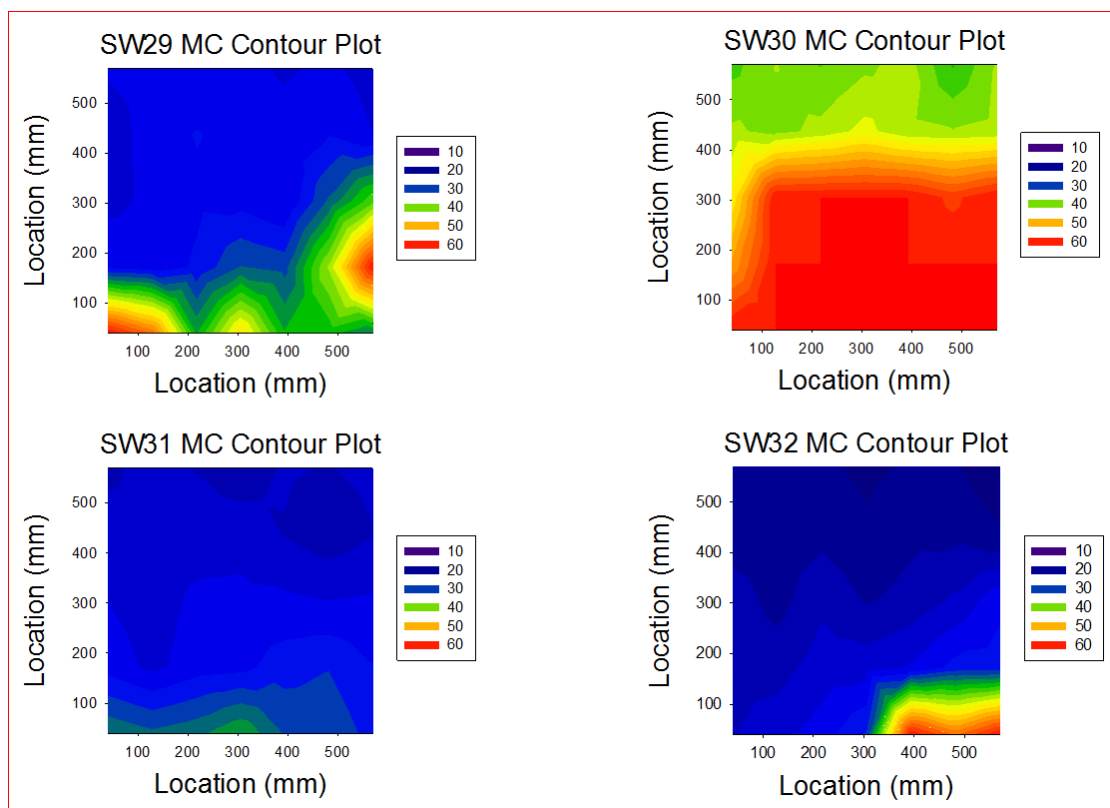


Figure H-6. Moisture Content Contour Plots of SW29, SW30, SW31, and SW32

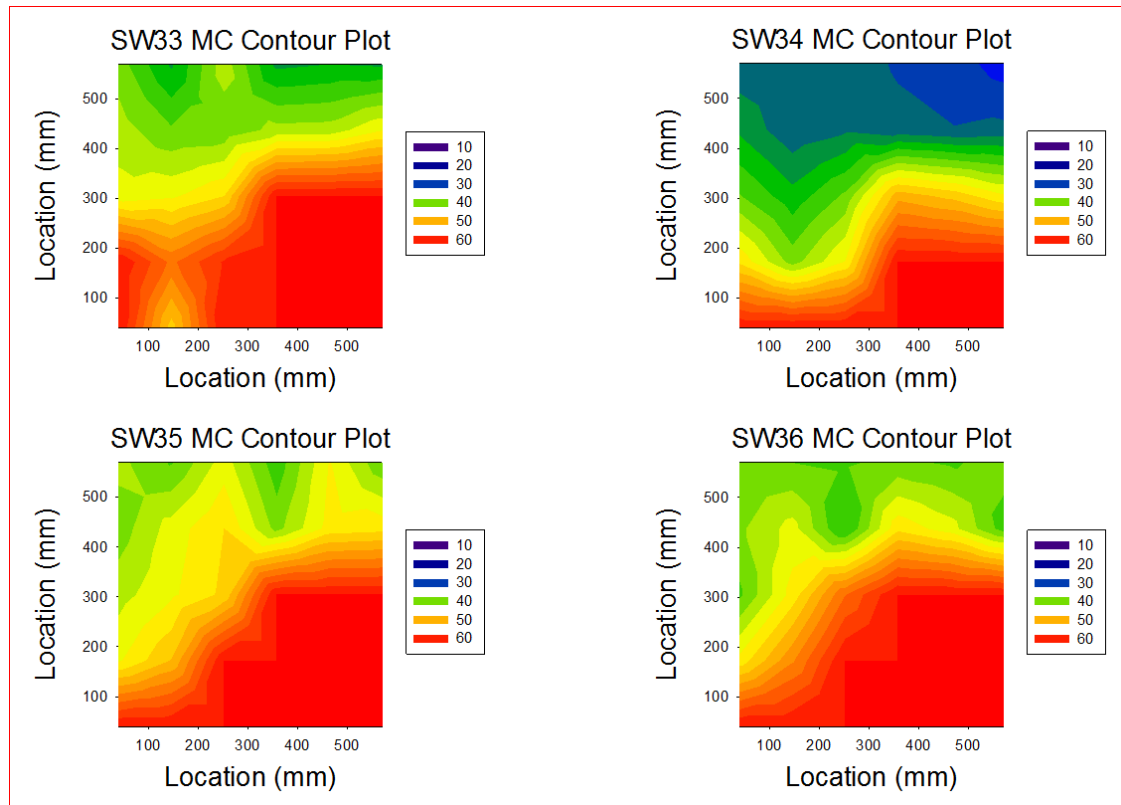


Figure H-7. Moisture Content Contour Plots of SW33, SW34, SW35, and SW36

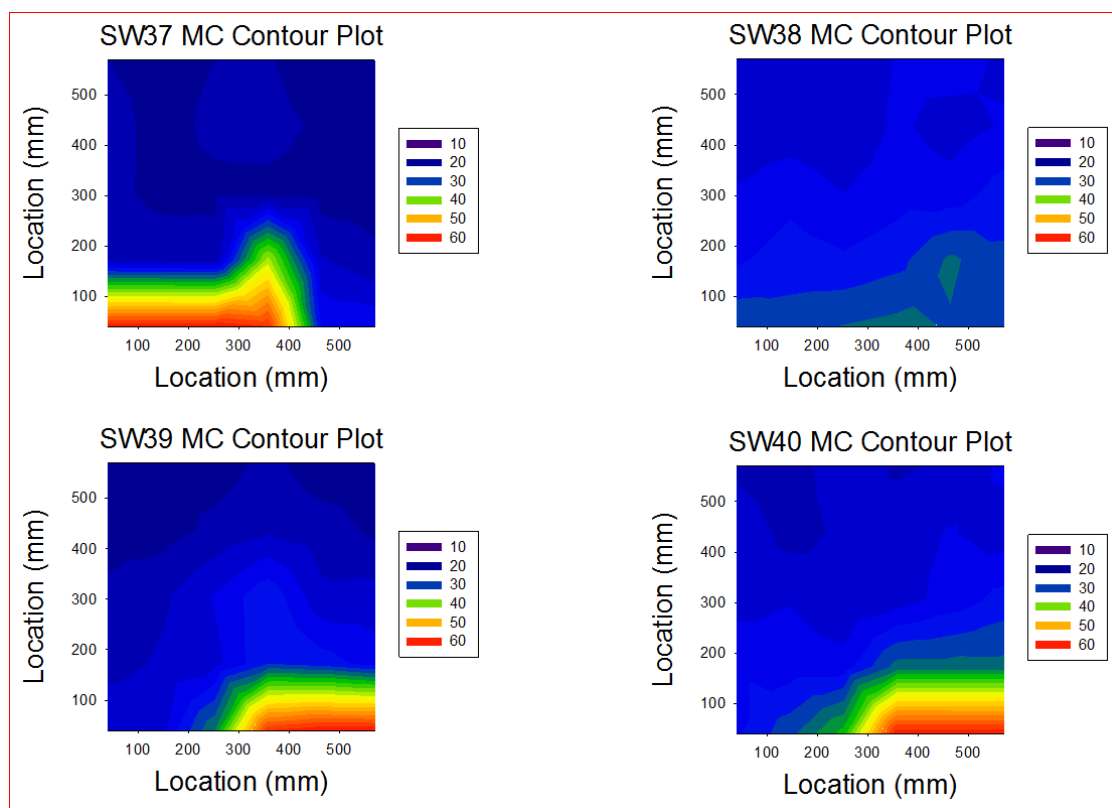


Figure H-8. Moisture Content Contour Plots of SW37, SW38, SW39, and SW40

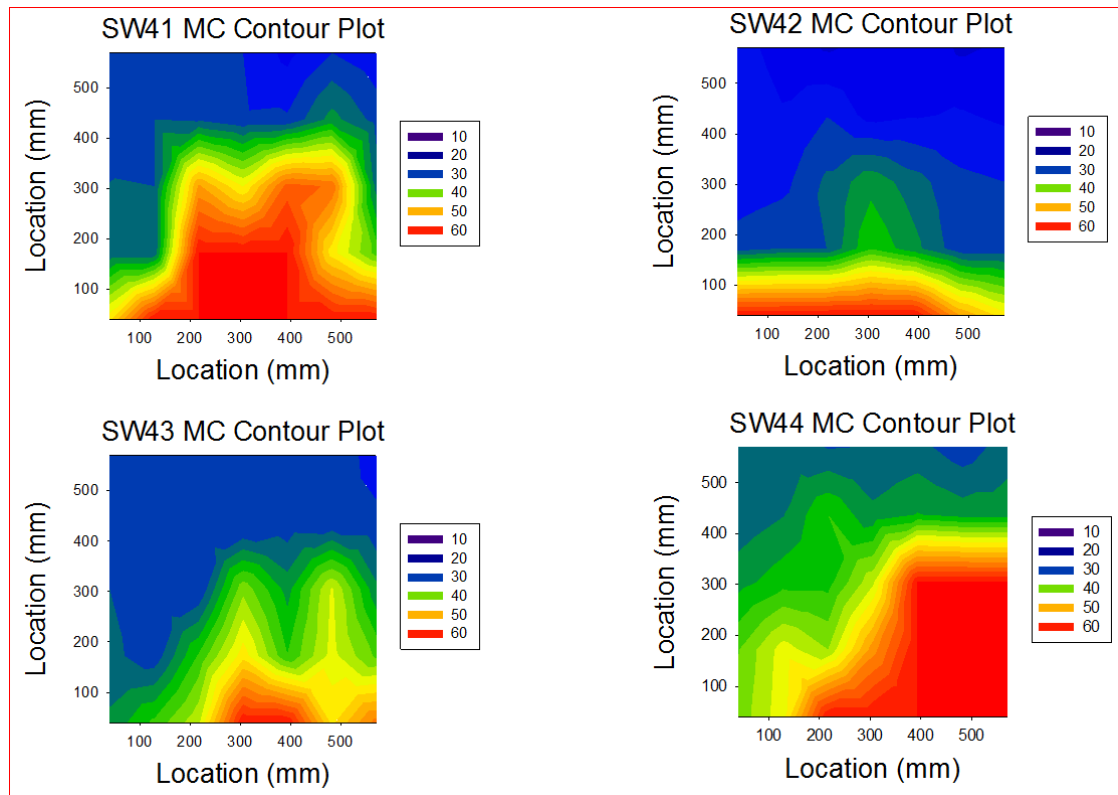


Figure H-9. Moisture Content Contour Plots of SW41, SW42, SW43, and SW44

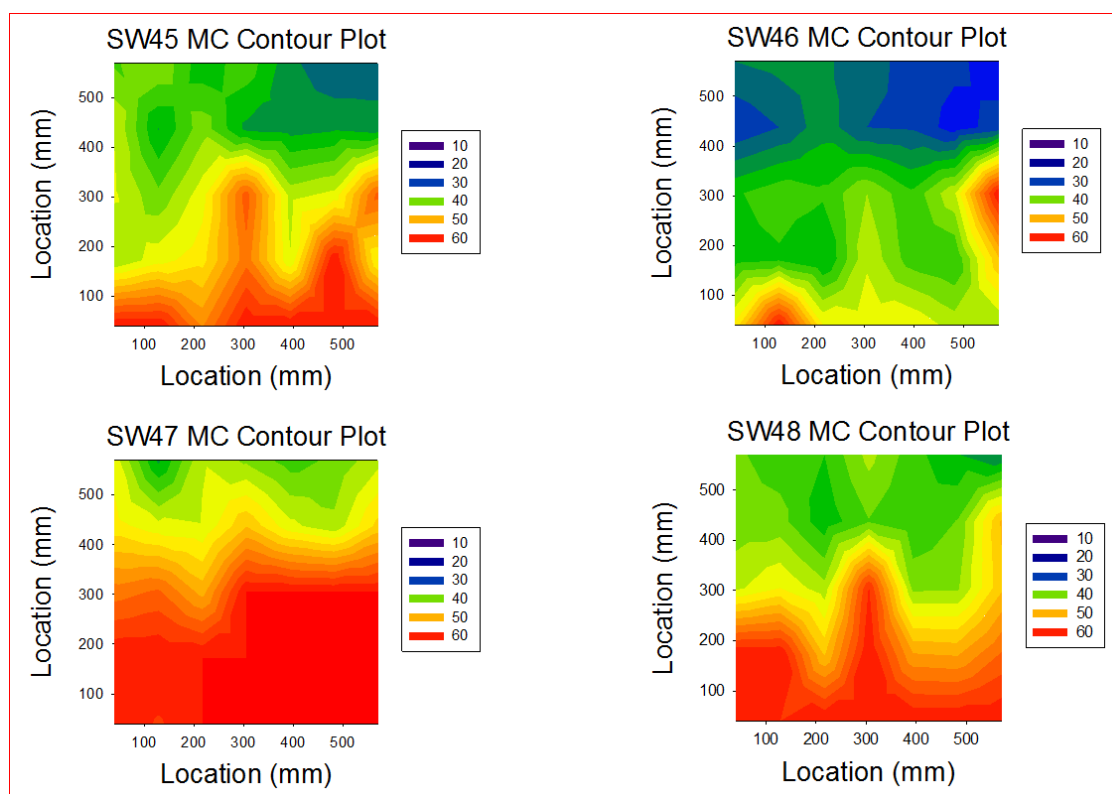


Figure H-10. Moisture Content Contour Plots of SW45, SW46, SW47, and SW48

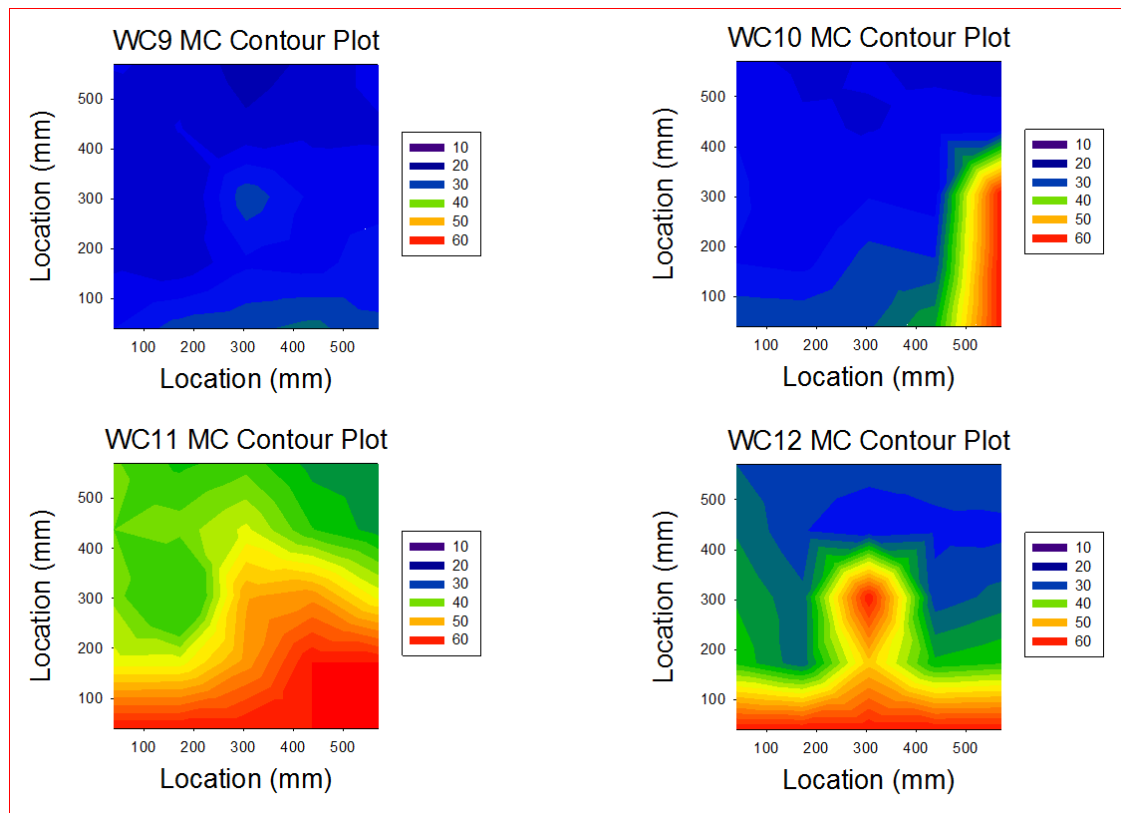


Figure H-11. Moisture Content Contour Plots of WC9, WC10, WC11, and WC12

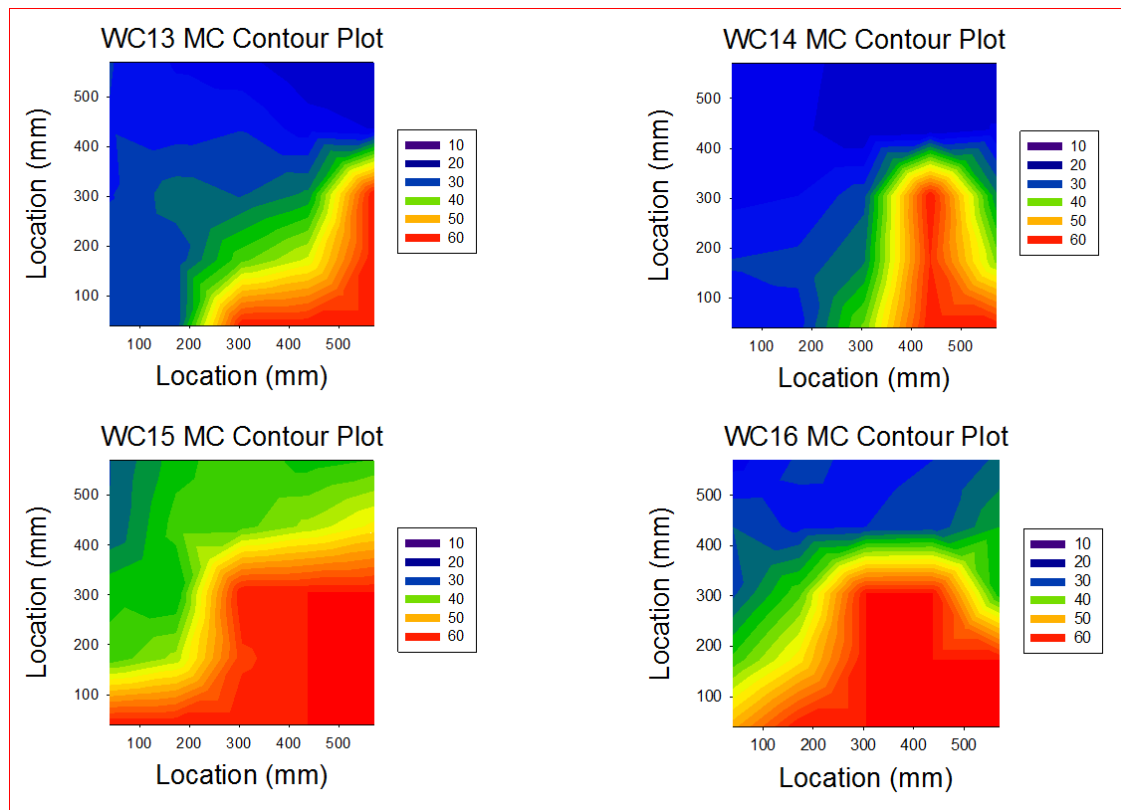


Figure H-12. Moisture Content Contour Plots of WC13, WC14, WC15, and WC16

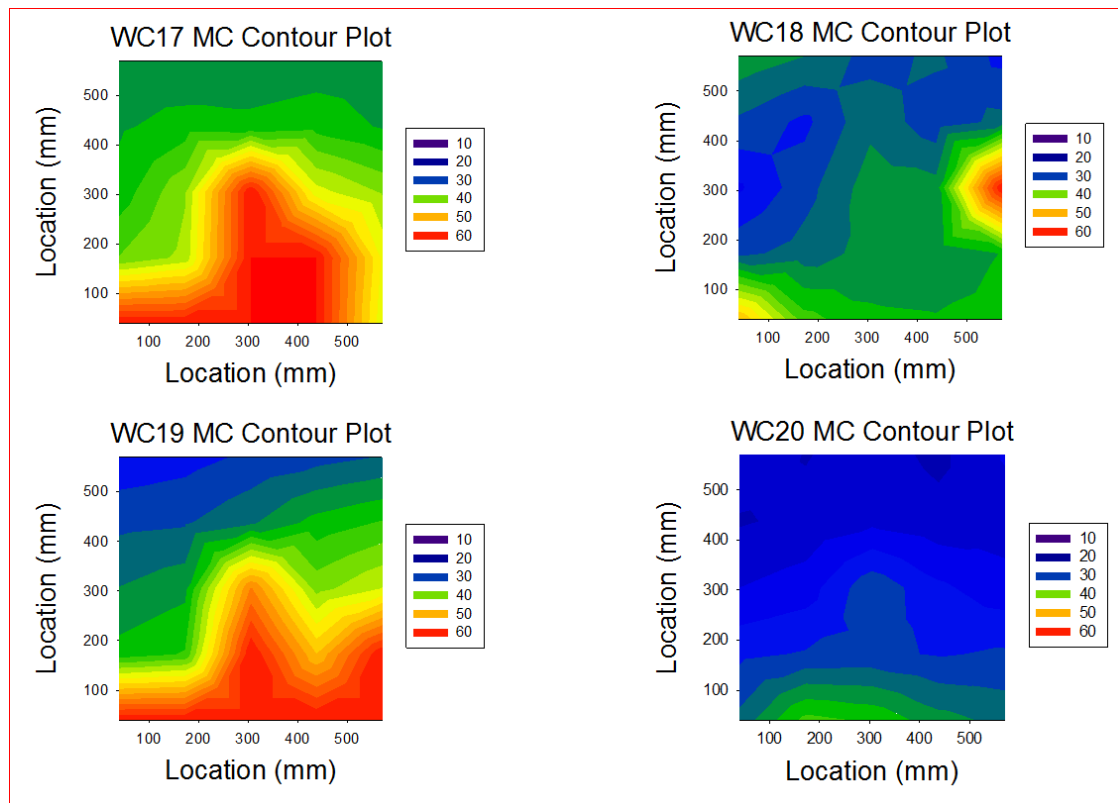


Figure H-13. Moisture Content Contour Plots of WC17, WC18, WC19, and WC20

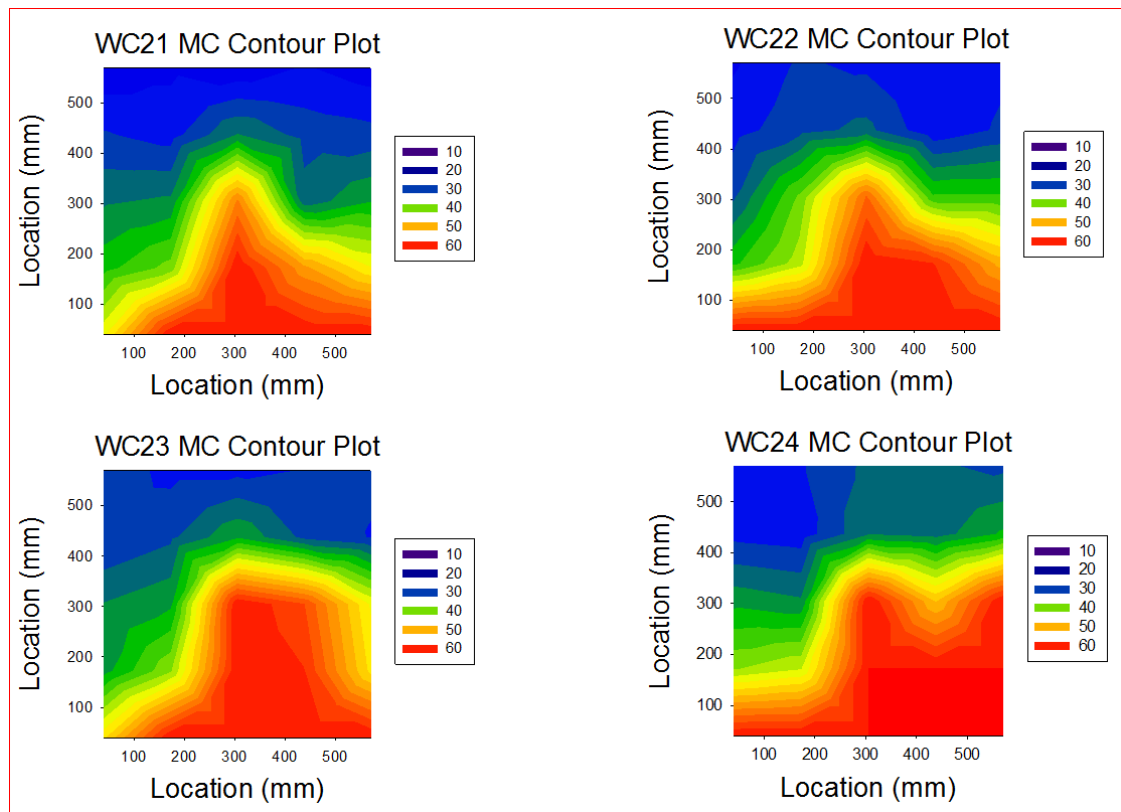


Figure H-14. Moisture Content Contour Plots of WC21, WC22, WC23, and WC24

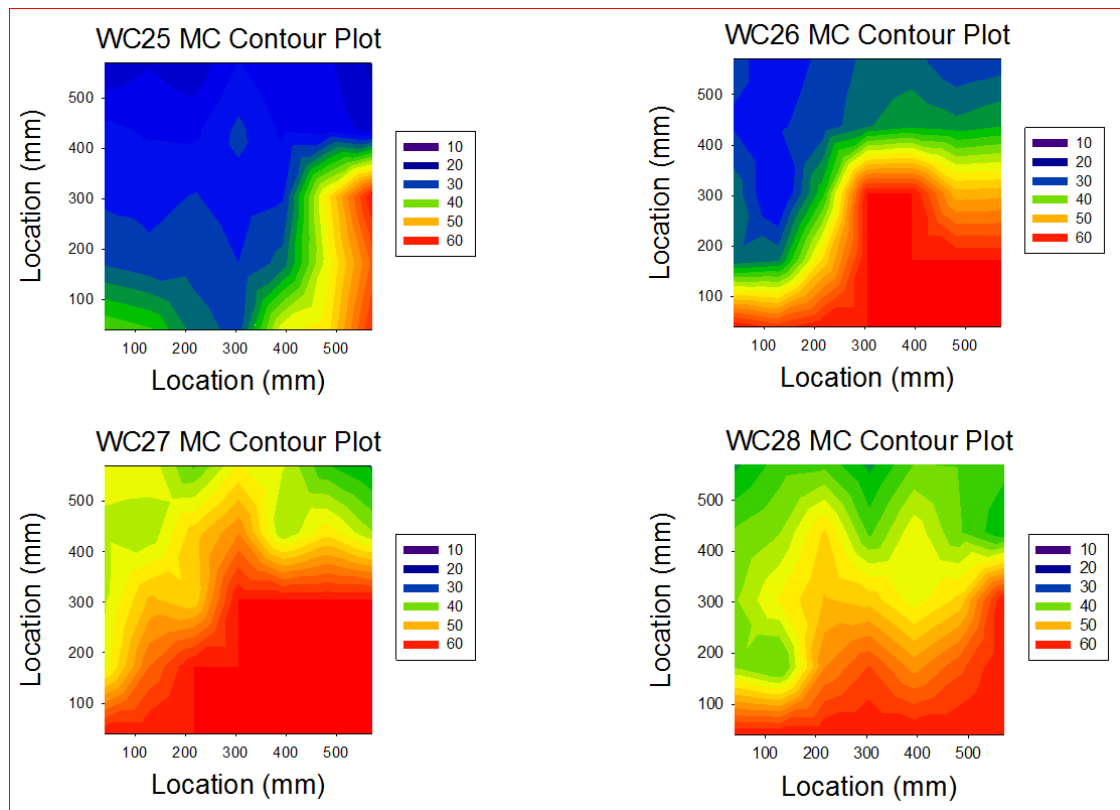


Figure H-15. Moisture Content Contour Plots of WC25, WC26, WC27, and WC28

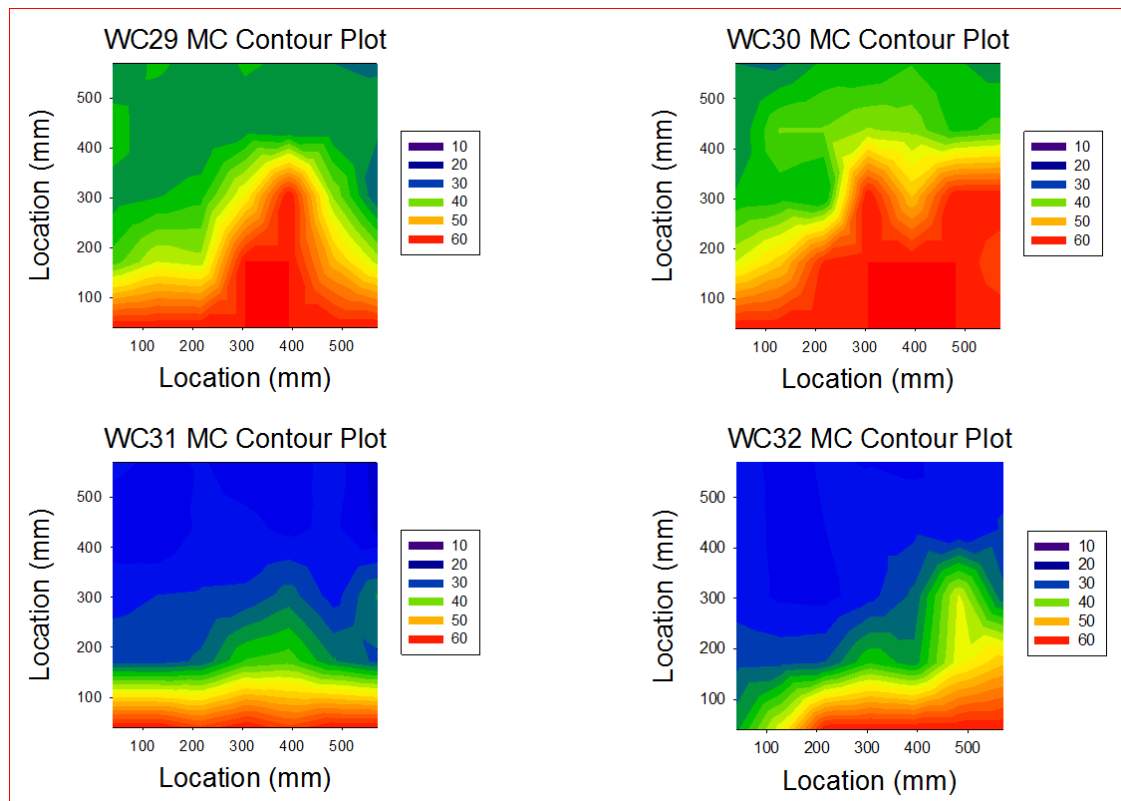


Figure H-16. Moisture Content Contour Plots of WC29, WC30, WC31, and WC32

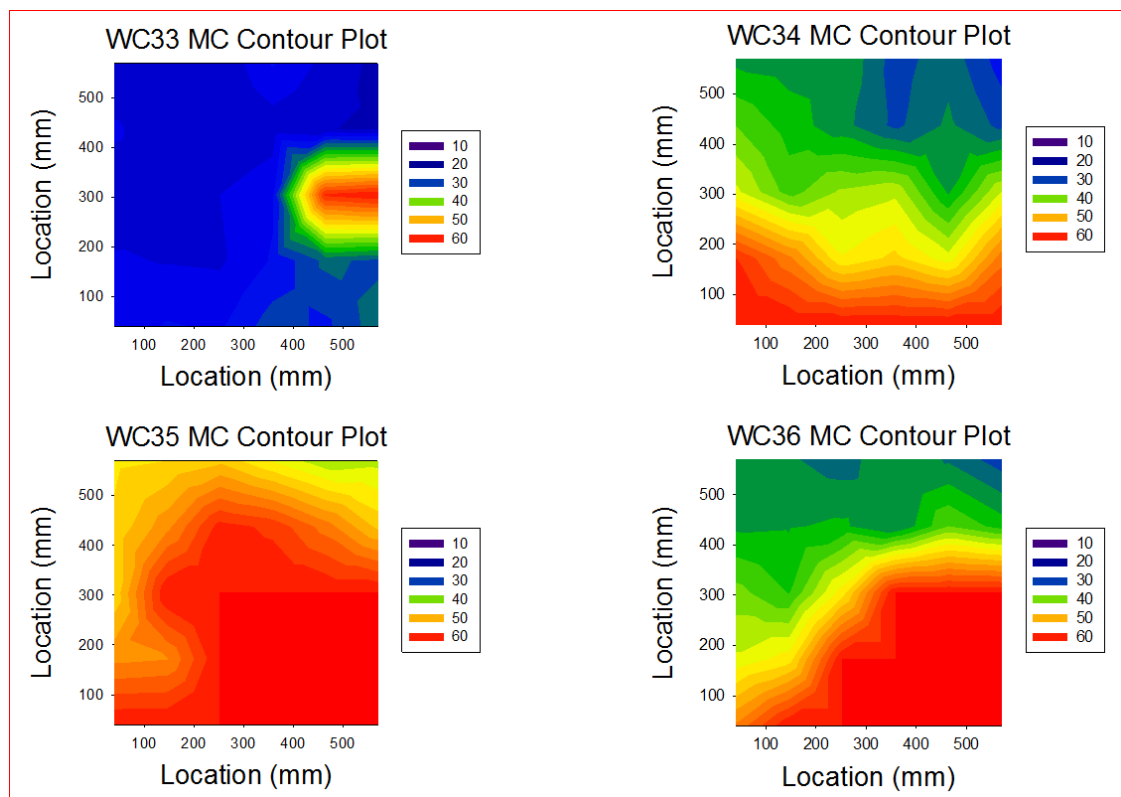


Figure H-17. Moisture Content Contour Plots of WC33, WC34, WC35, and WC36

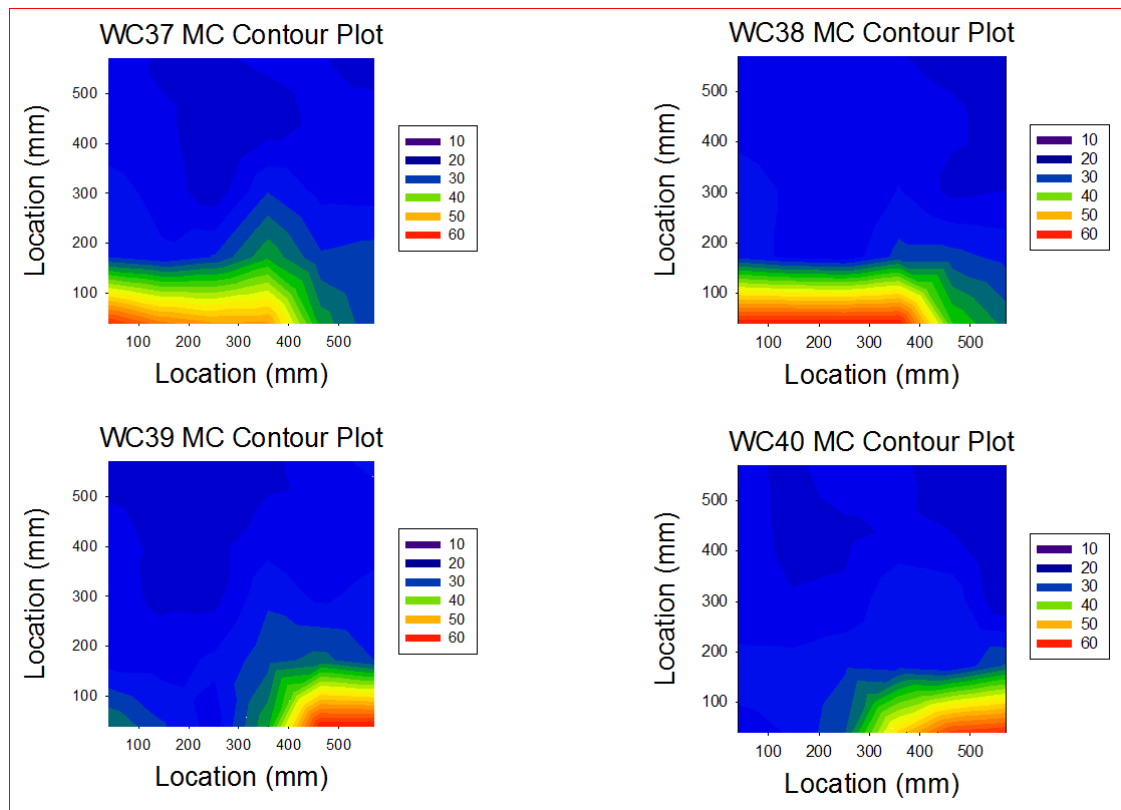


Figure H-18. Moisture Content Contour Plots of WC37, WC38, WC39, and WC40

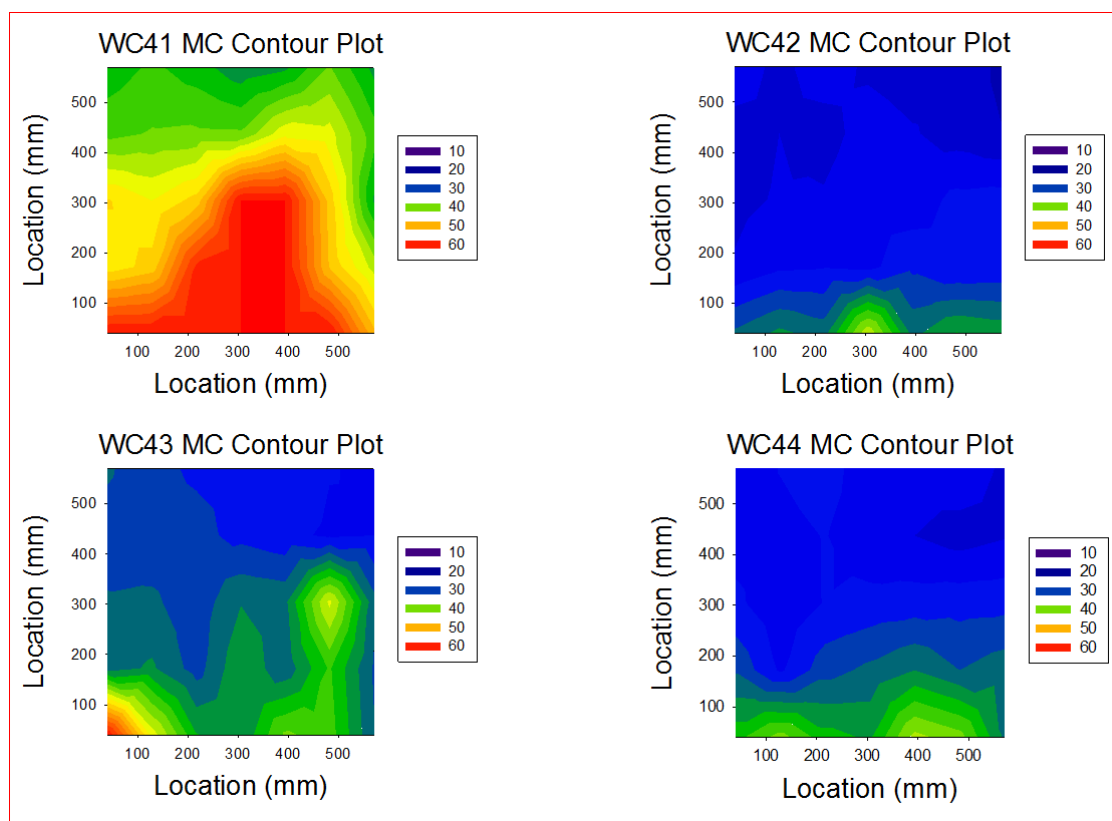


Figure H-19. Moisture Content Contour Plots of WC41, WC42, WC43, and WC44

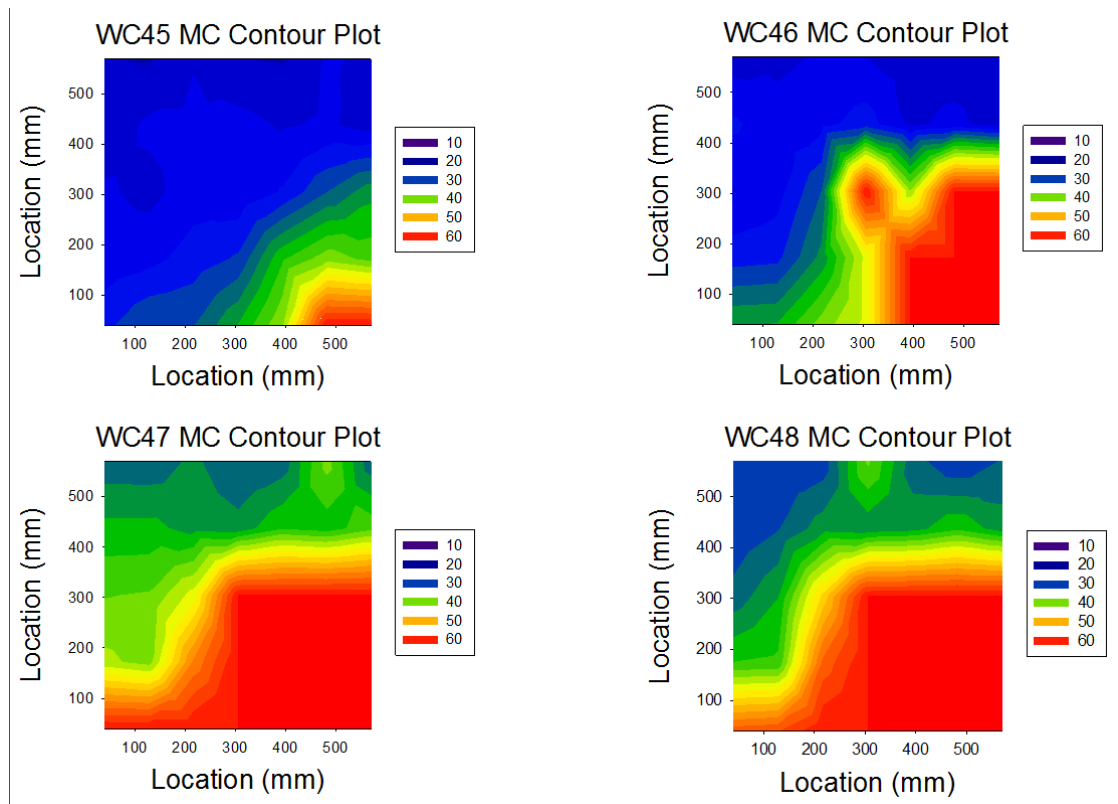


Figure H-20. Moisture Content Contour Plots of WC45, WC46, WC47, and WC48

Appendix I – Pilodyn Contour Plots

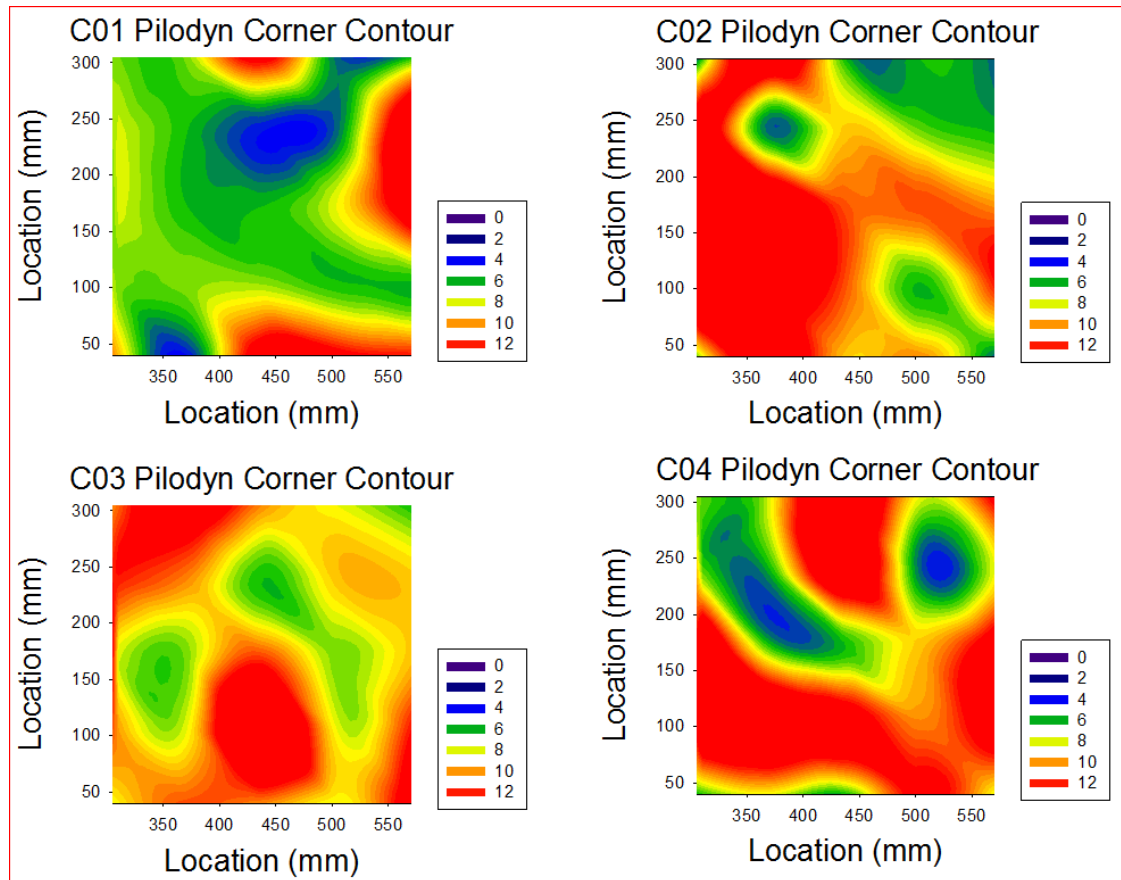


Figure I-1. Pilodyn Corner Contour Plots of C01, C02, C03, and C04

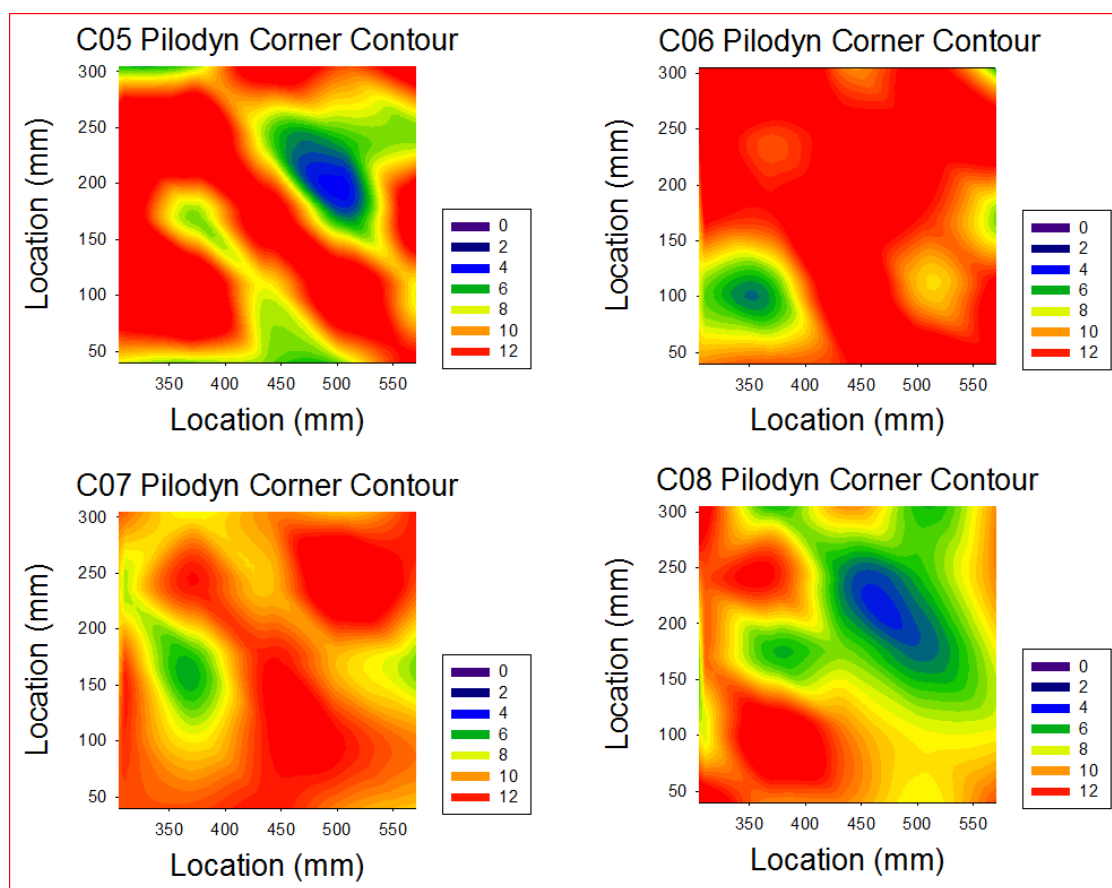


Figure I-2. Pilodyn Corner Contour Plots of C05, C06, C07, and C08

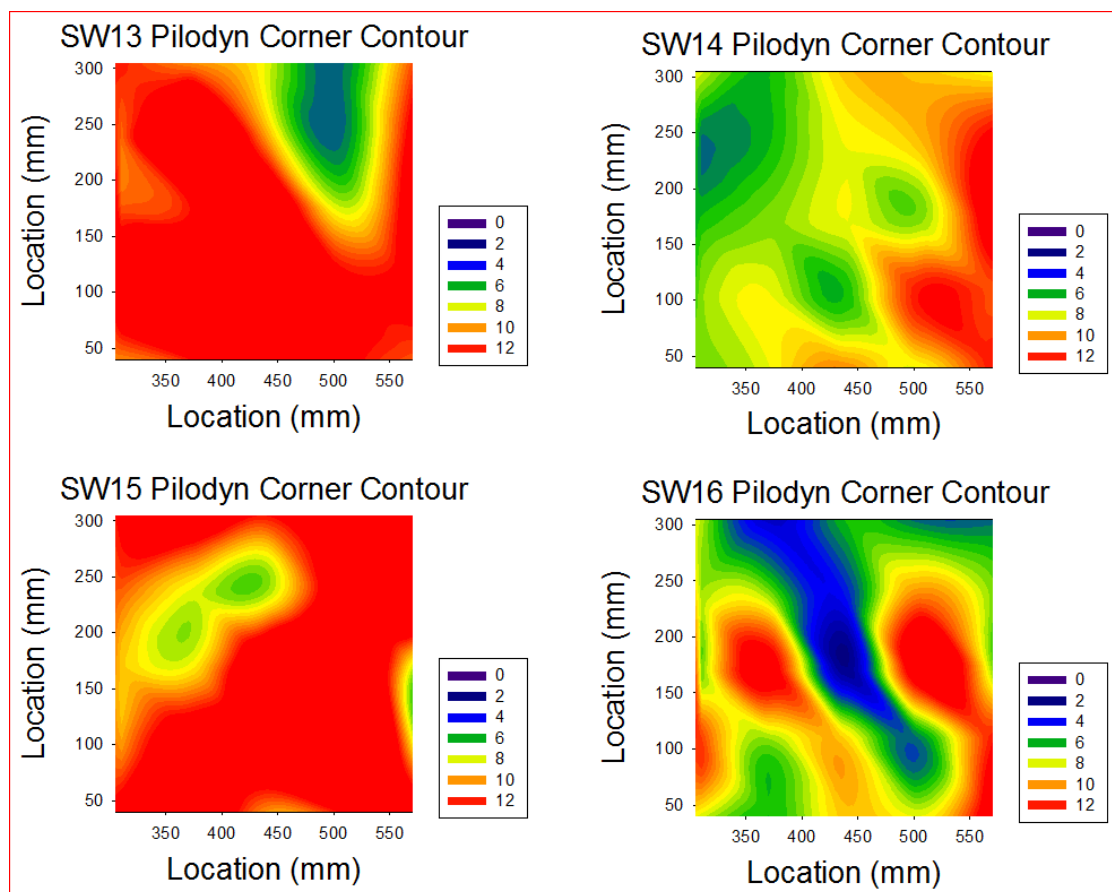


Figure I-3. Pilodyn Corner Contour Plots of SW13, SW14, SW15, and SW16

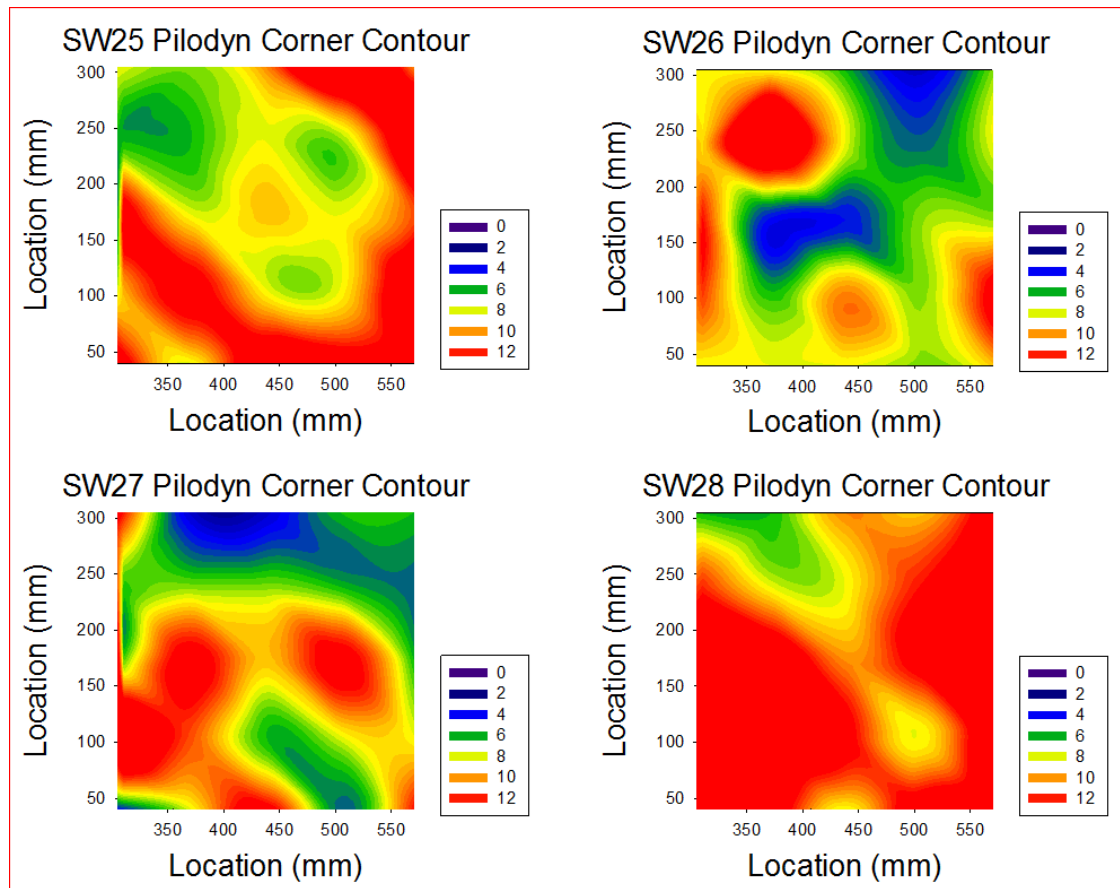


Figure I-4. Pilodyn Corner Contour Plots of SW25, SW26, SW27, and SW28

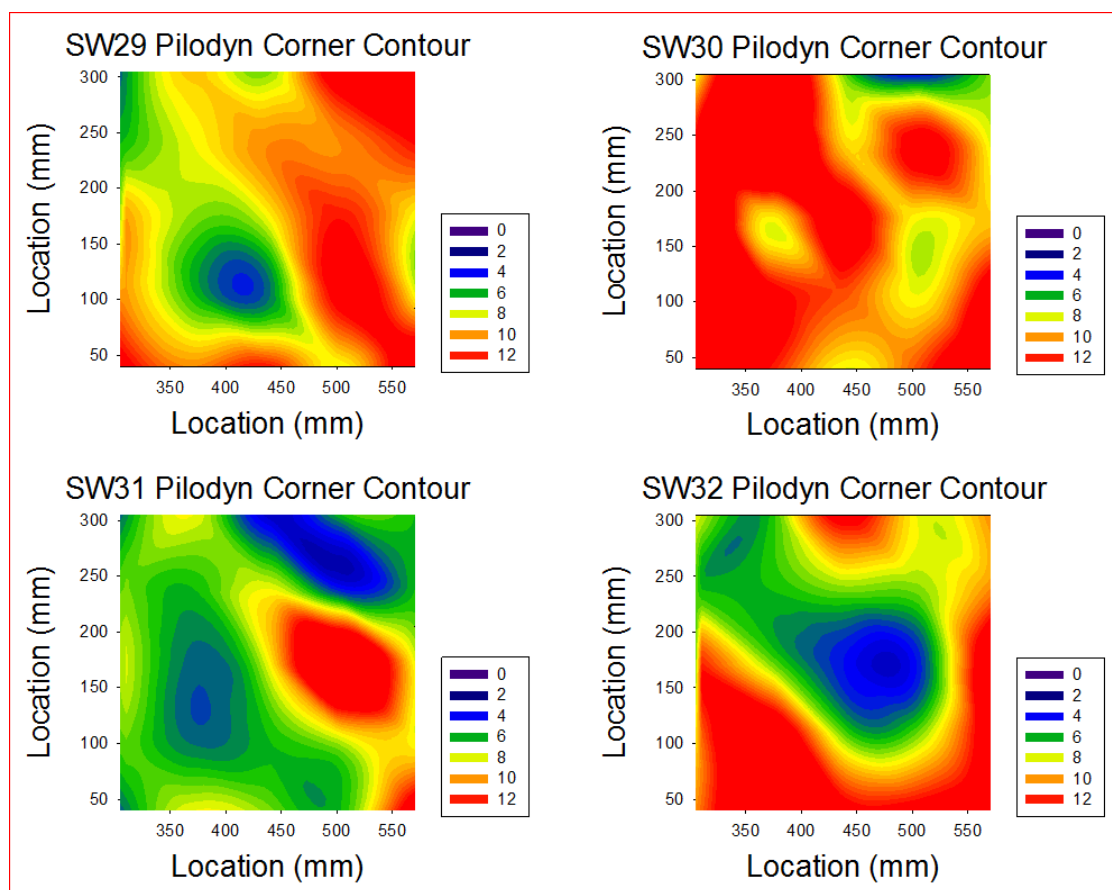


Figure I-5. Pilodyn Corner Contour Plots of SW29, SW30, SW31, and SW32

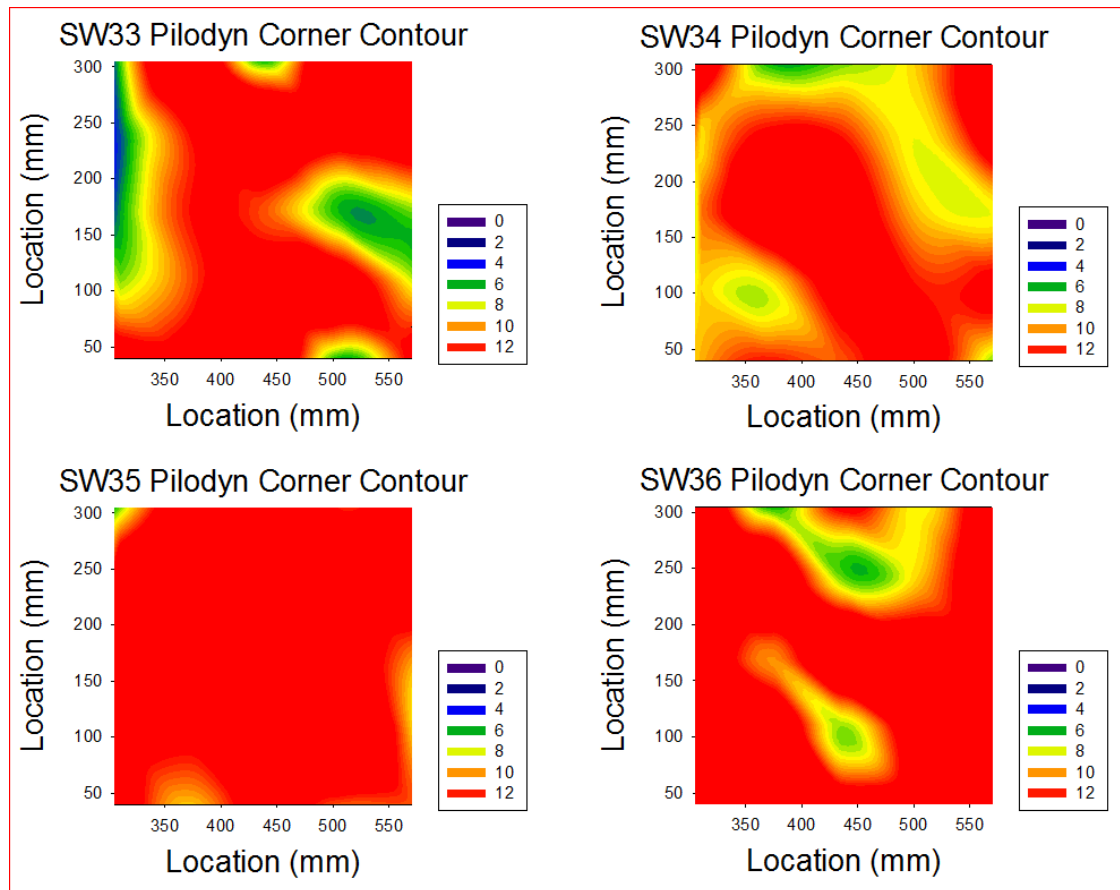


Figure I-6. Pilodyn Corner Contour Plots of SW33, SW34, SW35, and SW36

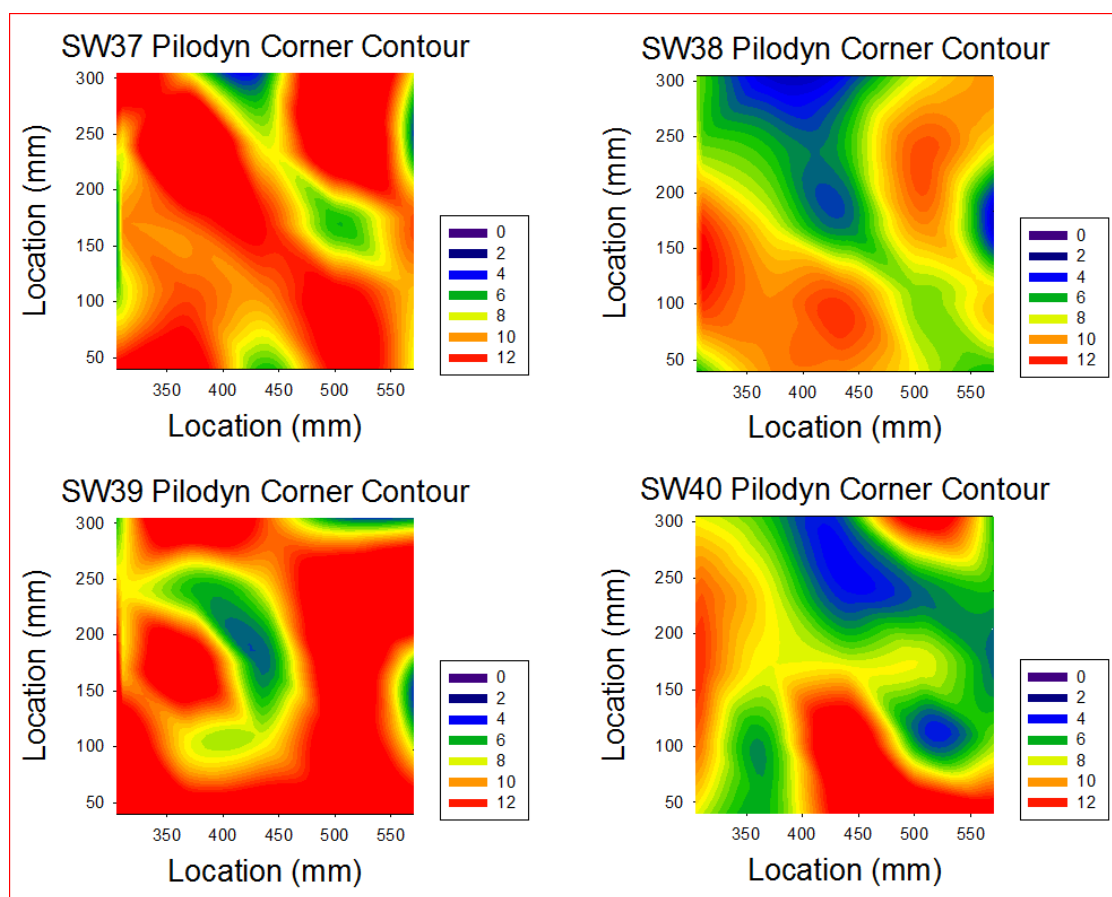


Figure I-7. Pilodyn Corner Contour Plots of SW37, SW38, SW39, and SW40

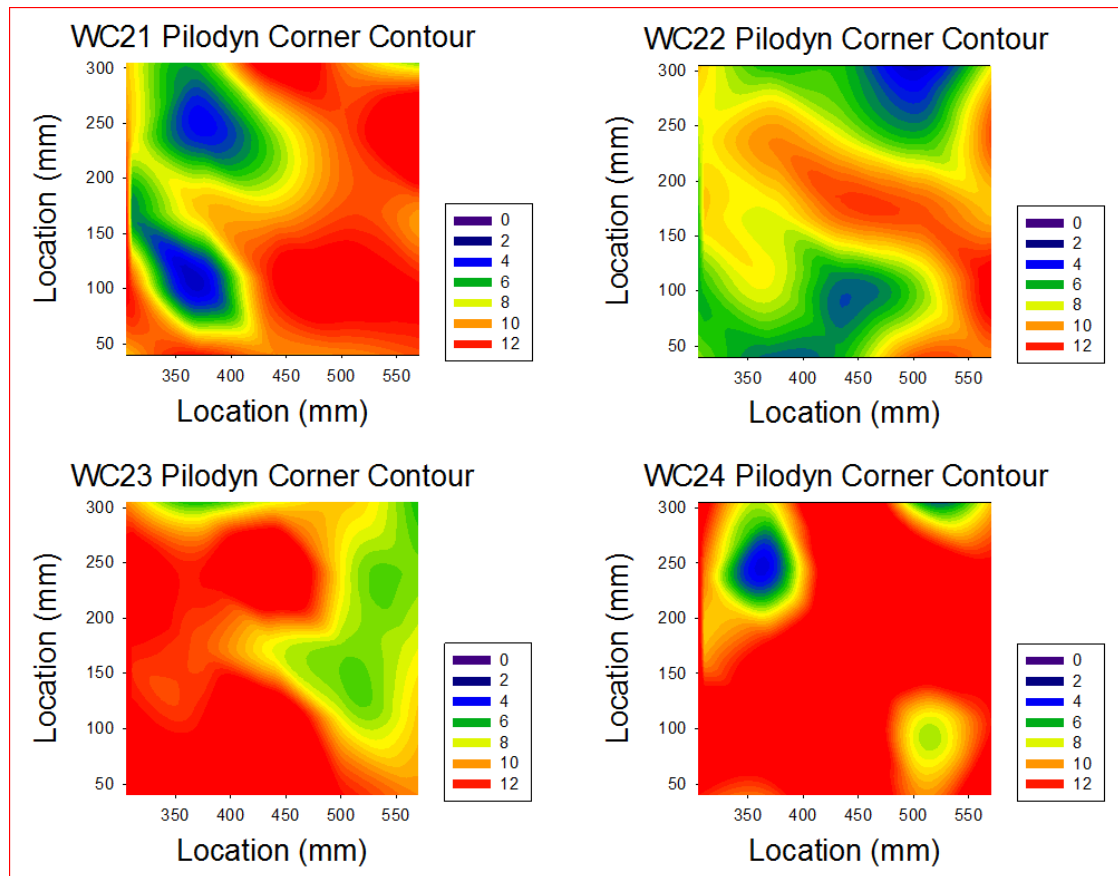


Figure I-8. Pilodyn Corner Contour Plots of WC21, WC22, WC23, and WC24

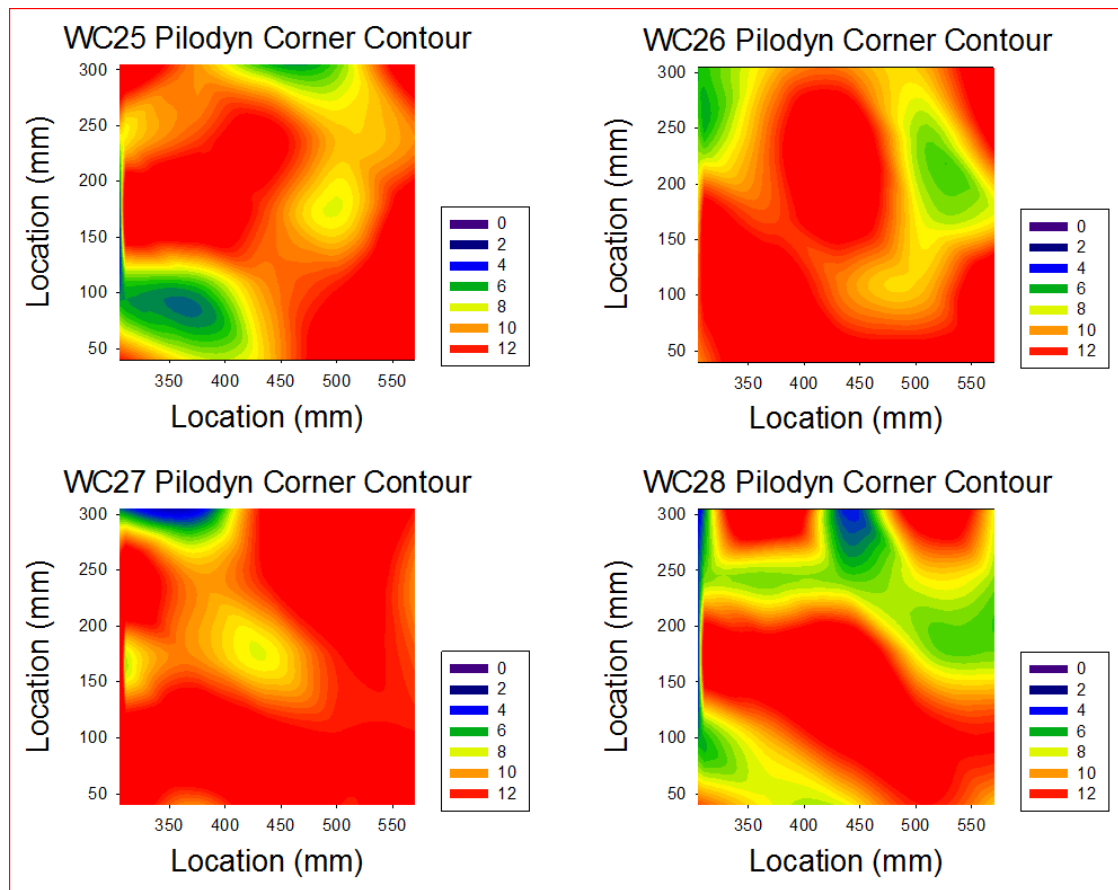


Figure I-9. Pilodyn Corner Contour Plots of WC25, WC26, WC27, and WC28

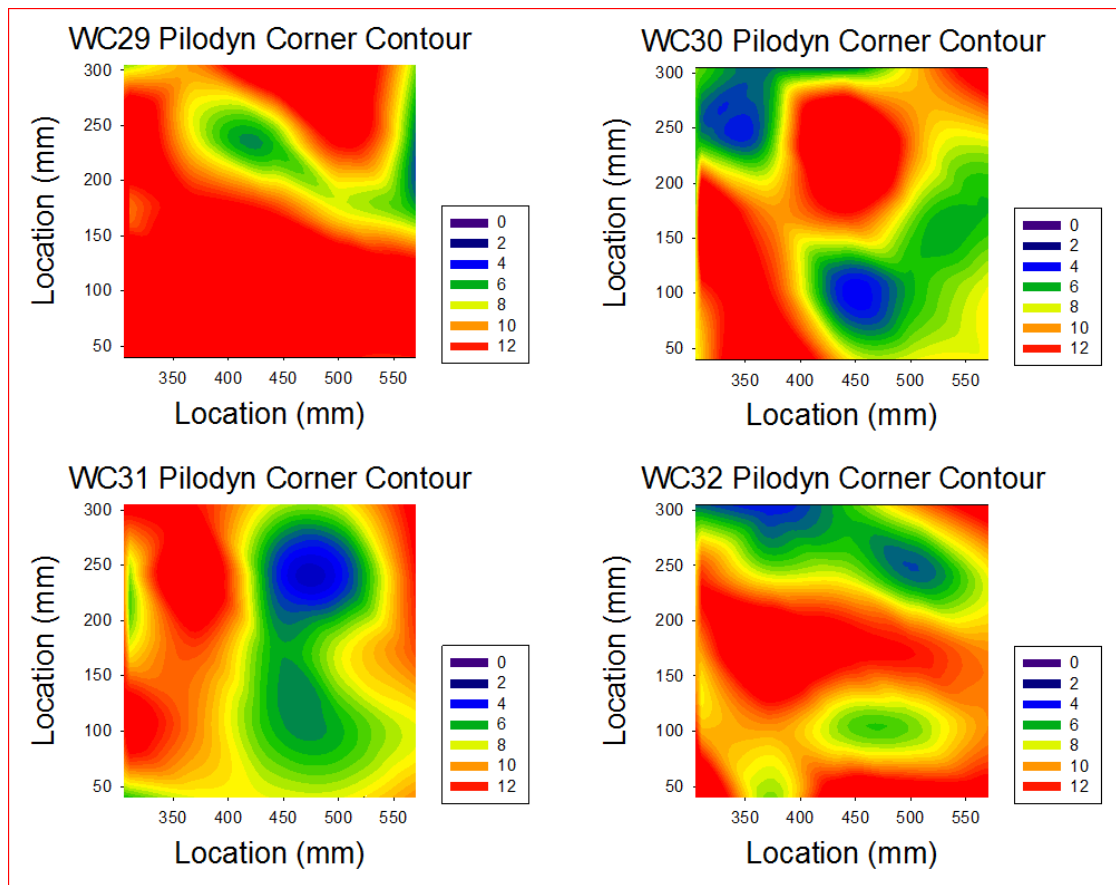


Figure I-10. Pilodyn Corner Contour Plots of WC29, WC30, WC31, and WC32

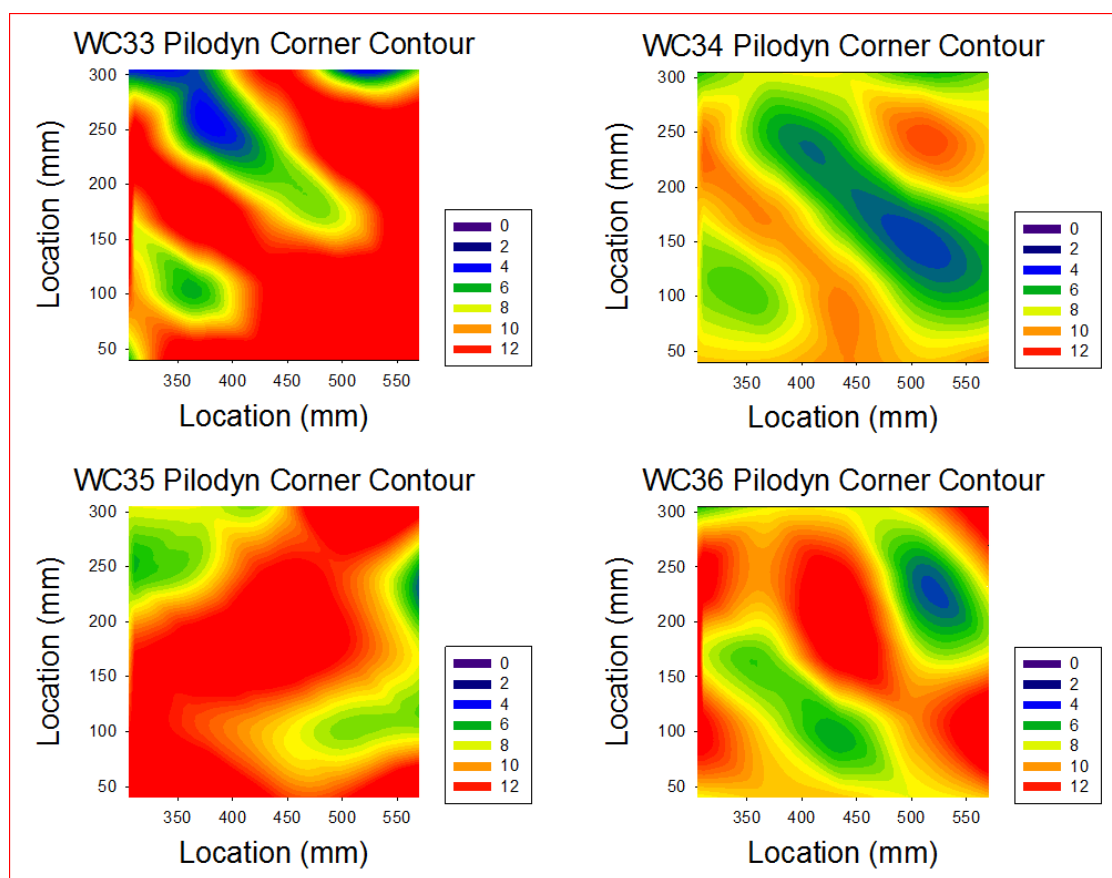


Figure I-11. Pilodyn Corner Contour Plots of WC33, WC34, WC35, and WC36

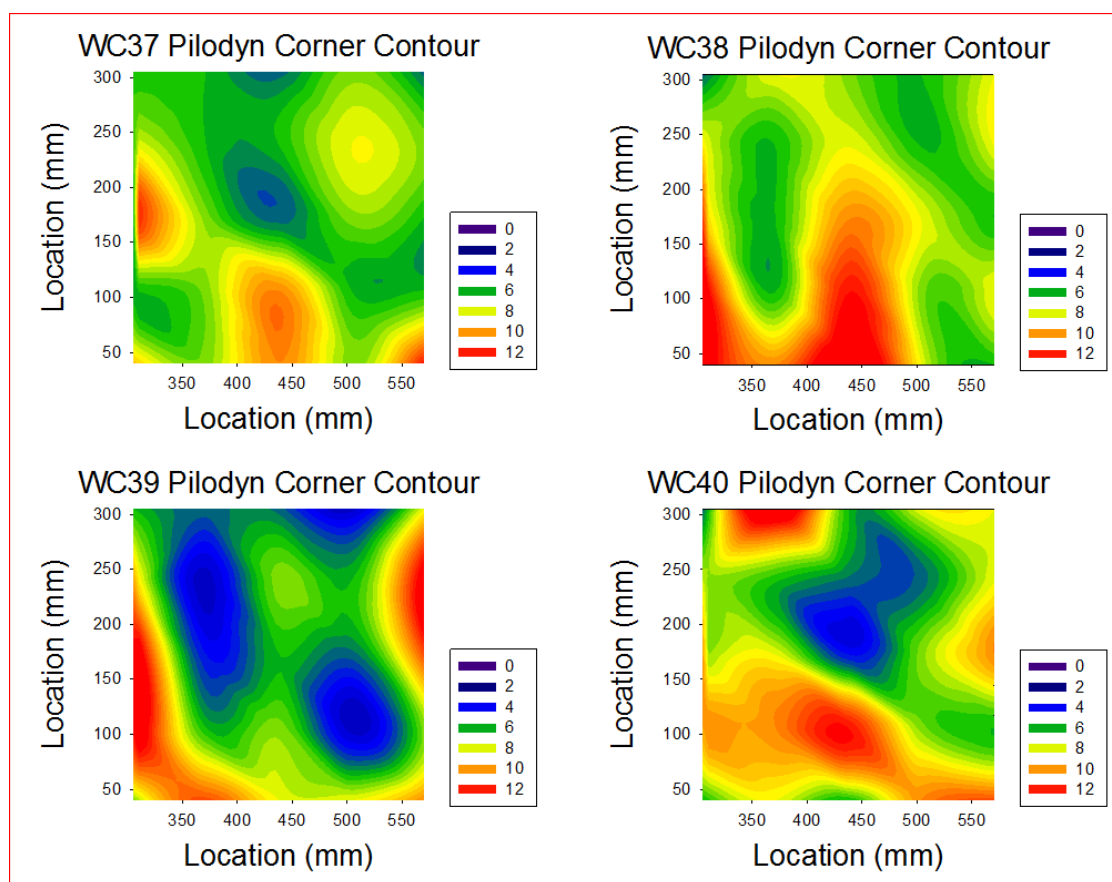


Figure I-12. Pilodyn Corner Contour Plots of WC37, WC38, WC39, and WC40

Appendix J - Shear Wall Load and Deflection Curves

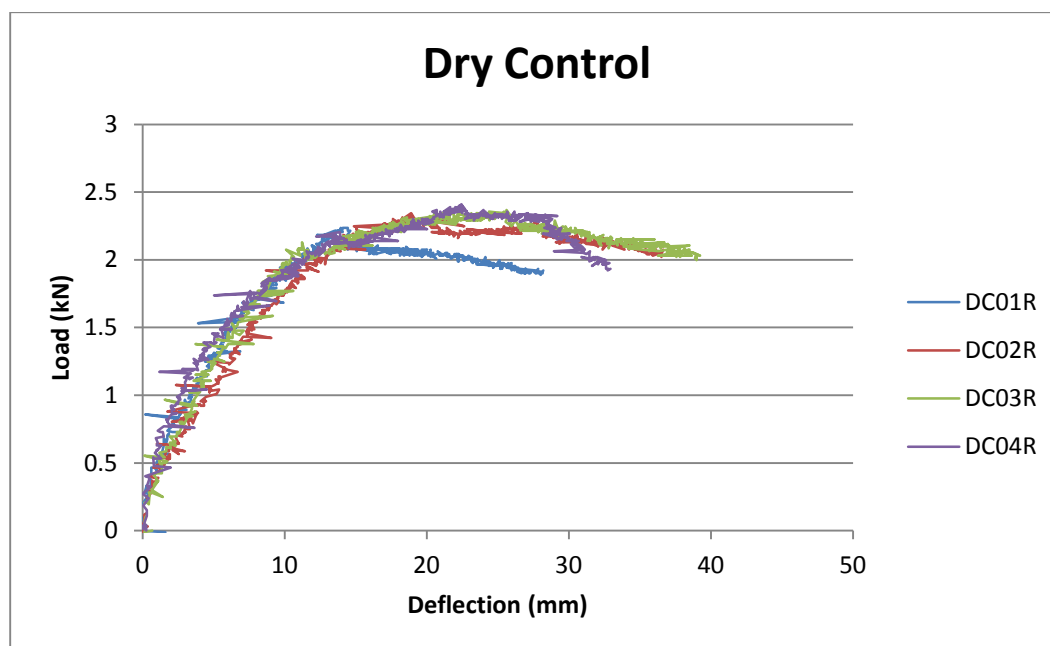


Figure I-1. Dry Control for DC01R, DC02R, DC03R, and DC04R

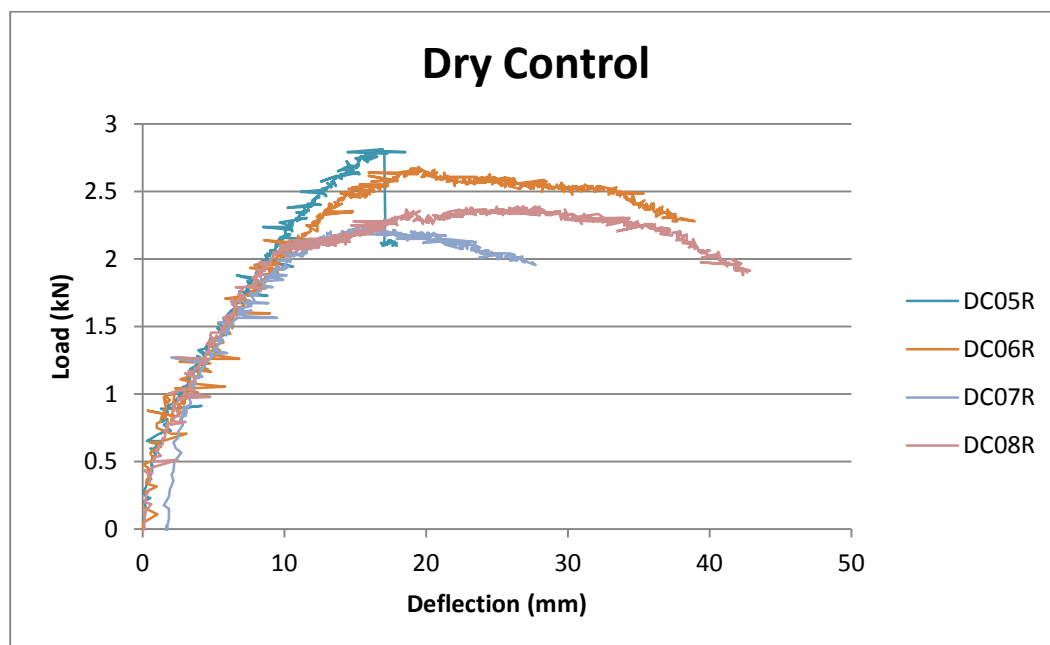


Figure I-2. Shear Wall Load and Deflection Curve for DC05R, DC06R, DC07R, and DC08R

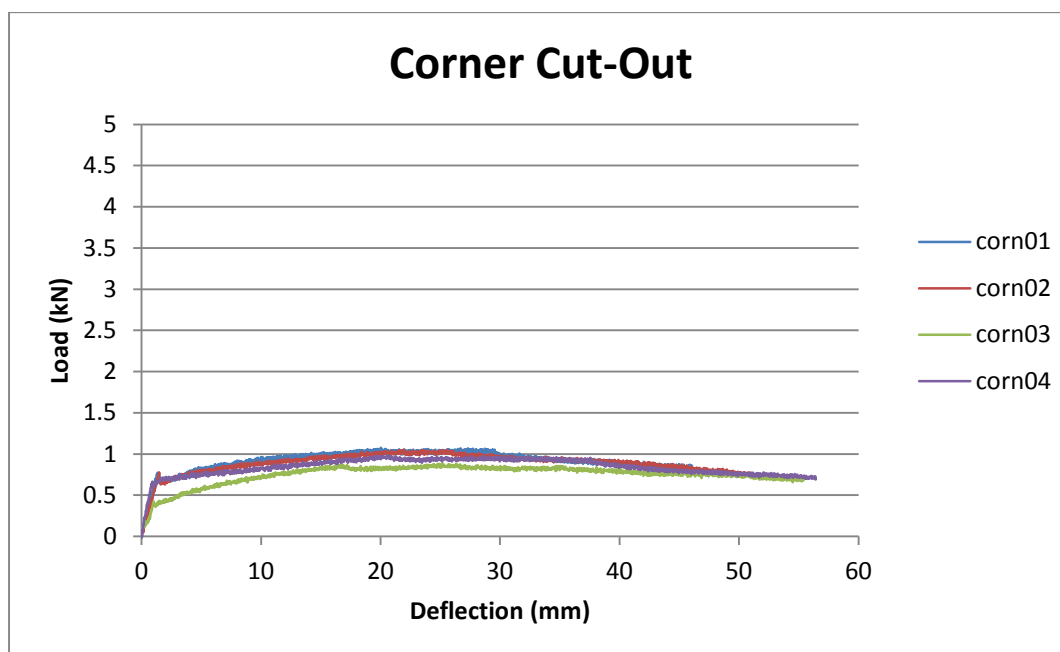


Figure I-3. Shear Wall Load and Deflection Curve for corn01, corn02, corn03, and corn04

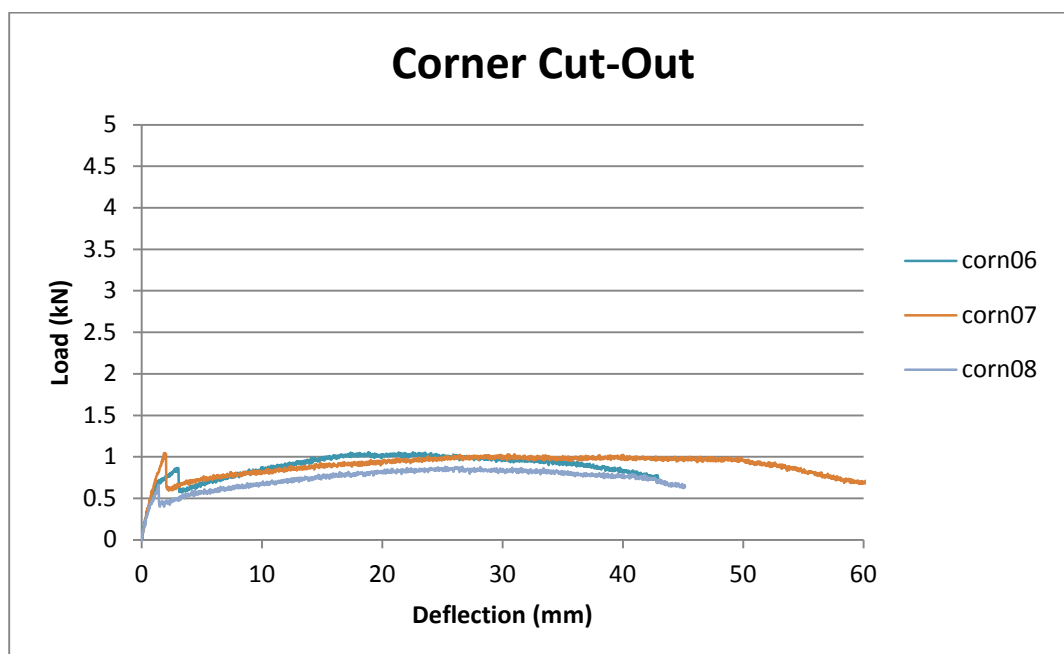


Figure I-4. Shear Wall Load and Deflection Curve for corn06, corn07, and corn08

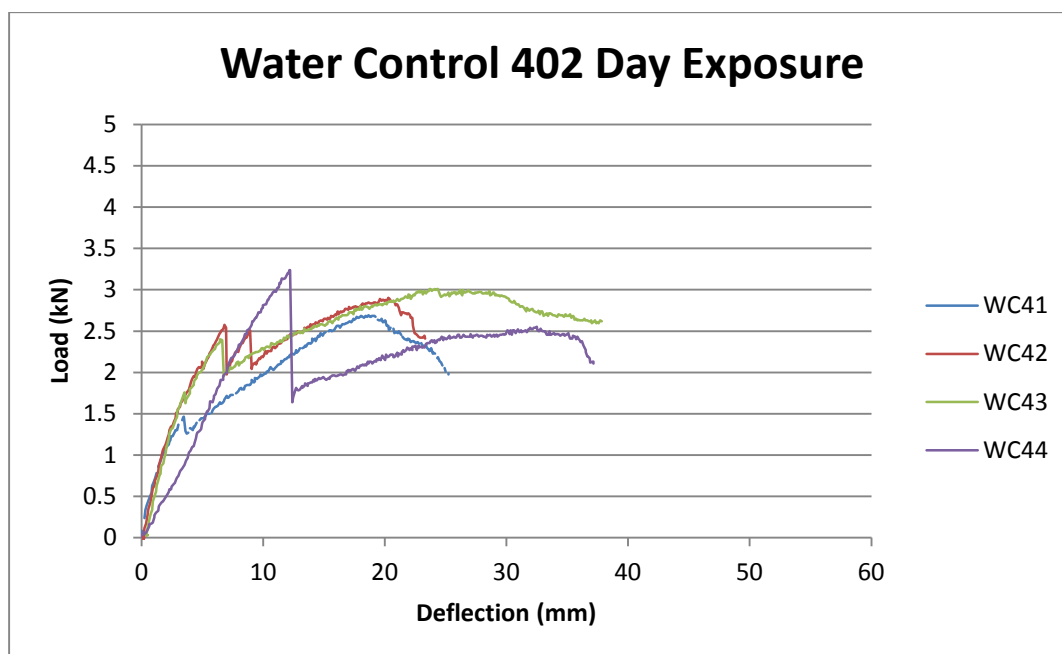


Figure I-5. Shear Wall Load and Deflection Curve for WC41, WC42, WC43, and WC44

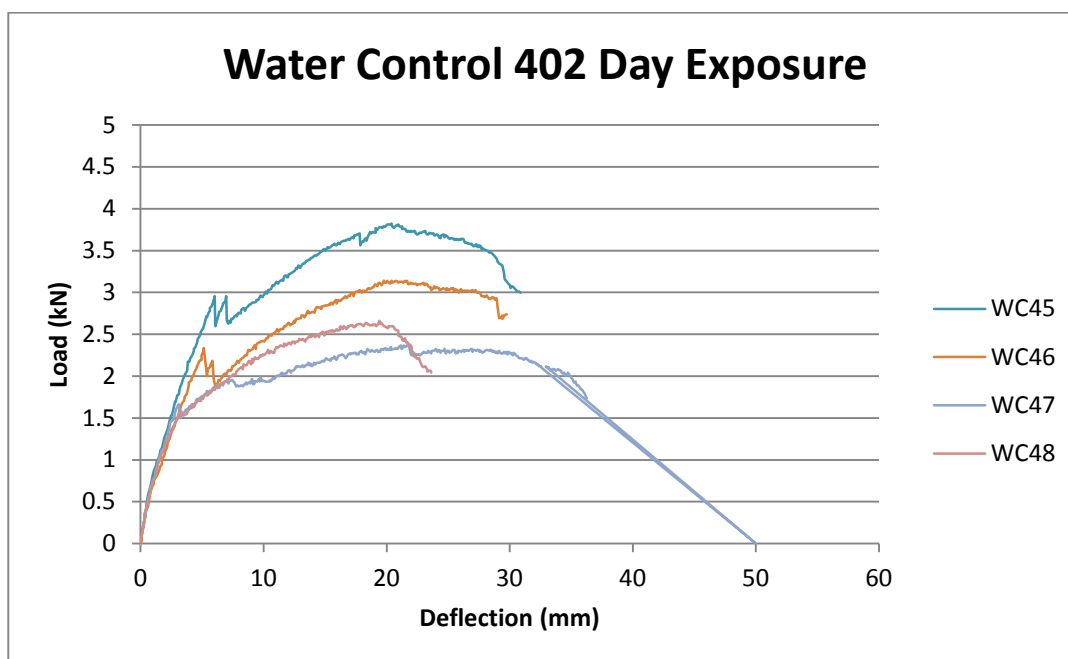


Figure I-6. Shear Wall Load and Deflection Curve for WC45, WC46, WC47, and WC48

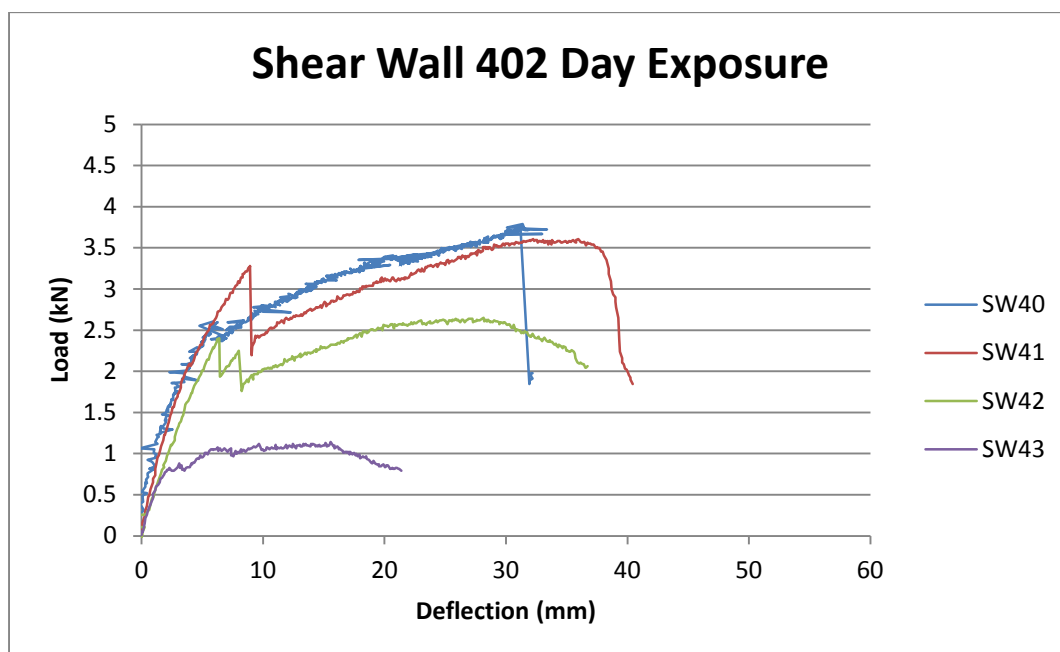


Figure I-7. Shear Wall Load and Deflection Curve for SW40, SW41, SW42, and SW43

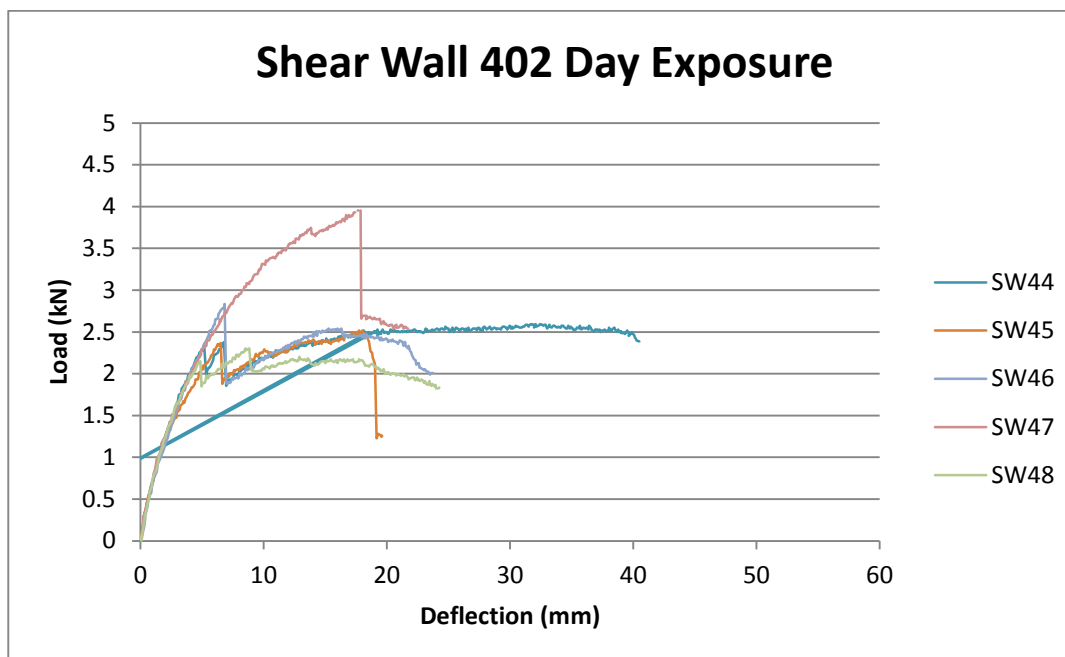


Figure I-8. Shear Wall Load and Deflection Curve for SW44, SW45, SW46, SW47, and SW48

Appendix K - Digital Image Correlation Strain Maps

Strain at failure

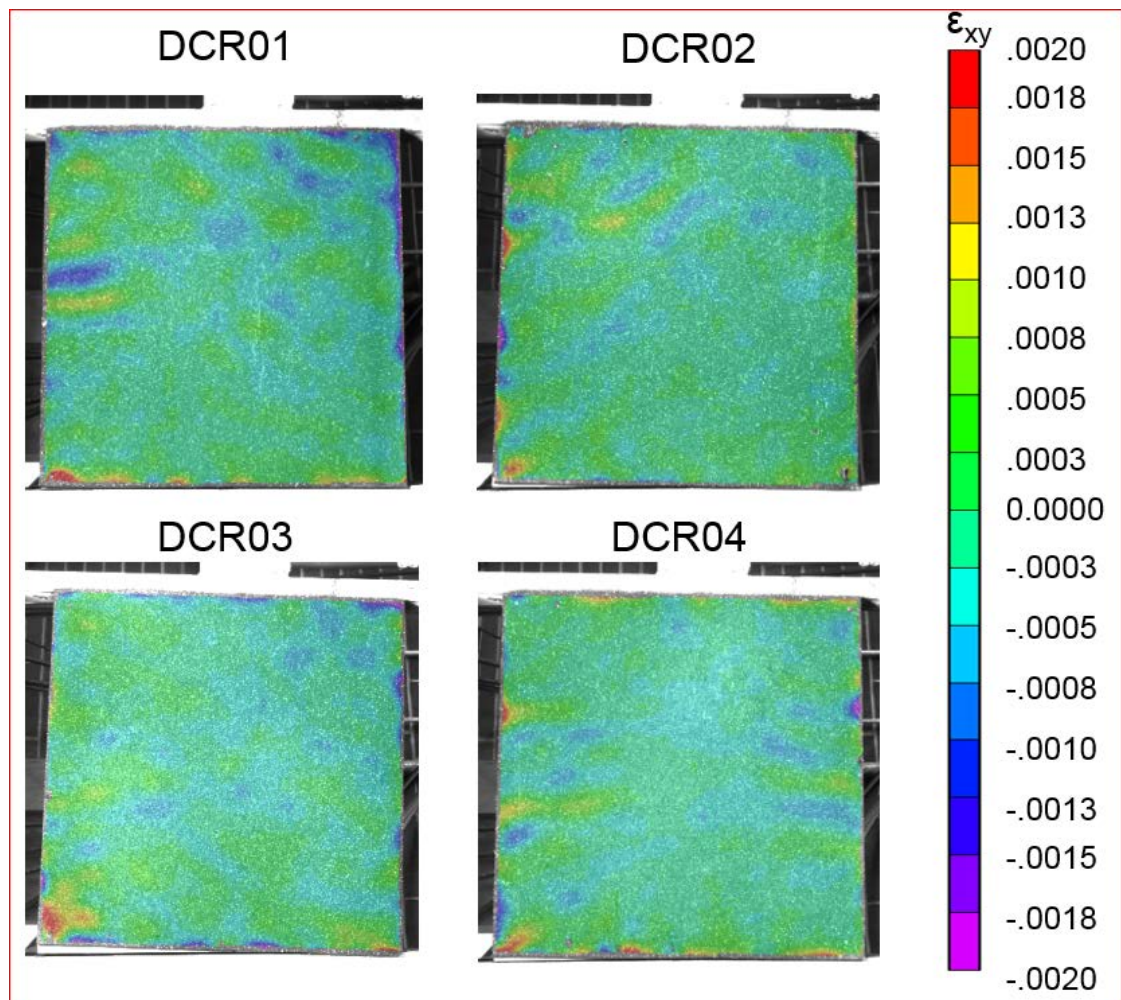


Figure K-1. Strain at Maximum Load for DC01, DC02, DC03, and DC04

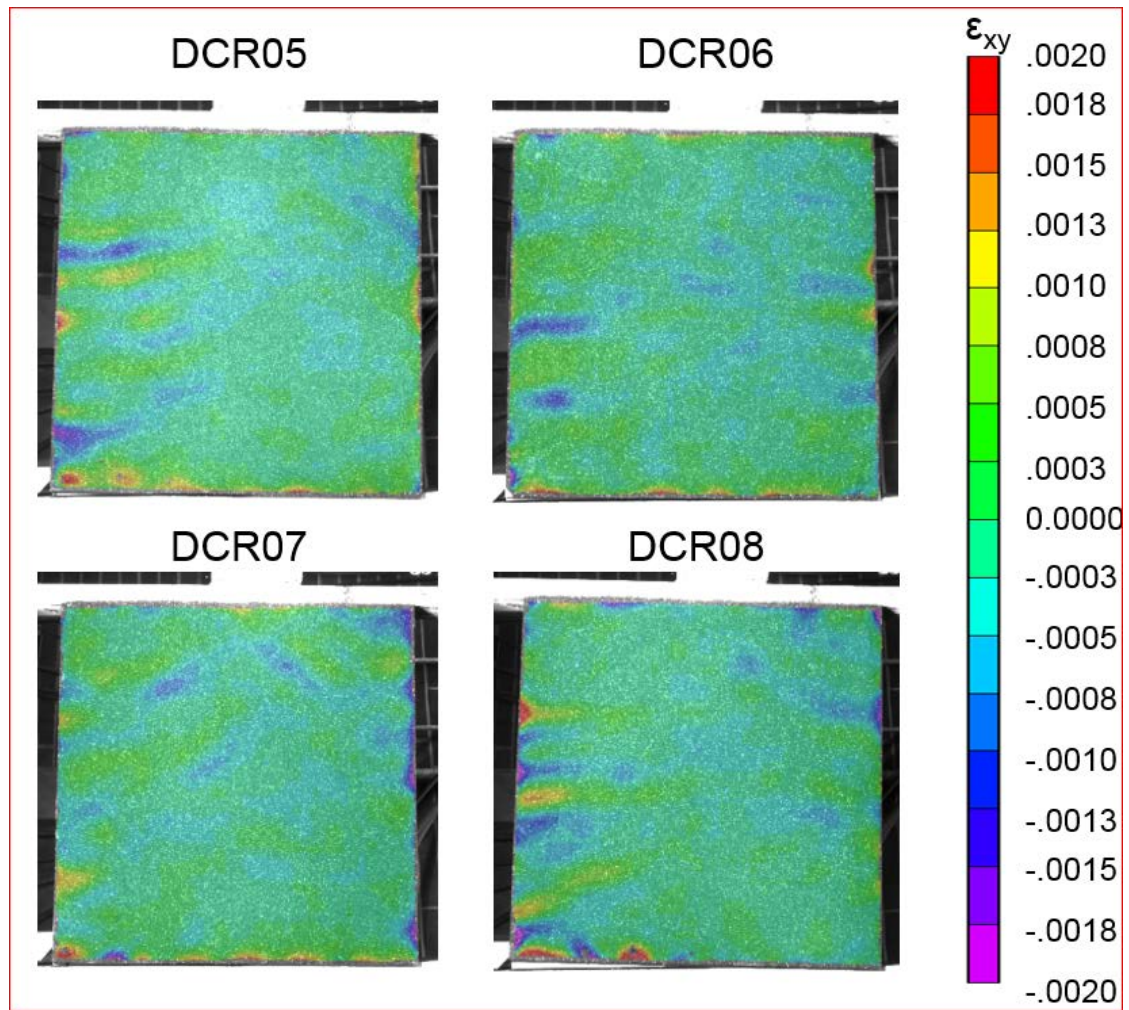


Figure K-2. Strain at Maximum Load for DC05, DC06, DC07, and DC08

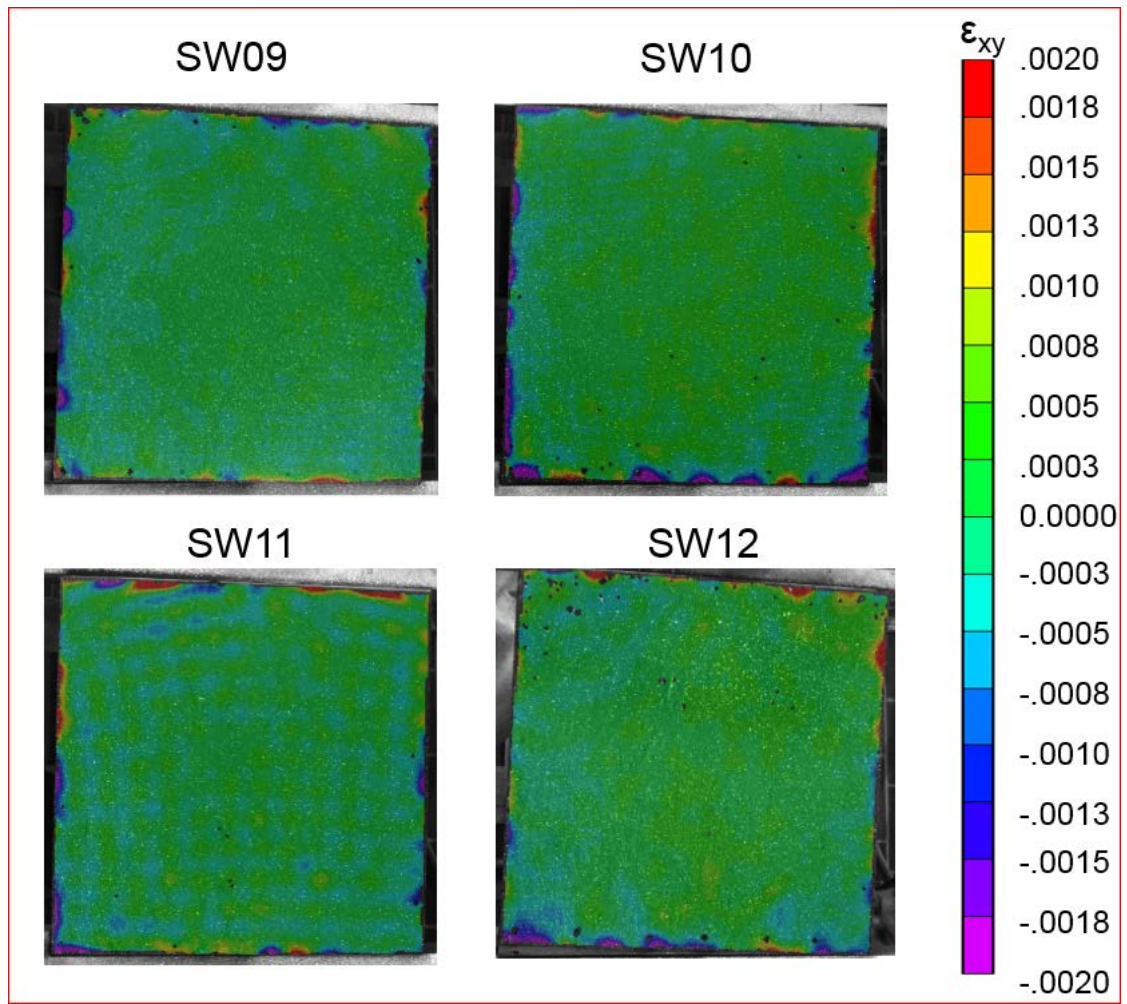


Figure K-3. Strain at Maximum Load for SW09, SW10, SW11, and SW12

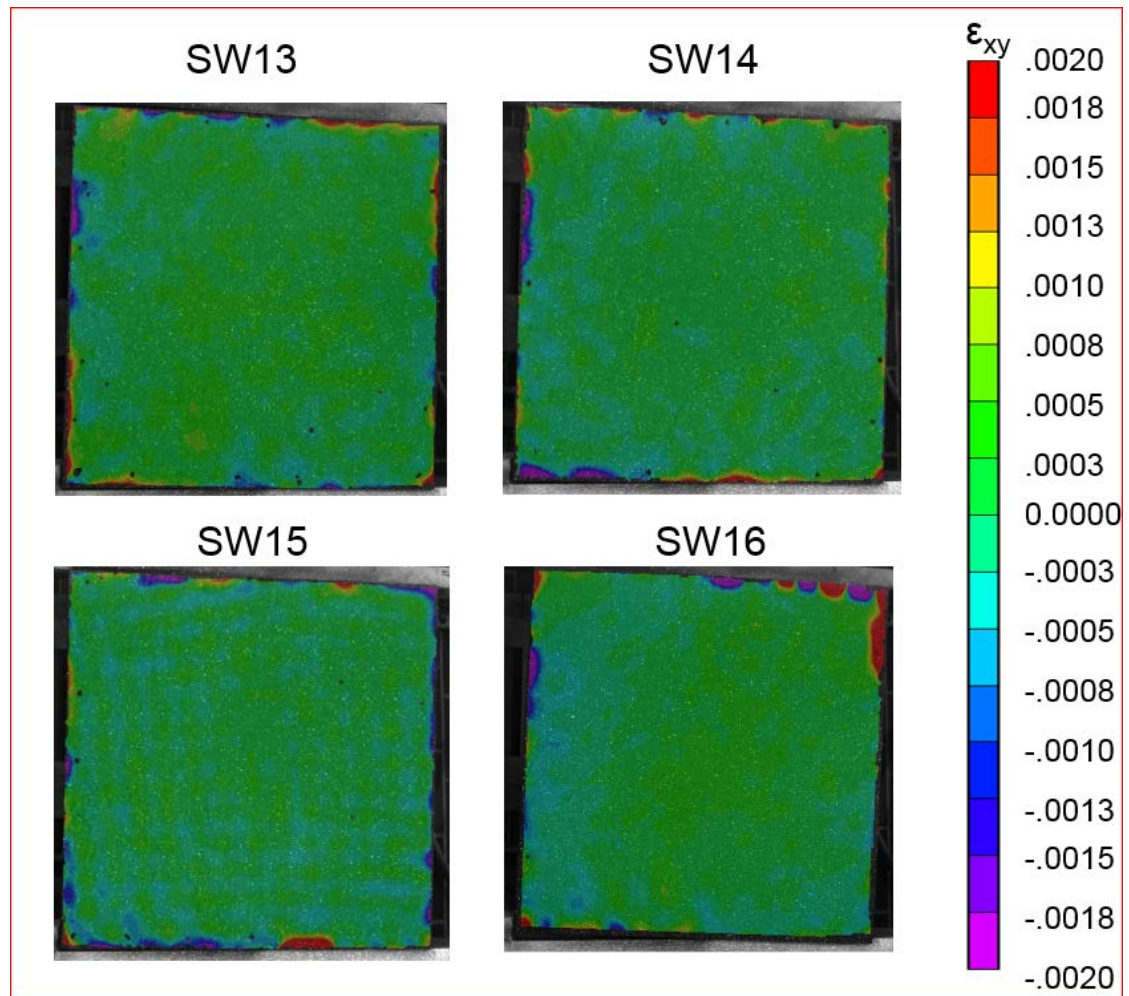


Figure K-4. Strain at Maximum Load for SW13, SW14, SW15, and SW16

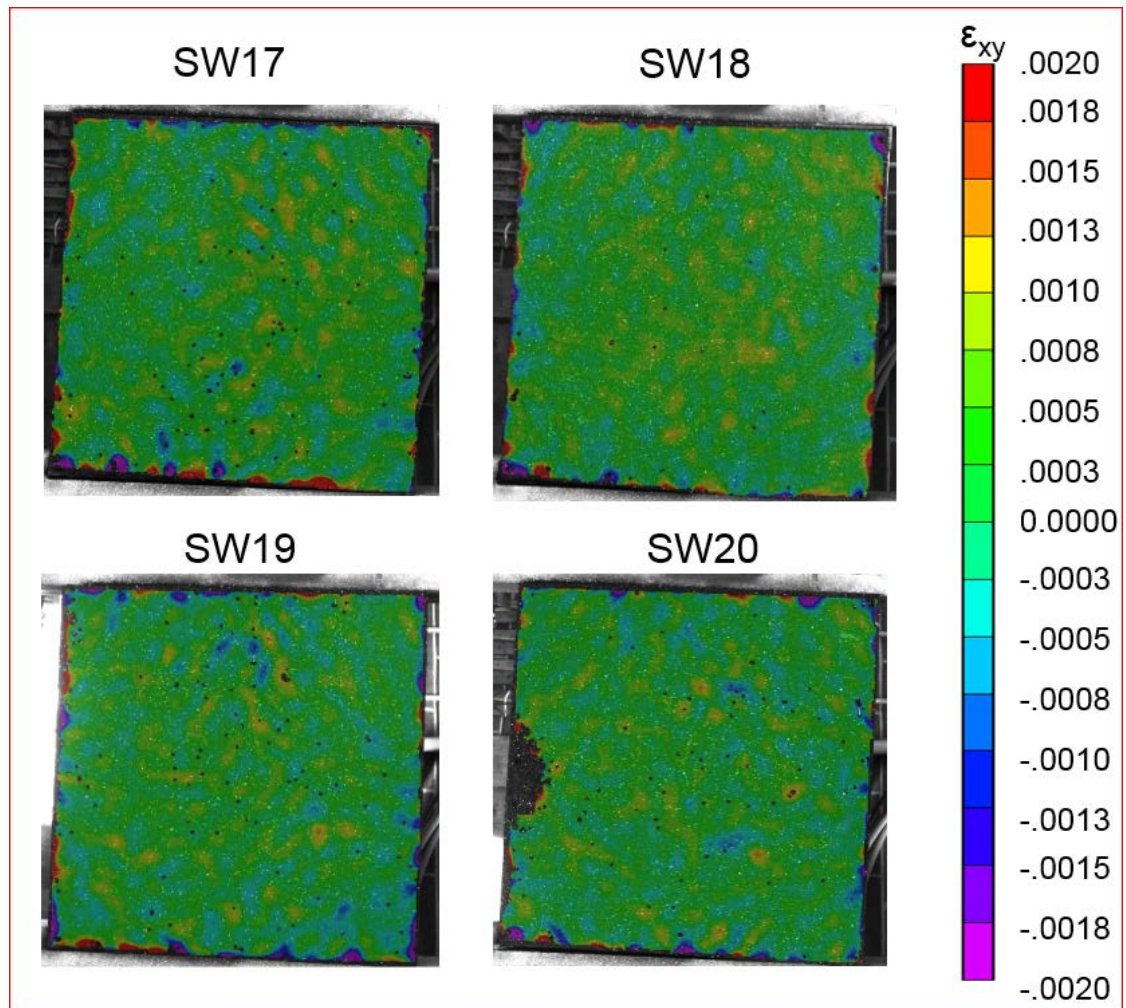


Figure K-5. Strain at Maximum Load for SW17, SW18, SW19, and SW20

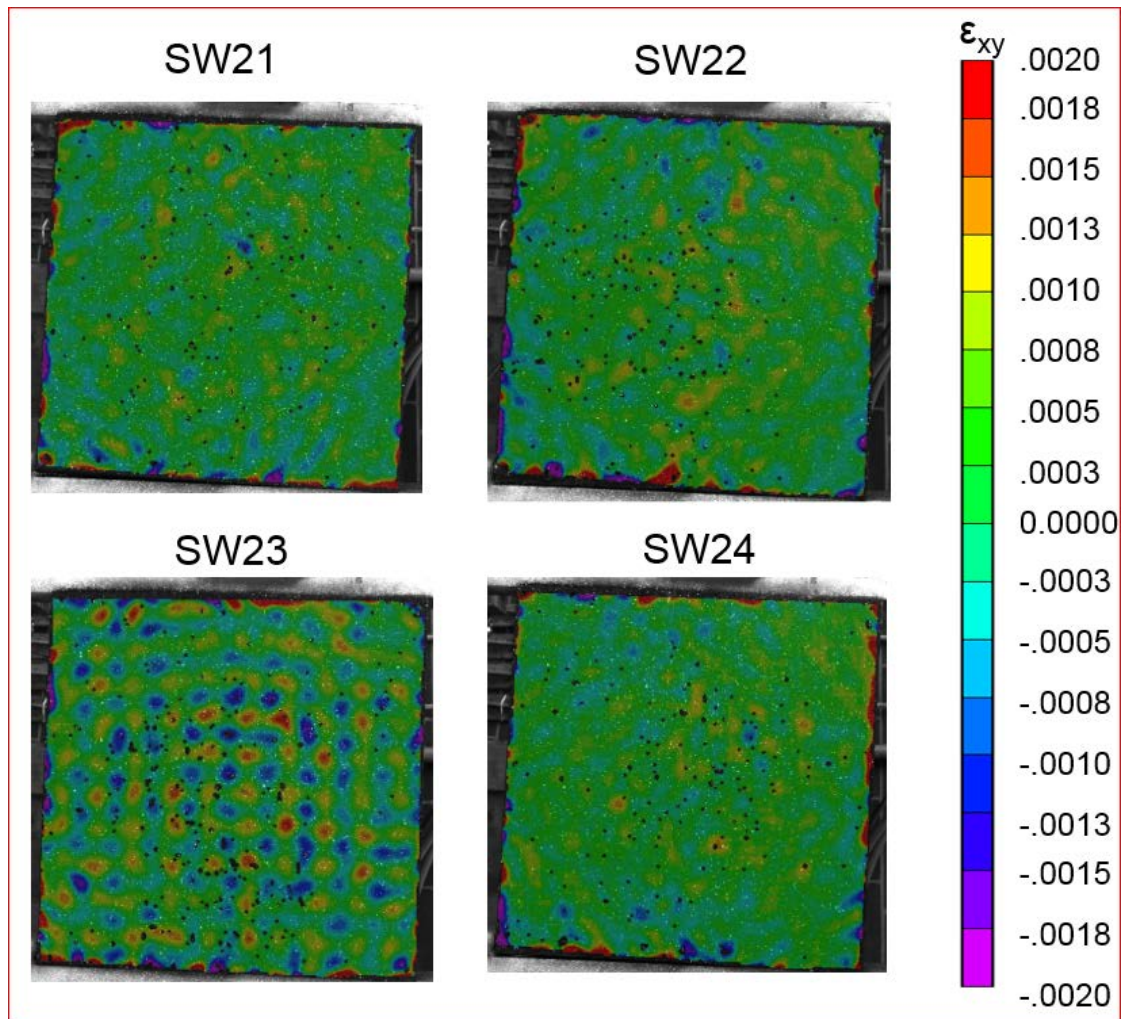


Figure K-6. Strain at Maximum Load for SW21, SW22, SW23, and SW24

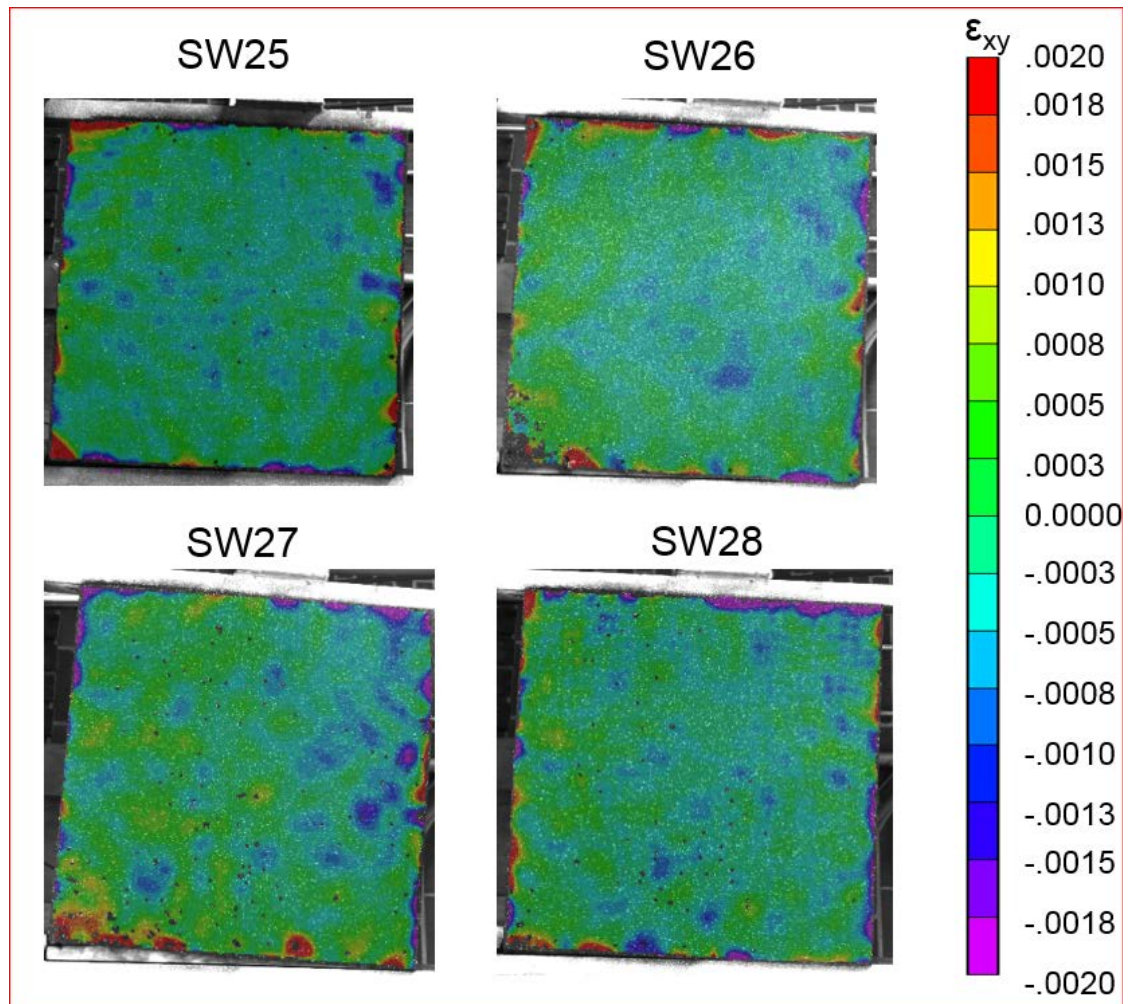


Figure K-7. Strain at Maximum Load for SW25, SW26, SW27, and SW28

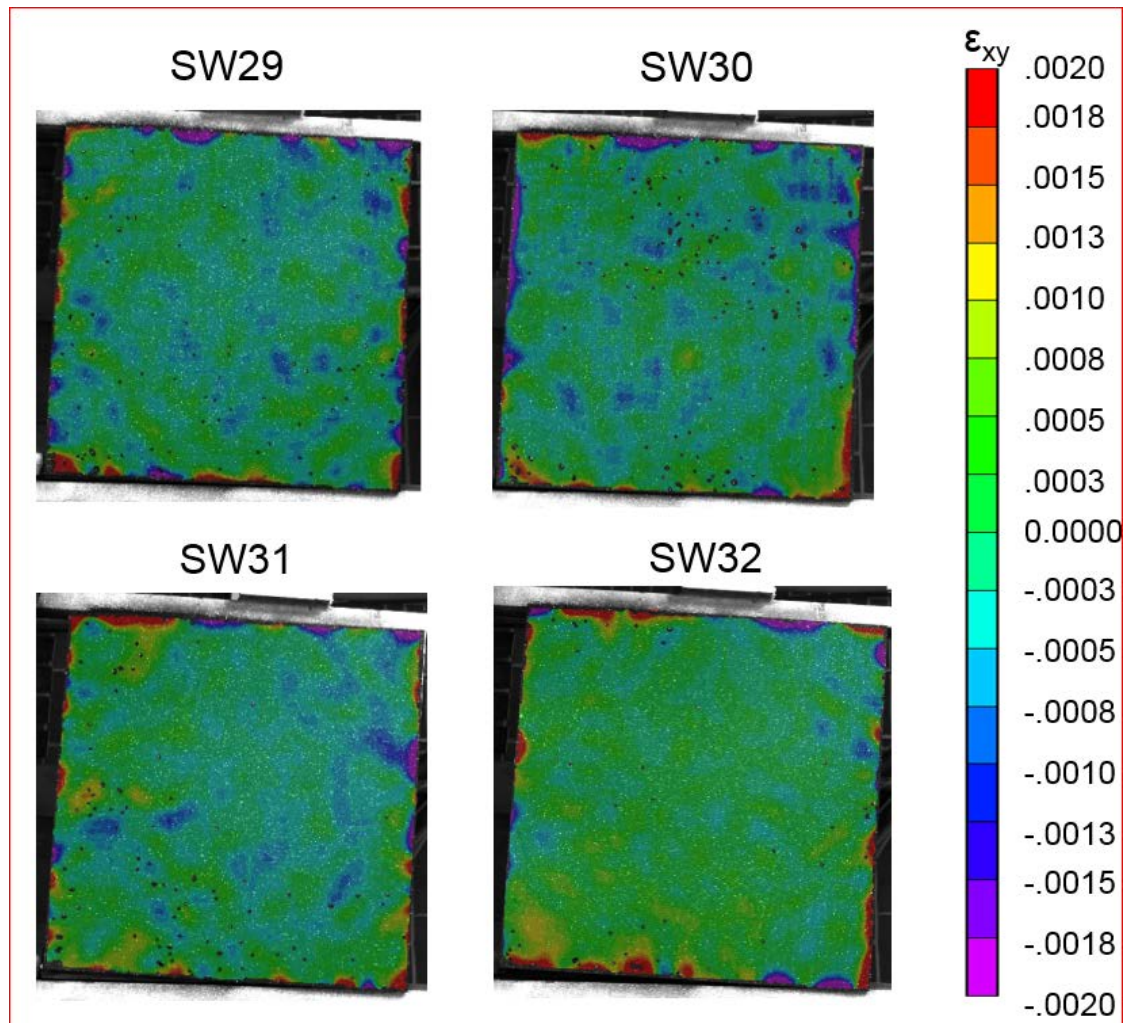


Figure K-8. Strain at Maximum Load for SW29, SW30, SW31, and SW32

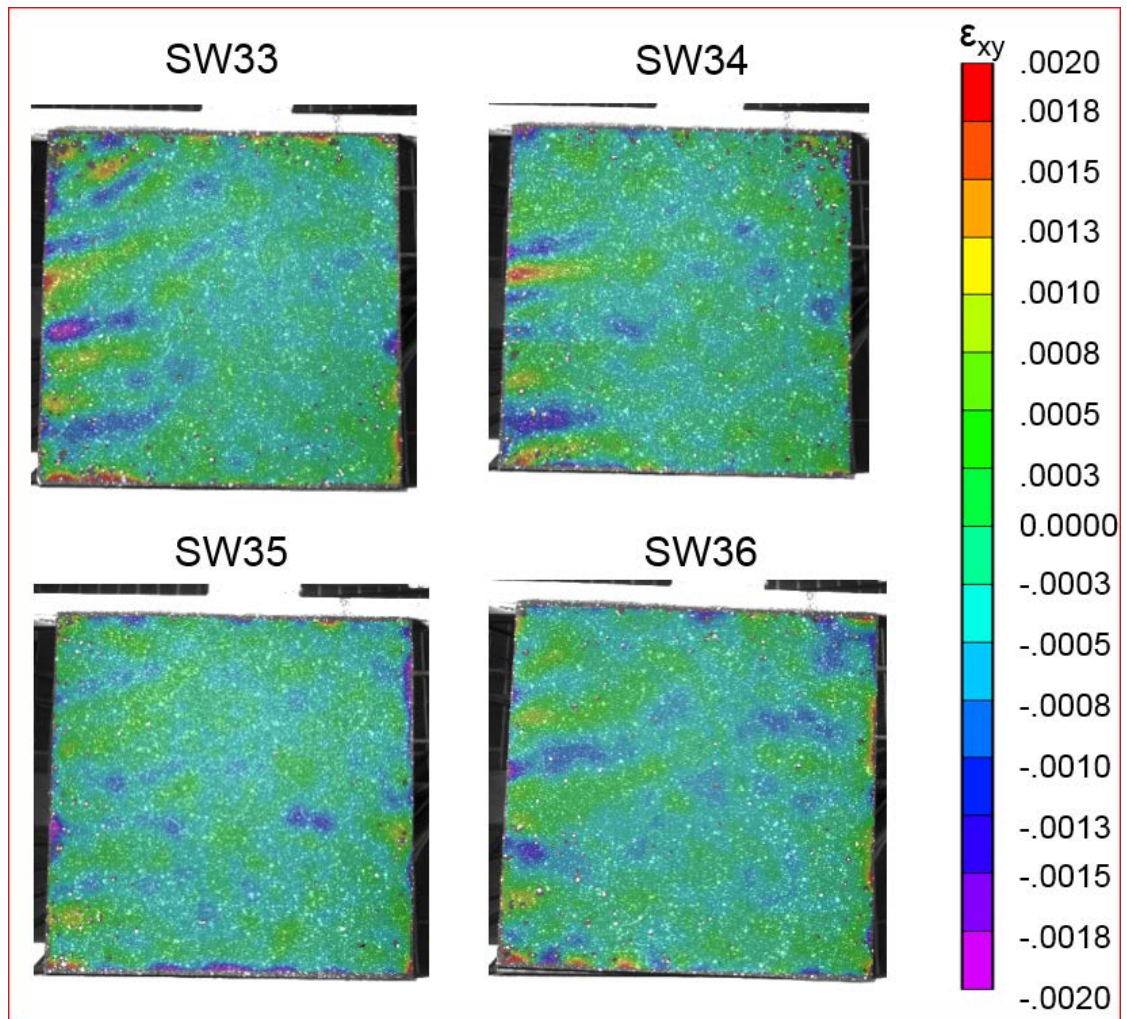


Figure K-9. Strain at Maximum Load for SW33, SW34, SW35, and SW36

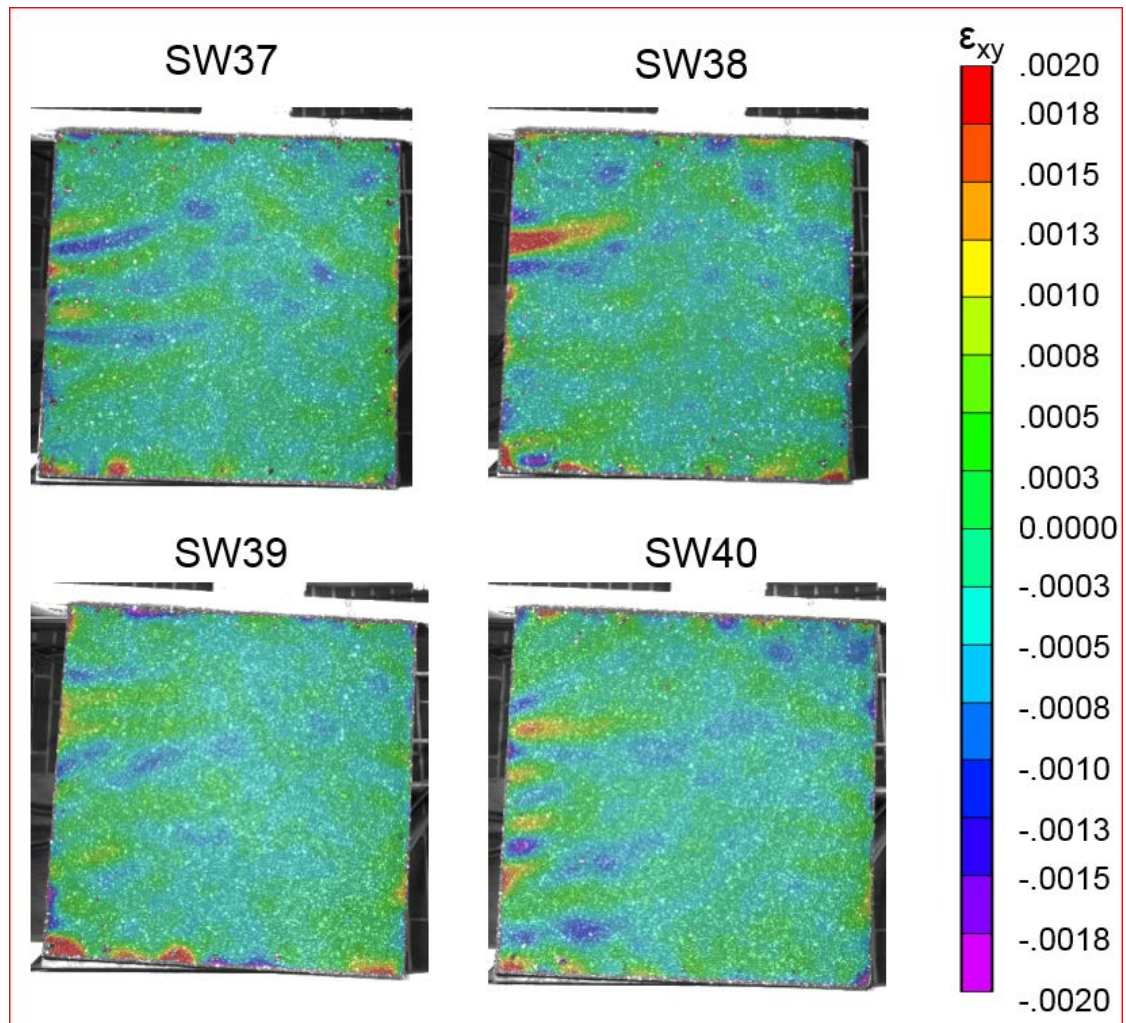


Figure K-10. Strain at Maximum Load for SW37, SW38, SW39, and SW40